LATERALLY-DRIVEN STOCHASTIC MOTIONS IN THE TROPICS

by

Man-Kin Mak

B.A. Sc., University of Toronto, 1963

M.S., Massachusetts Institute of Technology, 1966

SUBMITTED IN PARTIAL FULFILLMENT OF THE REQUIREMENTS

FOR THE DEGREE OF DOCTOR OF PHILOSOPHY

at the

MASSACHUSETTS INSTITUTE OF TECHNOLOGY

June, 1968

Signature of Author .....
Department of Meteorology, May 10, 1968

Certified by .....
Thesis Supervisor

Accepted by .....
Chairman, Departmental Committee on Graduate Students

Laterally-Driven Stochastic Motions in the Tropics

by

Man-Kin Mak

Submitted to the Department of Meteorology on May 10, 1968
in partial fulfillment of the requirement for the
Degree of Doctor of Philosophy

ABSTRACT

A two-layer model is used to investigate the asymmetric motions in the tropical atmosphere as small perturbations on a symmetric basic state which contains a vertical shear in the zonal wind. The physics used to describe them ignore latent heat, but include parameterized dissipation and non-geostrophic effects. The perturbed motion is treated as stationary random process driven by forcing at lateral boundaries located at 30^{o}N and 30^{o}S. The forcing motions are prescribed statistically in terms of spectra determined from 23 months of data at 30^{o}N, and with the assumption that the forcing at the two boundaries are statistically independent but otherwise are statistically similar.

The mathematical problem is to express second moment statistics of the internal motions in terms of the basic state parameters and the boundary statistics. This can be resolved into two separate steps: (1) to construct the response functions of the statistics from the fundamental solutions of the governing spectral equations, (2) to combine the response functions with a closed set of statistical boundary conditions.

The fundamental solutions are obtained numerically. Their properties are discussed with the aid of those obtained analytically in the case of no dissipation and shear in the basic zonal current.

The variance of the horizontal velocity components decreases with latitude, and are much larger at the uppper level. Variance of horizontal divergence, variance of temperature, and the correlation between velocity components at the two levels decrease markedly with latitude. A weak equatorward eddy sensible heat flux, a strong equatorward wave energy flux, and a poleward momentum flux are predicted. Comparison with observed values show good quantitative agreement for temperature

variance and sensible heat flux, but only qualitative agreement for meridional velocity variance and momentum flux. The results for the horizontal divergence and correlation between velocities at the two levels are compatible with synoptic experience. Physical implications are discussed for each statistic; in particular, as they bear upon earlier theoretical conclusions by Charney and by Eliassen and Palm.

A significant part of the meridional velocity variance in equatorial region at the upper level arises from motions of periods close to 5 days and wavelength of about 10,000 km, and westward phase propagation. These are similar to the disturbances in the equatorial lower stratosphere recently discovered by Yanai and Maruyama.

The eddy kinetic energy balance consists of a gain from pressure work on the boundaries, and losses to friction and conversions to eddy available potential energy and zonal kinetic energy. The gain in eddy available potential energy from this source is balanced by losses to radiative cooling and conversion to zonal available potential energy.

This study demonstrates that consistently reasonable statistics of the asymmetric motions can be obtained from a crude model that explicitly incorporates empirical forcing. Thus it lends support to the idea that lateral coupling between the low-latitude eddies and the mid-latitude motions is significant for the existence of the former.

Thesis Supervisor: Prof. Norman A. Phillips

Title : Professor of Meteorology

Dedication

To my father and mother whose instinctive love of education has always been a source of inspiration.

And to my wife, Pauline, who has contributed an element of fun to this research.

Acknowledgment

This work was undertaken on the suggestion of Prof. Norman A. Phillips whose active interest and critical advice have been most valuable throughout the course of this research. I wish to express my deep gratitude to him as my thesis supervisor.

The author is grateful to Prof. C. Wunsch for his suggestions concerning the spectral analysis; to Mr. John W. Kidson of the Planetary Circulations Project at M.I.T. for offering his unpublished results of several statistics in the tropics quoted in this work; and to the National Center for Atmospheric Research for providing two years' stream-function data.

Appreciation is due to Mrs. Marie L. Gabbe for typing this manuscript and to Miss Isabel Cole for drafting the figures.

The numerical computations were made at the M.I.T. Computation Center. This work was supported by the National Science Foundation under contract G-18985 with the Massachusetts Institute of Technology.

Finally the author acknowledges with gratitude the fellowship support from the Ford Foundation.

Table of Contents

Partial list of notation

c_ℓ, s_ℓ	Fourier cosine and sine coefficients in x-expansion of v_ℓ .	18
dC_ℓ, dS_ℓ	Increment of the random point functions associated with c_ℓ , s_ℓ .	20
V_ℓ, U_ℓ, P_ℓ	Complex Fourier coefficients in x-expansion of v_ℓ , u_ℓ , ϕ_ℓ .	18
$dV_\ell, dU_\ell, dP_\ell$	Increment of the random point functions associated with V_ℓ , U_ℓ , P_ℓ .	24
$\hat{V}_\ell^j, \hat{U}_\ell^j, \hat{P}_\ell^j$	$j=1,2,3,4$ Fundamental solutions of dV_ℓ , dU_ℓ , dP_ℓ .	26
$\hat{H}_{\xi\eta}^j$	Four response functions of the statistic $\langle \xi\eta \rangle$	38
F_j	Four non-trivial statistical boundary conditions.	38

1. Introduction

This study is a theoretical attempt to investigate the large scale zonally asymmetric motions in the tropics. The data analysis performed thus far are rather fragmentary, Starr and White (1954), Obasi (1963) and Peixoto (1960). Those studies only indicate that asymmetric motions have a progressively smaller role towards the equator in so far as transporting momentum and heat is concerned. We have yet to determine how far south the influence of eddies extends into the tropics. We understand very little about the energetics associated with the asymmetric tropical motions. The available data is sparser than in higher latitudes, but it has posed some interesting questions. Riehl (1954, 1963) noted that the flow in the lower tropical troposphere is relatively steady, whereas that at higher altitudes has considerably more variability and day to day changes in the large-scale disturbances. Furthermore, the low level systems in the Marshall Island region of the Western Pacific and in the Caribbean Sea have often been found to move quite independently of the upper level systems. This situation is quite different from what is usually observed in middle latitudes. Such observations suggest that the vertical scale of asymmetric motions in the tropics could be so small that motions at one level exert very little influence upon the motions at another level. Charney (1963) has applied a scaling argument to substantiate that possibility. He showed that on the basis of the generally accepted typical length and velocity scales and static stability in the tropics, the large scale motions there (in the absence of condensation)

should be even more quasi-horizontal and horizontally nondivergent than those in the middle latitudes. It follows that the vertical coupling should be of only second order. Such large scale eddy motions must then in the absence of condensation derive their energy either locally from barotropic instability or through lateral coupling with the motions in higher latitudes. This type of lateral coupling would be associated with a significant cross-latitude flux of wave energy. This aspect of the coupling has been hinted at by Eliassen and Palm (1960) when they made an analysis of stationary waves. They showed that these waves of planetary scale in a realistic mean state have a cross-latitude momentum flux in opposite direction to the wave energy flux. Should this also be true for the transient waves, the presumed lateral coupling would supply considerable wave energy into the tropics. How far equatorward such a flux of wave energy can penetrate depends upon the rate of dissipation the effect of the Coriolis parameter and the interaction with the mean flow.

In view of the suggestive evidence mentioned above concerning the plausibility of significant lateral coupling between the middle and low latitude circulation patterns, it is certainly of some interest to test that concept quantitatively. This paper does so with a model tropics that explicitly incorporates this mechanism. The role of local barotropic instability as an energy source will be excluded by using a model containing no lateral shear in the basic current. Specifically, we shall examine the statistics of the circulation in a model tropics driven solely by lateral forcing that is prescribed only statistically in terms of second

moment statistics. The latter will be deduced from actual data at 30^{o}N. If the resulting asymmetrical motions in the model tropics have statistical properties similar to those in the real tropics, we then will have established quantitative evidence for lateral coupling as an important energy source of their motions.

The dynamical design of the model is described in Section 2. Its simplicity underlies the limited objective of this study. Yet it is precisely in virtue of the model's simplicity that a statistical analysis is feasible and an unambiguous physical interpretation of the theoretical results can be given.

Section 3 is an exposition of the stochastic aspect of the analysis. It will be shown that the problem of deducing the second moment statistics can be resolved into two separate steps. One is to determine the fundamental solutions which can in turn be combined to obtain the response functions of the system. The other is to formulate and compute the statistical boundary conditions. These results can then be combined to give unique solutions for such statistics within the tropics.

Section 4 is devoted to the discussion of the statistical boundary conditions. A crucial assumption is made here that the variable part of the flow at 30^{o}S is statistically independent but otherwise similar to that at 30^{o}N; this is necessary since no sufficient data at 30^{o}S is available. In this section we will see how the boundary statistics at 30^{o}N from data are computed and how they may be interpreted in terms of wave motions in the east-west direction.

Section 5 shows the results for the first step of the analysis outlined in Section 3. The fundamental solutions are solved analytically for the special case of no dissipation and no shear in basic state, and numerically for the general case. A brief discussion is given of the manner in which the fundamental solutions are related to Rossby waves and internal gravity waves.

Finally Section 6 presents the predicted second moment statistics for the model tropics. The following statistics are computed: variance of each of the three velocity components, covariance between the horizontal velocities at the upper and lower levels, variance of temperature, eddy cross-latitude fluxes of momentum, sensible heat and wave energy, and the energy conversion terms. Wherever possible comparison between the theoretical statistics and the corresponding "observed" values will be made.

2. Description of the model tropics

The atmospheric model is designed for a rather limited objective. As pointed out in the Introduction, it is chosen for studying the statistical properties of large scale asymmetric motions in the tropics in the absence of condensation. Thus a dry model with hydrostatic approximation is used. In particular we use a two-layer model. It is sometimes known as a $2\frac{1}{2}$ dimensional model because it has only two degrees of freedom in the vertical dimension for the horizontal velocity field, and one for the thermal field and the vertical velocity field. The vertical coordinate consists of five pressure levels: 0, 250, 500, 750 and 1000 mb. The horizontal coordinates are those of a Mercator projection covering the tropical region from 30°S to 30°N. The effects of the spherical geometry of the earth are approximated by an equatorial β-plane representation. In order to see precisely how an equatorial β-plane approximation is introduced, let us start with the complete set of governing equations for a dry hydrostatic atmospheric system in (x, y, p) coordinates where p is pressure and x and y are horizontal coordinates of any conformal projection. (They are sometimes referred to as the "primitive" equations in meteorology literature.)

$$\frac{\partial \vec{V}}{\partial t} = -\nabla\left(\phi + \frac{\vec{V}^2}{2}\right) - \left(\vec{k}\cdot 2\vec{\Omega} + \frac{1}{h^2}\left(\frac{\partial hv}{\partial x} - \frac{\partial hu}{\partial y}\right)\right)\vec{k}\times\vec{V} - \omega\frac{\partial \vec{V}}{\partial p} + \vec{F}$$

$$\frac{\partial \phi}{\partial p} = -\frac{RT}{p} \qquad (2.1)$$

$$\frac{\partial \omega}{\partial p} + \frac{1}{h^2}\left(\frac{\partial hu}{\partial x} + \frac{\partial hv}{\partial y}\right) = 0$$

$$\left(\frac{\partial}{\partial t} + \vec{V}\cdot\nabla\right)\frac{\partial \phi}{\partial p} - \omega\frac{RT}{p}\frac{\partial \ln \Theta}{\partial p} = -\frac{\kappa Q}{p}$$

where $\vec{V} \equiv (u, v)$ horizontal velocity

$\nabla \equiv \left(\frac{1}{h}\frac{\partial}{\partial x}, \frac{1}{h}\frac{\partial}{\partial y}\right)$ horizontal del operator (at constant p)

h scale factor of the conformal projection

ϕ geopotential

T temperature

Θ potential temperature, $\Theta = T\left(\frac{p_0}{p}\right)^{\kappa}$

$\vec{\Omega}$ earth's rotation vector

$\vec{k}$ unit vector normal to isobaric surfaces

$\omega = \frac{dp}{dt}$ "p" velocity

Q rate of heating per unit mass

$\kappa = \frac{R}{c_p}$ = 0.286 for dry air

θ latitude, $\vec{k}\cdot 2\vec{\Omega} = 2\Omega \sin\theta$

In particular, if a Mercator projection centered at the equator is used, x , y and h would be related to longitude λ , latitude θ and earth's radius a as follows.

$$\begin{aligned} x &= \lambda \\ y &= \ln\left(\frac{1+\sin\theta}{\cos\theta}\right) \\ h &= a\cos\theta \\ 2\Omega\sin\theta &= 2\Omega\tanh y \end{aligned} \tag{2.2}$$

By "equatorial β -plane" approximation, we mean that the last two relations in (2.2) are approximated by

$$\begin{aligned} h &= a \\ 2\Omega\sin\theta &= 2\Omega y \end{aligned} \tag{2.3}$$

We also assume that ω vanishes at the top and bottom pressure levels. This simplification, amounting to no net divergence in a vertical column, eliminates the fast moving "external gravity" waves. Since we are only interested in motions with a long time scale, this assumption is reasonable.

A unique feature of the model is the use of statistical lateral forcing at 30^{o}N and 30^{o}S. They are prescribed in terms of second moment statistics. We consider the total circulation in the model tropics as consisting of a time and zonally averaged state and a deviation from it, which arises from the lateral forcing. The deviation component is assumed to be governed by linearized form of the "primitive" equations. It is the purpose of this study to demonstrate that the statistical properties

of the resulting response, treated as a stochastic process, can be uniquely deduced.

The mathematical analysis will be made in terms of the meridional velocity, v , at the 250- and 750-mb levels in the model tropics. The lateral forcing will be given in terms of the statistics of v at these levels at both 30^{o}N and 30^{o}S. This information at 30^{o}N is obtained from 23 months (June 1963 to May 1965) of streamfunction data that covers north of about 15^{o} latitude of the northern hemisphere. Unfortunately there is no similar data at 30^{o}S. We introduce instead the assumption that v at 30^{o}S is statistically independent of v at 30^{o}N, but is otherwise statistically identical to the latter. A detailed discussion on how to formulate and compute the statistical boundary conditions is given in Section 4.

Some type of dissipative mechanism must be incorporated, or else the possibility of having resonance may render impossible the existence of a statistically stationary state. We will use three simple types of parameterised dissipation. Two are frictional; an internal friction at the middle level and surface friction at the lower level. The former is assumed to be proportional to the shear of the velocity perturbation and the latter proportional to the velocity perturbation itself. The third is a simple radiational cooling, proportional to the temperature perturbation. Three empirical proportional constants must therefore be chosen.

We finally come to the problem of choosing a time and zonally averaged basic state. The choice is made on the basis of published in-

formation about the mean state of the tropical atmosphere. Let us first consider the static stability defined as $-\frac{T}{\Theta}\frac{\partial \Theta}{\partial p}$. It is generally recognised that this quantity does not vary significantly from low to middle latitudes. Table 1 shows the value of this quantity for the atmospheric layer, 750-250 mb, from several sources.

January	July	Average	Source
.0545	.0472	.0508	U.S. (Gates, 1961)
		.0493	U.S. standard atmosphere
		.0515	West Indies (Jordan, 1958)

Table 1. $-\frac{T}{\Theta}\frac{\partial \Theta}{\partial p}$ in deg mb^{-1}.

A value of .050 deg mb^{-1} is chosen for $-\frac{T}{\Theta}\frac{\partial \Theta}{\partial p}$ in the model tropics. The two-layer model to be developed in Section 3 contains internal gravity waves as one mode of oscillation. In the absence of rotation and zonal current, their phase speed is given by

$$c_g = \sqrt{\frac{-RT}{\Theta}\frac{\partial \Theta}{\partial p}\frac{p_0}{4}} = 60 \quad m\ sec^{-1}$$

We next consider the choice of an averaged zonal velocity. Table 2 shows the zonal velocities obtained by Palmen (1963) and by Obasi (1963) for the northern and southern hemispheres respectively.

Pressure mb / Latitude	200	500	850
30^{o}N	20.0	10.0	2.0
20	10.0	3.0	-1.0
10	0.0	-2.0	-4.0
0	-4.0	-2.5	-4.0
Average	6.5	2.1	-1.8
30^{o}S	29.6	11.2	2.2
20	17.8	5.6	-1.9
10	4.5	-1.0	-3.5
0	0.4	-4.5	-3.3
Average	13.0	2.8	-3.2

Table 2. Zonal velocities in m sec^{-1}.

It should be pointed out that Palmen's values are based on Crutcher's data (1959) which is considerably more abundant than that which was available to Obasi. The northern hemispheric values may therefore be more reliable than the southern hemispheric values. In any case, within the uncertainty margin of the two sets of values, we may say that the zonal wind is by and large symmetrical about the equator. There is a vertical as well as a horizontal shear. However, we will only incorporate the vertical shear in our basic state, and choose uniform values of 8 m sec^{-1} and -2 m sec^{-1} for the basic zonal current at the 250- and 750-mb levels.

The omission of lateral shear gives some simplification in the analysis. However it was omitted primarily to eliminate lateral shear as a source of wave energy in the tropics and to focus attention on the amount of energy that would appear in the absence of this source. The zonally averaged geopotential and temperature fields are taken as in geostrophic balance with the prescribed zonal wind.

The effect of a mean meridional circulation in the basic state on the asymmetric motion will be disregarded. The reasons for this simplification are that the present model is too crude to incorporate these effects and the actual meridional circulation is not well determined.

3. Formulation of an analysis for stochastic perturbations

Before we proceed to a mathematical formulation, it may be helpful to have a brief discussion of exactly what we mean by stochastic motion in our context. The concept of ensemble developed in studies of probability seems to be necessary in this discussion. An ensemble may be thought of as a collection of individual realisations of which we have only partial knowledge. Now let us imagine an infinite number of models as the one described in Section 2. The fluid in each of these models is subject to lateral forcings of same amplitude but randomly different phase. (Precise discussion will be given in Section 4 about the terms, "amplitude" and "phase".) The circulation in each model is then a realisation. Because of the randomly different phase in the forcings, each realisation is then naturally different from others in detail. But one may suspect that since the "amplitude" of the forcings in the ensemble are the same, there may be some properties common to all realisations. Our problem is to deduce these properties which can be properly called ensemble-average properties.

3.1 Perturbation spectral equations

We may make one definite statement about the realisations discussed above. It is that each realisation, however indeterministic it may be, must not violate the known physical laws that describe the dynamical and thermodynamical processes. Hence the stochastic process must be governed by equations (2.1). Let us first write (2.1) with an

equatorial β-plane on a Mercator projection, i.e. with (2.3), in a non-dimensional form using $(2\Omega)^{-1}$, a and p_0 (=1000 mb) as time, length and pressure units. We define:

$$
\begin{aligned}
(u', v') &= \frac{1}{2\Omega a}(u, v) \\
\omega' &= \frac{\omega}{2\Omega p_0} \\
\phi' &= \frac{\phi}{(2\Omega a)^2} \\
\vec{F}' &= \frac{\vec{F}}{4\Omega^2 a} \\
\epsilon &= \frac{-RT}{(2\Omega a)^2}\frac{\partial \ln \Theta}{\partial p}\frac{p_0}{4} \\
Q' &= \frac{\kappa Q}{8\Omega^3 a^2} \\
t' &= 2\Omega t \\
p' &= \frac{p}{p_0}
\end{aligned}
\qquad (3.1)
$$

For simplicity we will now omit the prime superscript in the following equations.

$$\frac{\partial u}{\partial t} + u\frac{\partial u}{\partial x} + v\frac{\partial u}{\partial y} + \omega\frac{\partial u}{\partial p} = -\frac{\partial \phi}{\partial x} + yv + F_x$$

$$\frac{\partial v}{\partial t} + u\frac{\partial v}{\partial x} + v\frac{\partial v}{\partial y} + \omega\frac{\partial v}{\partial p} = -\frac{\partial \phi}{\partial y} - yu + F_y$$

$$\frac{\partial \omega}{\partial p} + \frac{\partial u}{\partial x} + \frac{\partial v}{\partial y} = 0 \qquad (3.2)$$

$$\left(\frac{\partial}{\partial t} + u\frac{\partial}{\partial x} + v\frac{\partial}{\partial y}\right)\left(\frac{\partial \phi}{\partial p}\right) + \frac{4}{p}\omega\epsilon = \frac{-Q}{p}$$

The range of the independent variables are

$$0 \leq x \leq 2\pi$$

$$-Y \leq y \leq Y \quad ; \quad Y = \ln\left(\frac{1+\sin 30^\circ}{\cos 30^\circ}\right) = 0.548$$

$$0 \leq p \leq 1$$

$$-\infty < t < \infty$$

t = 1 is equal to 12 hours.

The basic features of the two-layer model tropics are summarized in Fig. 1.

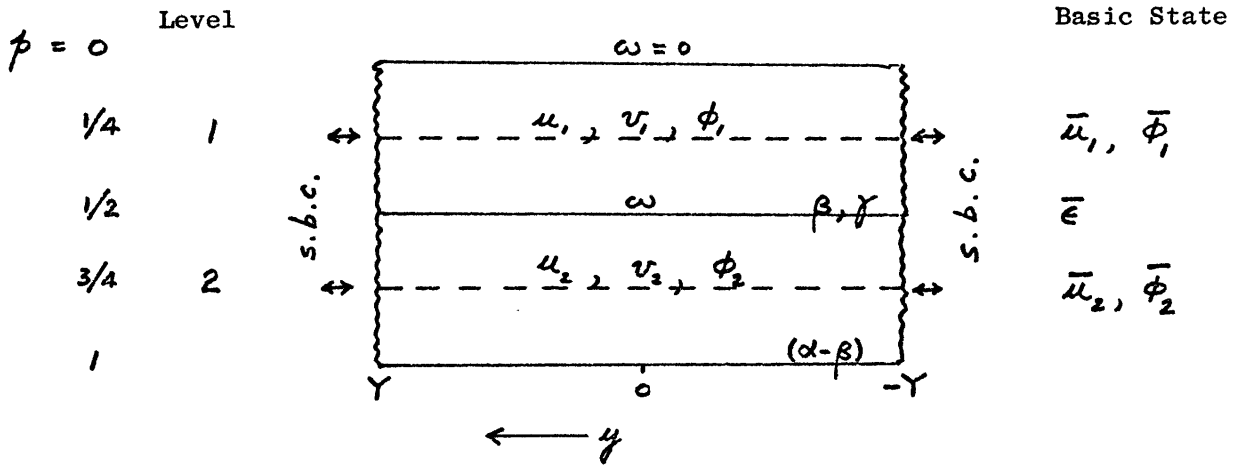

↔ s.b.c. stands for statistical boundary conditions

Figure 1. Model tropics

The numerical values of the basic state are:

$$\bar{u}_1 = \frac{8 \text{ m sec}^{-1}}{2\Omega a} = .0086$$

$$\bar{u}_2 = \frac{-2 \text{ m sec}^{-1}}{2\Omega a} = -.00215$$

$$\bar{u} = \tfrac{1}{2}(\bar{u}_1 + \bar{u}_2) \qquad (3.3)$$

$$\Lambda = \tfrac{1}{2}(\bar{u}_1 - \bar{u}_2)$$

$$\bar{\epsilon} = \left(\frac{c_g}{2\Omega a}\right)^2 = 4.16 \times 10^{-3}$$

$$\frac{d\bar{\phi}_1}{dy} = -y\bar{u}_1 \quad , \quad \frac{d\bar{\phi}_2}{dy} = -y\bar{u}_2$$

The horizontal momentum equations are each written at levels 1 and 2. The vertical advection term in these equations is written using the assumption $(\vec{V})_{p=\frac{1}{2}} = \frac{1}{2}(\vec{V}_1 + \vec{V}_2)$ in the following way.

$$\left(\omega \frac{\partial \vec{V}}{\partial p}\right)_1 = \left(\frac{\partial \omega \vec{V}}{\partial p} - \vec{V}\frac{\partial \omega}{\partial p}\right)_1$$

$$= 2(\vec{V}_{p=\frac{1}{2}} - \vec{V}_1)\omega_{p=\frac{1}{2}}$$

$$= (\vec{V}_2 - \vec{V}_1)\omega_{p=\frac{1}{2}}$$

Similarly

$$\left(\omega \frac{\partial \vec{V}}{\partial p}\right)_2 = (\vec{V}_2 - \vec{V}_1)\omega_{p=\frac{1}{2}}$$

By using the boundary conditions $\omega = 0$ at $p = 0$ and $p = 1$ we write the continuity equation as follows.

$$\omega_{p=\frac{1}{2}} = -\frac{1}{2}\nabla\cdot\vec{V}_1 = \frac{1}{2}\nabla\cdot\vec{V}_2 \qquad (3.4)$$

The thermodynamic equation is written at $p = \frac{1}{2}$ by treating ϵ at this level as a given constant.

The linearized version of the resulting equations, in which u_1, v_1, u_2, v_2 and ϕ_1, ϕ_2 now denote the perturbation variables, is:

$$\frac{\partial u_1}{\partial t} + (\bar{u}+\Lambda)\frac{\partial u_1}{\partial x} + \Lambda\left(\frac{\partial u_1}{\partial x} + \frac{\partial v_1}{\partial y}\right) = -\frac{\partial \phi_1}{\partial x} + y v_1 + \beta(u_2 - u_1)$$

$$\frac{\partial v_1}{\partial t} + (\bar{u}+\Lambda)\frac{\partial v_1}{\partial x} = -\frac{\partial \phi_1}{\partial y} - y u_1 + \beta(v_2 - v_1)$$

$$\frac{\partial u_2}{\partial t} + (\bar{u}-\Lambda)\frac{\partial u_2}{\partial x} - \Lambda\left(\frac{\partial u_2}{\partial x} + \frac{\partial v_2}{\partial y}\right) = -\frac{\partial \phi_2}{\partial x} + y v_2 + \beta u_1 - \alpha u_2$$

$$\frac{\partial v_2}{\partial t} + (\bar{u}-\Lambda)\frac{\partial v_2}{\partial x} = -\frac{\partial \phi_2}{\partial y} - y u_2 + \beta v_1 - \alpha v_2 \qquad (3.5)$$

$$\frac{\partial u_1}{\partial x} + \frac{\partial u_2}{\partial x} + \frac{\partial v_1}{\partial y} + \frac{\partial v_2}{\partial y} = 0$$

$$\left(\frac{\partial}{\partial t} + \bar{u}\frac{\partial}{\partial x}\right)(\phi_2 - \phi_1) + \Lambda y (v_1 + v_2) - 2\bar{\epsilon}\left(\frac{\partial u_1}{\partial x} + \frac{\partial v_1}{\partial y}\right) = -\gamma(\phi_2 - \phi_1)$$

$\omega_{p=\frac{1}{2}}$ has been eliminated by using (3.4). The frictional and heating effects have been parameterized by linear laws:

$$\vec{F}_1 = -\beta(\vec{V}_1 - \vec{V}_2)$$

$$\vec{F}_2 = \beta(\vec{V}_1 - \vec{V}_2) - (\alpha-\beta)\vec{V}_2$$

$$Q = -\gamma(\phi_1 - \phi_2)$$

β represents a small-scale vertical exchange of horizontal momentum between levels 1 and 2; $(\alpha-\beta)$ represents a surface drag coefficient; and γ can be thought of as a very crude representation of radiative cooling. The numerical values assigned to them were taken from Charney (1959).

$$\beta = 0.343 \times 10^{-2}$$

$$\alpha - \beta = 2.74 \times 10^{-2}$$

$$\gamma = 0.206 \times 10^{-2}$$

They correspond to decay times of 23, 6 and 39 days, respectively.

The x-dependence in (3.5) can be represented by a Fourier series expansion for each dependent variable. Thus, if the subscript $\ell = 1$ or 2 represents the pressure level, we write

$$v_\ell(x,y,t) = \sum_{n=1}^{\infty}\left[\mathcal{C}_\ell(y,t;n)\cos nx + \mathcal{S}_\ell(y,t;n)\sin nx\right]$$

$$= \mathrm{Re}\left\{\sum_{n=1}^{\infty} V_\ell(y,t;n)\, e^{inx}\right\} \tag{3.6}$$

where

$$V_\ell = \mathcal{C}_\ell - i\mathcal{S}_\ell$$

n is the zonal wave number. In the same way we have

$$u_\ell = \mathrm{Re}\left\{\sum_{n=1}^{\infty} \mathcal{U}_\ell\, e^{inx}\right\}$$

$$\phi_\ell = \mathrm{Re}\left\{\sum_{n=1}^{\infty} \mathcal{P}_\ell\, e^{inx}\right\}$$

In order to formulate our statistical boundary value problem, we must seek a spectral representation for the time variability of the six random functions, $\mathcal{U}_\ell$, $\mathcal{V}_\ell$ and $\mathcal{P}_\ell$, and their derivatives. A mathematical theory exists which permits us to do so under a mild condition. A thorough exposition of it can be found in Yaglom (1962). It is sometimes referred to as correlation theory, because it is developed only for examining the second moments of stationary random functions. According to this theory, if each of the six functions has a unique non-negative definite auto-correlation function which is at least twice differentiable with respect to the lag at zero lag, then each of them and their time derivatives has a spectral representation. The spectral representation is in the form of Fourier-Stieltjes integrals and their inverse integrals. We postulate that this condition is valid for the random functions in our model. In Yaglom's terminology, we define a random point function $Z(\sigma)$ for each of the six stationary random functions $\xi(t)$:

$$
\begin{aligned}
\xi(t) &= \int_{-\infty}^{\infty} e^{i\sigma t}\, dZ \\
Z(\sigma) &= \lim_{T\to\infty} \frac{1}{2\pi} \int_{-T}^{T} \frac{e^{-i\sigma t}-1}{-it}\, \xi(t)\, dt \\
\frac{d\xi}{dt} &= \int_{-\infty}^{\infty} e^{i\sigma t}\, i\sigma\, dZ \\
dZ &\equiv Z(\sigma+\Delta\sigma) - Z(\sigma)
\end{aligned}
\qquad (3.7)
$$

The identification is:

$$\xi : \mathcal{U}_\ell , \mathcal{V}_\ell , \mathcal{P}_\ell , \mathcal{C}_\ell , \mathcal{S}_\ell$$

$$Z : U_\ell , V_\ell , P_\ell , C_\ell , S_\ell$$

The spectral form of the definition (3.6) is

$$dV_\ell = dC_\ell - i\, dS_\ell$$

Since $dC_\ell(-\sigma) = dC_\ell^*(\sigma)$ and $dS_\ell(-\sigma) = dS_\ell^*(\sigma)$

(where * denotes complex conjugate),

we obtain

$$dC_\ell(\sigma) = \frac{1}{2}\left[dV_\ell(\sigma) + dV_\ell^*(-\sigma)\right]$$

$$dS_\ell(\sigma) = \frac{1}{2}\left[dV_\ell(\sigma) - dV_\ell^*(-\sigma)\right] \qquad (3.8)$$

We substitute the Fourier series expansion (3.6) into (3.5) and then take the Fourier-Stieltjes integral of the resulting equations according to (3.7). The following equations result, governing the increment dZ of these six random point functions.

$$
\begin{aligned}
(s+2n\Lambda-i\beta)\,dU_1 - i(\Lambda D-y)\,dV_1 + i\beta\,dU_2 &= -n\,dP_1 \\
y\,dU_1 + i(s+n\Lambda-i\beta)\,dV_1 - \beta\,dV_2 &= -D\,dP_1 \\
(s-2n\Lambda-i\alpha)\,dU_2 + i(\Lambda D+y)\,dV_2 + i\beta\,dU_1 &= -n\,dP_2 \\
y\,dU_2 + i(s-n\Lambda-i\alpha)\,dV_2 - \beta\,dV_1 &= -D\,dP_2 \\
n\,dU_1 + n\,dU_2 - iD\,dV_1 - iD\,dV_2 &= 0 \\
2\bar{\epsilon}n\,dU_1 - i(2\bar{\epsilon}D-\Lambda y)\,dV_1 + i\Lambda y\,dV_2 &= (s-i\gamma)(dP_2-dP_1)
\end{aligned}
\tag{3.9}
$$

where

$\frac{s}{n} = \bar{u} + \frac{\sigma}{n}$ is the longitudinal phase speed relative to the vertically averaged basic flow, and

$D \equiv \frac{d}{dy}$ is the latitudinal derivative operator at constant n and σ .

The six spectral equations in (3.9) can be reduced to two coupled equations by the relatively straightforward but algebraically involved procedure described in Appendix A. The final perturbation spectral equations governing dV_1 and dV_2 are:

$$
\begin{aligned}
L_1\{dV_1\} + L_2\{dV_2\} &= 0 \\
L_3\{dV_1\} + L_4\{dV_2\} &= 0
\end{aligned}
\tag{3.10}
$$

where L_j ($j = 1,2,3,4$) are second-order operators in y .

$$L_j = a_j \frac{d^2}{dy^2} + b_j\, y \frac{d}{dy} + c_j + d_j\, y^2$$

a_j , b_j , c_j and d_j are functions of the parameters. dV_1 and dV_2 are related to dU_1 , dU_2 , dP_1 and dP_2 as follows.

$$\begin{aligned} dU_2 &= M_1\{dV_1\} + M_2\{dV_2\} \\ dU_1 &= A_1\, dU_2 + M_3\{dV_1\} + M_4\{dV_2\} \\ dP_1 &= A_2\, dU_1 + A_3\, dU_2 + M_5\{dV_1\} \\ dP_2 &= A_3\, dU_1 + A_4\, dU_2 + M_6\{dV_2\} \end{aligned} \tag{3.11}$$

where A_j $(j=1,\cdots,4)$ are functions of the parameters and are independent of y , and M_m $(m=1,\cdots,6)$ are first order differential operators in y .

3.2 Fundamental solutions

Equations (3.10) and the associated relations (3.11) have as dependent variables the increments dZ of the six random point functions Z . The boundary conditions at $y = \pm Y$ are formally in terms of $dV_{l\pm}$ which cannot be uniquely specified. In this sense our problem is fundamentally different from the usual boundary value problem

where the dependent variables and boundary conditions are deterministic quantities. Nevertheless it will be shown that the formal properties of (3.10) play an important role in determining the response of the model to statistically prescribed forcing. We therefore first consider the derivation of the fundamental solutions which is based on the formal properties of (3.10). The manipulation of the resulting form of statistically indeterminate solutions to give determinate statistics will then be considered in the following subsection, with the aid of the Wiener-Khintchin theorem.

The operators L_j ($j = 1,2,3,4$) in (3.10) are second-order differential operators, and are even operators with respect to y . These facts imply that each of dV_1 and dV_2 must have four independent solutions, two of which are even functions of y and two of which are odd functions of y . The solutions can therefore be written in the following symbolic form,

$$dV_1 = \sum_{j=1}^{4} \beta_j w_j(y)$$
$$dV_2 = \sum_{j=1}^{4} \beta_j r_j(y) \qquad (3.12)$$

where β_j are constants of integration. Without loss of generality, let us consider w_1 , w_2 , r_1 , r_2 as even solutions and w_3 , w_4 , r_3 , r_4 as odd solutions. The constants of integration are related as usual to the boundary values of the eight dependent solutions and $dV_{l\pm}$.

The boundary relations are

$$\beta_1 = \frac{1}{2(r_{2+}w_{1+} - w_{2+}r_{1+})}\left[r_{2+}(dV_{1+} + dV_{1-}) - w_{2+}(dV_{2+} + dV_{2-})\right]$$

$$\beta_2 = \frac{1}{2(r_{2+}w_{1+} - w_{2+}r_{1+})}\left[-r_{1+}(dV_{1+} + dV_{1-}) + w_{1+}(dV_{2+} + dV_{2-})\right] \qquad (3.13)$$

$$\beta_3 = \frac{1}{2(r_{4+}w_{3+} - r_{3+}w_{4+})}\left[r_{4+}(dV_{1+} - dV_{1-}) - w_{4+}(dV_{2+} - dV_{2-})\right]$$

$$\beta_4 = \frac{1}{2(r_{4+}w_{3+} - r_{3+}w_{4+})}\left[-r_{3+}(dV_{1+} - dV_{1-}) + w_{3+}(dV_{2+} - dV_{2-})\right]$$

where subscript $\pm$ again indicates functions evaluated at $y = \pm Y$.

If we substitute (3.13) into (3.12) and rearrange the terms, we would then be able to write the solutions in the following form

$$dV_1 = \sum_{j=1}^{4} d\alpha_j \hat{V}_1^j(y)$$

$$dV_2 = \sum_{j=1}^{4} d\alpha_j \hat{V}_2^j(y) \qquad (3.14)$$

where

$$
\begin{aligned}
d\alpha_1 &= dV_{1+} + dV_{1-} \\
d\alpha_2 &= dV_{2+} + dV_{2-} \\
d\alpha_3 &= dV_{1+} - dV_{1-} \\
d\alpha_4 &= dV_{2+} - dV_{2-}
\end{aligned}
\tag{3.14a}
$$

$$
\begin{aligned}
\hat{V}_1^1 &= 0.5\,(r_{2+}w_{1+} - r_{1+}w_{2+})^{-1}(r_{2+}w_1 - r_{1+}w_2) \\
\hat{V}_1^2 &= 0.5\,(r_{2+}w_{1+} - r_{1+}w_{2+})^{-1}(-w_{2+}w_1 + w_{1+}w_2) \\
\hat{V}_1^3 &= 0.5\,(r_{4+}w_{3+} - w_{4+}r_{3+})^{-1}(r_{4+}w_3 - r_{3+}w_4) \\
\hat{V}_1^4 &= 0.5\,(r_{4+}w_{3+} - w_{4+}r_{3+})^{-1}(-w_{4+}w_3 + w_{3+}w_4) \\
\hat{V}_2^1 &= 0.5\,(r_{2+}w_{1+} - r_{1+}w_{2+})^{-1}(r_{2+}r_1 - r_{1+}r_2) \\
\hat{V}_2^2 &= 0.5\,(r_{2+}w_{1+} - r_{1+}w_{2+})^{-1}(-w_{2+}r_1 + w_{1+}r_2) \\
\hat{V}_2^3 &= 0.5\,(r_{4+}w_{3+} - w_{4+}r_{3+})^{-1}(r_{4+}r_3 - r_{3+}r_4) \\
\hat{V}_2^4 &= 0.5\,(r_{4+}w_{3+} - w_{4+}r_{3+})^{-1}(-w_{4+}r_3 + w_{3+}r_4)
\end{aligned}
$$

The superscript j of the solutions $\hat{V}_1^j$ and $\hat{V}_2^j$ are chosen such that $\hat{V}_1^1$ and $\hat{V}_2^1$ are to satisfy (3.10) simultaneously, and similarly for pairs where $j = 2,3,4$. Furthermore it is easy to see from their definitions that $\hat{V}_1^j$ and $\hat{V}_2^j$ are either equal to 0.0 or 0.5 at $y = Y$; and because of their even or odd properties

another condition for each of them can be specified at $y = 0$. The boundary conditions for them are summarized in Table 3.

j	y = 0		y = Y	
	$\hat{V}_1^j$	$\hat{V}_2^j$	$\hat{V}_1^j$	$\hat{V}_2^j$
1	d/dy = 0	d/dy = 0	0.5	0.0
2	d/dy = 0	d/dy = 0	0.0	0.5
3	0.0	0.0	0.5	0.0
4	0.0	0.0	0.0	0.5

Table 3.

The fundamental solutions $\hat{V}_1^j$ and $\hat{V}_2^j$ can then be obtained by solving the governing equations (3.10) four times using the four different sets of boundary conditions summarized in Table 3.

The statistical properties of dV_1 and dV_2 are now contained only in the $d\alpha_j$, whereas $\hat{V}_\ell^j$ are deterministic functions and will be referred to as the fundamental solutions.

The general solutions for dU_ℓ and dP_ℓ , $\ell = 1, 2$, associated with those for dV_ℓ in (3.14) are

$$dU_\ell = \sum_{j=1}^{4} d\alpha_j \hat{U}_\ell^j$$

$$dP_\ell = \sum_{j=1}^{4} d\alpha_j \hat{P}_\ell^j \qquad (3.15)$$

$\hat{U}_\ell^j$, $\hat{P}_\ell^j$ are related to $\hat{V}_\ell^j$ for each j in the same way that dU_ℓ and dP_ℓ are related to dV_ℓ in equations (3.11).

3.3 Response functions for second moment statistics

A theorem for stationary random functions known as Wiener-Khintchin theorem will be applied in the following argument. It consists of a set of interlocking equations relating the correlation function $\varphi_{\xi\eta}(\tau)$ of two stationary random functions $\xi(t)$ and $\eta(t)$ to the associated random point functions $Z(\sigma)$ and $W(\sigma)$ through a quantity known as the spectral density functions $\Phi_{\xi\eta}(\sigma)$. It is stated below for the sake of reference.

$$\varphi_{\xi\eta}(\tau) = \lim_{T\to\infty} \frac{1}{2T}\int_{-T}^{T} \xi(t)\,\eta(t-\tau)\,dt$$

$$\Phi_{\xi\eta}(\sigma) = \frac{1}{2\pi}\int_{-\infty}^{\infty} \varphi_{\xi\eta}(\tau)\, e^{-i\sigma\tau}\, d\tau \qquad (3.16)$$

$$\langle dZ\, dW^* \rangle = \Phi_{\xi\eta}(\sigma)\,\Delta\sigma$$

$$\therefore\ \varphi_{\xi\eta}(\tau) = \int_{-\infty}^{\infty} e^{i\sigma\tau} \langle dZ\, dW^* \rangle$$

dZ and dW are related to ξ and η respectively by the definitions (3.7). The symbol $\langle\ \rangle$ is an ensemble average operator.

The first statement in (3.16) contains the ergodic hypothesis. The only other assumption involved in this theorem is that the correlation function is integrable, which is invariably true in all known physical situations. Thus we postulate this mild condition for the statistical forcing in this study.

For clarity let us consider a particular correlation function, namely the zonally averaged correlation function between $v_1(t,x)$ and $v_2(t,x)$. An overbar will represent an x-average. By direct substitution from the Fourier series representation (3.6) of v_1 and v_2, we obtain

$$\langle \overline{v_1 v_2} \rangle = \sum_{n=1}^{\infty} \frac{1}{2}\left[\varphi_{\epsilon_1\epsilon_2}(\tau) + \varphi_{\sigma_1\sigma_2}(\tau) \right] \tag{3.17}$$

The subscripts on φ denote $\xi = \epsilon_1$, $\eta = \epsilon_2$; $\xi = \sigma_1$, $\eta = \sigma_2$ in the definition (3.16) of $\varphi_{\xi\eta}$. The dependence of ϵ and σ on n is not denoted explicitly. By the Wiener-Khintchin theorem, we can write (3.16) when $\tau = 0$ as:

$$\langle \overline{v_1 v_2} \rangle = \sum_{n=1}^{\infty} \frac{1}{2} \int_{-\infty}^{\infty} \left[\langle dC_1 dC_2^* \rangle + \langle dS_1 dS_2^* \rangle \right] . \tag{3.18}$$

<u>It will now be assumed, without further specification, that all variances refer to x-averaged expressions and the overbar will be omitted for convenience.</u>

By using (3.8) we can rewrite (3.17) as

$$\langle v_1 v_2 \rangle = \sum_{n=1}^{\infty} \frac{1}{4} \int_{-\infty}^{\infty} \langle dV_1(\sigma)\, dV_2^*(\sigma) \rangle + \langle dV_1^*(-\sigma)\, dV_2(-\sigma) \rangle \tag{3.19}$$

It is clear that the integrand at negative value of σ is equal to its complex conjugate at positive value of σ . Because of this symmetry in frequency (3.19) can be written as

$$\langle v_1 v_2 \rangle = \sum_{n=1}^{\infty} \frac{1}{2} \int_{-\infty}^{\infty} \mathcal{R}_e \{ \langle dV_1\, dV_2^* \rangle \} \tag{3.20}$$

The reason for this symmetry is simple. It arises from our choice of dealing with two-sided spectra, i.e. for both positive and negative frequency. But as far as the covariance is concerned, there is no physical difference between positive and negative frequency and thus contributions from them are necessarily equal.

Substituting the general solutions for dV_ℓ in the form of (3.4), we obtain

$$\langle v_1 v_2 \rangle = \frac{1}{2} \sum_{n=1}^{\infty} \int_{-\infty}^{\infty} \mathcal{R}_e \left\{ \sum_{j=1}^{4} \sum_{m=1}^{4} \langle d\alpha_j \hat{V}_1^j\, d\alpha_m^* \hat{V}_2^{m*} \rangle \right\}$$

$$= \frac{1}{2} \sum_{n=1}^{\infty} \int_{-\infty}^{\infty} \mathcal{R}_e \left\{ \sum_{j=1}^{4} \sum_{m=1}^{4} \hat{V}_1^j \hat{V}_2^{m*} \langle d\alpha_j\, d\alpha_m^* \rangle \right\} \tag{3.21}$$

That the $\hat{V}_\ell^i$ are deterministic functions makes possible the last step which is critical in this analysis.

The $d\alpha_j$ are given by the boundary values of dV_ℓ at $y = \pm Y$, as defined in (3.14). By the third statement in (3.15), each of the 16 $\langle d\alpha_j\, d\alpha_m^* \rangle$ can be expressed in the general form $\Phi^k d\sigma$ $k = 1,2,\ldots,16$, (3.21) thereby reduces to an expression of the general form

$$\langle v_1 v_2 \rangle = \int_{-\infty}^{\infty} \left[\sum_{n=1}^{\infty} \sum_{k=1}^{16} H^k(y,\sigma;n)\, \Phi^k(\sigma;n) \right] d\sigma \tag{3.22}$$

The $H^k(y,\sigma;n)$ play the role of the "response functions" (or "system functions") used in electrical systems. The square bracketed quantity is the spectrum for the covariance of v_1 and v_2, and we see that it is a superposition of the responses associated with the 16 "input" spectra Φ^k for each wavenumber n. This is the statement for our linear model of the general law that the "output" spectrum of a linear system is equal to the system function times the input spectrum

(3.21) can be generalized to determine other variances and covariances in the model. Let ξ and η denote any pair of the six variables v_ℓ, u_ℓ and ϕ_ℓ and let $\hat{Z}^i$ and $\hat{W}^i$ denote the corresponding deterministic solutions $\hat{V}_\ell^i$, $\hat{U}_\ell^i$ and $\hat{P}_\ell^i$ as formulated in (3.14a) and the statement following (3.15). Then the

general form of covariance is

$$\langle \xi \eta \rangle = \frac{1}{2} \sum_{n=1}^{\infty} \int_{-\infty}^{\infty} Re \left\{ \sum_{j=1}^{4} \sum_{m=1}^{4} \hat{Z}^{j} \hat{W}^{m*} \langle d\alpha_j \, d\alpha_m^* \rangle \right\}$$

(3.23)

4. Statistical boundary conditions

This section consists of three parts. The first part formulates a closed set of statistical boundary conditions for the spectral equations (3.10) on the basis that only v_1 and v_2 at 30°N are known for a sufficiently long period of time. The second part describes how the boundary statistics are actually computed. The third part gives a physical interpretation of the results obtained in this way.

4.1 Formulation

For the moment let us assume that a long record of observations of v_1 and v_2 at both 30°N and 30°S is available. We first expand each of these functions into Fourier series of longitude, truncated at a certain wavenumber N

$$v_{l+}(t,x) = \sum_{n=1}^{N} \left[\mathcal{C}_{l+}(t;n) \cos nx + \mathcal{S}_{l+}(t;n) \sin nx \right]$$
$$v_{l-}(t,x) = \sum_{n=1}^{N} \left[\mathcal{C}_{l-}(t;n) \cos nx + \mathcal{S}_{l-}(t;n) \sin nx \right] \qquad (4.1)$$

$l = 1,2$; subscript $\pm$ stands for $y = \pm Y$

As shown in (3.23), any second moment statistic in the model can be uniquely determined if the statistical boundary conditions (s.b.c.) are such that they enable $\langle d\alpha_j \, d\alpha_m^* \rangle$, $j = 1,2,3,4$; $m = 1,2,3,4$ to be evaluated. According to the definition of $d\alpha_j$ in (3.14a), the required s.b.c. for the governing spectral equations (3.10) are

$\langle dV_{l\pm}\, dV^*_{k\pm}\rangle$, $l=1,2$; $k=1,2$. They can be synthesized from $\langle dC_{l\pm}\, dC^*_{k\pm}\rangle$, $\langle dS_{l\pm}\, dS^*_{k\pm}\rangle$, $\langle dC_{l\pm}\, dS^*_{k\pm}\rangle$ and $\langle dS_{l\pm}\, dC^*_{k\pm}\rangle$, since dV_l is related to dC_l and dS_l by $dV_l = dC_l - i\, dS_l$. By the Wiener-Khintchin theorem (3.16), the s.b.c. for each wavenumber n can therefore be constructed from all the independent spectra

$$\Phi_{\mathcal{C}(l\pm)\,\mathcal{C}(k\pm)} \quad , \quad \Phi_{\mathcal{S}(l\pm)\,\mathcal{S}(k\pm)} \quad , \quad \Phi_{\mathcal{C}(l\pm)\,\mathcal{S}(k\pm)} \quad , \quad \Phi_{\mathcal{S}(l\pm)\,\mathcal{C}(k\pm)}$$

These spectra can be obtained if $v_{l\pm}$, and thus $\mathcal{C}_{l\pm}$ and $\mathcal{S}_{l\pm}$ as defined in (4.1), is available. But as pointed out in Section 2, only observations for v_{l+} are available in detail sufficient for the Fourier expansion (4.1). The simplest and perhaps the most reasonable way to overcome this handicap is to assume that v_{l-} is statistically independent of v_{l+} , but is otherwise statistically similar to the latter. This is just a working assumption. The first part of the assumption is not unreasonable because there is unlikely to be significant correlation between the baroclinic activities at the mid-latitudes of the two hemispheres, which after all are primarily responsible for the flows near 30°N and 30°S. The second part of the assumption is reasonable only to the extent that hemispheric symmetry is a sufficiently good approximation. It cannot be rigorously justified, since topological differences do exist between the two hemispheres.

Much of the interhemispheric statistical difference presumably is expressed in seasonal fluctuations. Our detailed analysis, however, will consider only periods between 3 days and about 3 months. Therefore the assumption of symmetry is not as weak as it appears. For consistency the basic state must also be symmetric, as has already been assumed.

An approach commonly used in deducing the response of a linear fluid system to localized excitation is the so-called "radiation" argument, in which only those wave solutions are used which give energy propagation away from the source to a sink at infinity. Our situation, however, is more complicated — we cannot, for example, separate the observations of v at $y = Y$ into a source function plus the effect of a transmitted northward energy-propagating wave from $y = -Y$. The simple analogue to our model is more like a box of water contained between walls at $y = \pm Y$, where two statistically similar but independent demons are oscillating the boundary walls.

Let us first consider the consequence of postulating statistically independent forcings at $y = \pm Y$. If two stationary random functions, $\xi(t)$ and $\eta(t)$ with zero mean are statistically independent, their correlation function will be identically zero:

$$\begin{aligned} \langle \xi\eta \rangle &= \int_{-\infty}^{\infty}\int_{-\infty}^{\infty} \xi_0\, \eta_0\, P_{\xi\eta}(\xi_0, \eta_0; \tau)\, d\xi_0\, d\eta_0 \\ &= \int_{-\infty}^{\infty} \xi_0\, P_{\xi}(\xi_0) d\xi_0 \int_{-\infty}^{\infty} \eta_0\, P_{\eta}(\eta_0) d\eta_0 \\ &= \langle \xi \rangle \langle \eta \rangle \\ &= 0 \end{aligned} \tag{4.2}$$

$P_{\xi\eta}(\xi_0, \eta_0; \tau)$ is the joint probability density for $\xi(t_1) = \xi_0$, $\eta(t_2) = \eta_0$ when $t_1 - t_2 = \tau$; $P_\xi(\xi_0)$ is the probability density for $\xi(t_1) = \xi_0$ and $P_\eta(\eta_0)$ is the probability density for $\eta(t_2) = \eta_0$. By the ergodic assumption, we then have

$$\varphi_{\xi\eta}(\tau) = \langle \xi\eta \rangle = \langle \xi \rangle \langle \eta \rangle = 0$$

Thus the assumption of statistically independent forcing at $y = \pm\gamma$ is formulated by

$$\left\langle \overline{v_{\ell+}(x,t)\, v_{k-}(x-\delta, t-\tau)} \right\rangle = 0 \tag{4.3}$$

By assuming that $v_{\ell+}$ is statistically similar to $v_{\ell-}$, we mean

$$\left\langle \overline{v_{\ell+}(x,t)\, v_{k+}(x-\delta, t-\tau)} \right\rangle = \left\langle \overline{v_{\ell-}(x,t)\, v_{k-}(x-\delta, t-\tau)} \right\rangle$$

for all δ and τ for $\ell = 1,2$ and $k = 1,2$

With (4.1) this can be written as

$$\left[\varphi_{c(\ell+)c(k+)} + \varphi_{s(\ell+)s(k+)}\right]\cos\delta n + \left[-\varphi_{c(\ell+)s(k+)} + \varphi_{s(\ell+)c(k+)}\right]\sin\delta n$$

$$= \left[\varphi_{c(\ell-)c(k-)} + \varphi_{s(\ell-)s(k-)}\right]\cos\delta n + \left[-\varphi_{c(\ell-)s(k-)} + \varphi_{s(\ell-)c(k-)}\right]\sin\delta n$$

Thus, the assumption of symmetric forcing amounts to assuming

(4.4)

$$\varphi_{c(\ell+)c(k+)} + \varphi_{s(\ell+)s(k+)} = \varphi_{c(\ell-)c(k-)} + \varphi_{s(\ell-)s(k-)}$$

$$-\varphi_{c(\ell+)s(k+)} + \varphi_{s(\ell+)c(k+)} = -\varphi_{c(\ell-)s(k-)} + \varphi_{s(\ell-)c(k-)}$$

By the Wiener-Khintchin theorem, (4.3) and (4.4) can then be written as

$$\langle dC_{l+}\, dC^*_{k-}\rangle + \langle dS_{l+}\, dS^*_{k-}\rangle = 0$$

$$\langle dC_{l+}\, dS^*_{k-}\rangle - \langle dS_{l+}\, dC^*_{k-}\rangle = 0$$

$$\langle dC_{l+}\, dC^*_{k+}\rangle = \Phi_{\mathcal{C}(l+)\,\mathcal{C}(k+)}\,\Delta\sigma \qquad (4.5)$$

$$\langle dS_{l+}\, dS^*_{k+}\rangle = \Phi_{\mathcal{S}(l+)\,\mathcal{S}(k+)}\,\Delta\sigma$$

$$\langle dC_{l+}\, dS^*_{k+}\rangle = \Phi_{\mathcal{C}(l+)\,\mathcal{S}(k+)}\,\Delta\sigma$$

$$\langle dS_{l+}\, dC^*_{k+}\rangle = \Phi_{\mathcal{S}(l+)\,\mathcal{C}(k+)}\,\Delta\sigma$$

$$\langle dC_{l-}\, dC^*_{k-}\rangle + \langle dS_{l-}\, dS^*_{k-}\rangle = \langle dC_{l+}\, dC^*_{k+}\rangle + \langle dS_{l+}\, dS^*_{k+}\rangle$$

$$\langle dC_{l-}\, dS^*_{k-}\rangle - \langle dS_{l-}\, dC^*_{k-}\rangle = \langle dC_{l+}\, dS^*_{k+}\rangle - \langle dS_{l+}\, dC^*_{k+}\rangle$$

for $l = 1, 2$; $k = 1, 2$

The statistical boundary conditions for (3.10) now reduce to

$$\langle dV_{\ell+}\, dV_{k-}^{*} \rangle = 0$$

together with the four real functions F_1 , F_2 , F_3 and F_4 :

$$F_\ell \equiv \langle |dV_{\ell+}|^2 \rangle = \langle |dV_{\ell-}|^2 \rangle \qquad \ell = 1, 2$$

$$= \left[\Phi_{\mathcal{C}_+ \mathcal{C}_+} + \Phi_{\mathcal{S}_+ \mathcal{S}_+} - 2\,\mathrm{Im}\left\{ \Phi_{\mathcal{C}_+ \mathcal{S}_+} \right\} \right]_\ell \Delta\sigma \tag{4.6}$$

$$F_3 + i F_4 \equiv \langle dV_{1+}\, dV_{2+}^{*} \rangle = \langle dV_{1-}\, dV_{2-}^{*} \rangle$$

$$= \left[\Phi_{\mathcal{C}_{1+} \mathcal{C}_{2+}} + \Phi_{\mathcal{S}_{1+} \mathcal{S}_{2+}} + i \left(\Phi_{\mathcal{C}_{1+} \mathcal{S}_{2+}} - \Phi_{\mathcal{S}_{1+} \mathcal{C}_{2+}} \right) \right] \Delta\sigma$$

With the definition of $d\alpha_j$ in (3.14a), the $\langle d\alpha_j\, d\alpha_m^{*} \rangle$ appearing in (3.23) can then be written as

$$\langle |d\alpha_1|^2 \rangle = \langle |d\alpha_3|^2 \rangle = 2F_1$$

$$\langle |d\alpha_2|^2 \rangle = \langle |d\alpha_4|^2 \rangle = 2F_2$$

$$\langle d\alpha_1\, d\alpha_2^{*} \rangle = \langle d\alpha_3\, d\alpha_4^{*} \rangle = 2(F_3 + iF_4) \tag{4.7}$$

$$\langle d\alpha_1^{*}\, d\alpha_2 \rangle = \langle d\alpha_3^{*}\, d\alpha_4 \rangle = 2(F_3 - iF_4)$$

$$\langle d\alpha_1^{*}\, d\alpha_3 \rangle = \langle d\alpha_1^{*}\, d\alpha_4 \rangle = \langle d\alpha_2^{*}\, d\alpha_3 \rangle = \langle d\alpha_2^{*}\, d\alpha_4 \rangle = 0$$

$$\langle d\alpha_1\, d\alpha_3^{*} \rangle = \langle d\alpha_1\, d\alpha_4^{*} \rangle = \langle d\alpha_2\, d\alpha_3^{*} \rangle = \langle d\alpha_2\, d\alpha_4^{*} \rangle = 0$$

Finally the general form of any covariance can be written upon substitution from (4.7) as

$$\langle \xi\eta \rangle = \sum_{n=1}^{12} \int_{-\infty}^{\infty} \sum_{j=1}^{4} H_{\xi\eta}^{j}(y, \sigma; n)\, F_j(\sigma; n) \qquad (4.8)$$

where

$$H_{\xi\eta}^{1} = \mathcal{R}e\left\{\hat{Z}^{1}\hat{W}^{1*} + \hat{Z}^{3}\hat{W}^{3*}\right\}$$

$$H_{\xi\eta}^{2} = \mathcal{R}e\left\{\hat{Z}^{2}\hat{W}^{2*} + \hat{Z}^{4}\hat{W}^{4*}\right\}$$

$$H_{\xi\eta}^{3} = \mathcal{R}e\left\{\hat{Z}^{1}\hat{W}^{2*} + \hat{Z}^{2}\hat{W}^{1*} + \hat{Z}^{3}\hat{W}^{4*} + \hat{Z}^{4}\hat{W}^{3*}\right\}$$

$$H_{\xi\eta}^{4} = \mathcal{I}m\left\{-\hat{Z}^{1}\hat{W}^{2*} + \hat{Z}^{2}\hat{W}^{1*} - \hat{Z}^{3}\hat{W}^{4*} + \hat{Z}^{4}\hat{W}^{3*}\right\}$$

4.2 Data analysis

The actual data used for computing the statistical boundary conditions (4.6) is the streamfunction field analysed ψ with the "balance equation" by the National Meteorological Center. [See Shuman, 1957.] The data is given in a stereographic grid system which covers the northern hemisphere north of about 15°N, twice daily at 00 and 12 GMT. Data for the period June 1963 through April 1965 for the 200-mb and 850-mb levels was made available to the writer by the National Center for Atmospheric Research.

A linear interpolation scheme was used to obtain the value of ψ at every 5 degrees of longitude along 30°N at each observation time. These 72 values were then resolved into Fourier components in longitude. In view of the relatively sparse network over the major oceans, the Fourier series was truncated after wavenumber 12. ψ_ℓ is non-dimensionalized as $\psi'_\ell = \psi_\ell / (2\Omega a^2)$, so that the dimensionless meridional velocity is $v_{\ell+} = \frac{1}{\cos 30^\circ} \frac{\partial \psi'_\ell}{\partial x}$. These Fourier coefficients for ψ'_ℓ are readily related to those for $v_{\ell+}$:

$$v_{\ell+}(t, x_j) = \sum_{n=1}^{12} \left[\mathcal{C}_{\ell+}(t;n) \cos n x_j + \mathcal{S}_{\ell+}(t;n) \sin n x_j \right] \tag{4.9}$$

Each of the time series $\mathcal{C}_{\ell+}$ and $\mathcal{S}_{\ell+}$ was next modified by having its time mean value removed. From now on, $\mathcal{C}_{\ell+}$ and $\mathcal{S}_{\ell+}$ refer to these zero time mean series.

There are four basic considerations in making spectral estimates from discrete time series — aliasing, spectral smoothing, resolution, and reliability requirements. The overriding objective in the actual spectral analysis in this study was to make a simple analysis that can adequately avoid the difficulties associated with each of the four considerations. A brief discussion is now given for each of them separately.

Resolution and reliability requirements

Because of the nature of our stream function data, we shall only examine the spectra in the frequency range $|\sigma| \leq \frac{1}{6}$ cycles per 12 hrs, corresponding to a minimum period of 3 days. On the other hand we want a fairly large number of frequency bands within this range so that we can examine the variation of the response spectra. For a record length of 1351 data points 12 hours apart, these two requirements can be met only at the price of having a minimum tolerable reliability. We therefore chose a maximum lag equal to 1/10 of the record length. A rough guess of the reliability of the spectral estimate is [Blackman and Tukey, 1958]:

$$\frac{\text{variance}\left\{\text{spectrum estimate}\right\}}{\left[\text{average}\left\{\text{spectrum estimate}\right\}\right]^2} \approx \frac{\text{maximum lag}}{\text{record length}} = \frac{1}{10}$$

In other words, the standard deviation of each estimate is about one third of its average value. If we assume the noise in the record as Gaussian, we may arrive at a more detailed estimate of the spectral variability in terms of the Chi-square distribution with 20 equivalent degrees of freedom. But the rough estimate given above is sufficient for error estimation. With our

choice of maximum lag, the spectral estimates are then calculated every $(270)^{-1}$ cycles per 12 hours and the resolution of the spectra is $(135)^{-1}$ cycles per 12 hours.

Spectral smoothing

This is a necessary procedure because it can be shown that the variability of a periodogram (raw estimate) does not decrease with increased record length. In general, the Hanning lag window is quite sufficient for smoothing, and was therefore used. But one additional caution must be made for this data because its spectra must have a strong component or line at the annual period. The smoothing procedure would diffuse some of the energy of this peak to higher frequencies. To overcome this a high-pass prefiltering was used. (The filter is described in Appendix C).

Aliasing

This is not a significant problem here for two reasons. First the high frequency components must be fairly weak in the streamfunction data since the NMC analysis has already incorporated some spatial smoothing and considerations of time continuity. Secondly the highest frequency of the spectra that we are interested in is equal to 1/6 which is three times smaller than the folding frequency, σ_c = 1/2 cycles per 12 hours. Nevertheless the filter that was used (Appendix C) was designed to filter out all components of periods less than $1\frac{1}{2}$ days as well as periods longer than 6 months.

Analysis

A direct method was used to obtain periodograms from the prefiltered time series. This method is based upon the fact that the spectrum of a time series may be expressed directly in terms of the series itself instead of via its correlation function (ref. Blackman and Tukey, 1958, pp 87-88) and it can be generalized for the cross spectrum of two time series. It is generally recommended in text books (Bendat and Piersol, 1966) that the periodogram should be only calculated at m discrete frequencies

$$\sigma_k = \frac{k\,\sigma_c}{m} = \frac{5k}{L}$$

where m = maximum lag number, L = record length = $10\,m$, $k = 1, \cdots, m$.

Then according to the direct method, the raw estimate of the cross spectrum of two time series $\xi(t)$ and $\eta(t)$ is given by

$$\hat{\Phi}_{\xi\eta}\left(\frac{5k}{L}\right) = \frac{L}{4}\left(A_{5k} - iB_{5k}\right)\left(\mathcal{A}_{5k} + i\,\mathcal{B}_{5k}\right) \qquad (4.10)$$

where A_{5k} and B_{5k} are the $(5k)^{th}$ Fourier cosine and sine coefficients of ξ, and $\mathcal{A}_{5k}$ and $\mathcal{B}_{5k}$ are the $(5k)^{th}$ Fourier cosine and sine coefficients of η.

A Hanning lag window is now used to smooth the $\hat{\Phi}$ obtained by (4.10), and the results of hanning is

$$\Phi\left(\frac{5k}{L}\right) = \frac{1}{4}\hat{\Phi}\left(\frac{5(k-1)}{L}\right) + \frac{1}{2}\hat{\Phi}\left(\frac{5k}{L}\right) + \frac{1}{4}\hat{\Phi}\left(\frac{5(k+1)}{L}\right)$$

$$\Phi\left(\frac{5}{L}\right) = \frac{1}{2}\left[\hat{\Phi}\left(\frac{5}{L}\right) + \hat{\Phi}\left(\frac{5(2)}{L}\right)\right]$$

$$\Phi\left(\frac{5m}{L}\right) = \frac{1}{2}\left[\hat{\Phi}\left(\frac{5(m-1)}{L}\right) + \hat{\Phi}\left(\frac{5m}{L}\right)\right] \qquad (4.11)$$

Finally in order to compensate for the attenuation introduced by the pre-filtering, the spectrum obtained by (4.11) is divided by the attenuation factor to give the final spectra. These spectra are then used to compute the statistical boundary conditions F_1 , F_2 , F_3 , F_4 in (4.6).

4.3 Results and interpretation

A complete listing of the four statistical boundary conditions for the frequency range $|\sigma| \leq \frac{1}{6}$ cycles per 12 hours for each of the 12 wavenumbers is given in Appendix D. A simple interpretation for F_1 , F_2 , F_3 and F_4 is now given in terms of the amplitudes and the relative phase of the wave motions at 200-mb and 850-mb levels.

$$v_{l+} = \sum_{n=1}^{12}\left[C_{l+}(t)\cos nx + S_{l+}(t)\sin nx\right] \qquad (4.12)$$

$$= \sum_{n=1}^{12}\int_{-\infty}^{\infty}\cos nx\, e^{i\sigma t}\, dC_{l+} + \int_{-\infty}^{\infty}\sin nx\, e^{i\sigma t}\, dS_{l+}$$

$$= \sum_{n=1}^{12}\int_{-\infty}^{\infty}\frac{1}{2}\left[e^{i(nx+\sigma t)}(dC_{l+} - i\,dS_{l+}) + e^{-i(nx-\sigma t)}(dC_{l+} + i\,dS_{l+})\right]$$

Since $dC_{\ell+}(-\sigma) = dC^{*}_{\ell+}(\sigma)$, $dS_{\ell+}(-\sigma) = dS^{*}_{\ell+}(\sigma)$, we then can rewrite (4.12) as

$$v_{\ell+} = Re\left\{\sum_{n=1}^{12}\int_{0}^{\infty}(dC_{\ell+}+i\,dS_{\ell+})\,e^{i(\sigma t-nx)} + (dC_{\ell+}-i\,dS_{\ell+})\,e^{i(nx+\sigma t)}\right\} \tag{4.13}$$

The first integrand in (4.13) represents an eastward traveling wave with an amplitude equal to $\left(\langle |dC_{\ell+}+i\,dS_{\ell+}|^2\rangle\right)^{\frac{1}{2}}$ whereas the second integrand represents a westward traveling wave with an amplitude equal to $\left(\langle |dC_{\ell+}-i\,dS_{\ell+}|^2\rangle\right)^{\frac{1}{2}}$. Since, for ℓ = 1 and 2,

$F_{\ell}(\sigma) = \langle |dV_{\ell+}(\sigma)|^2\rangle = \langle |dC_{\ell+} - i\,dS_{\ell+}|^2\rangle$ and

$F_{\ell}(-\sigma) = \langle |dV_{\ell+}(-\sigma)|^2\rangle = \langle |dC_{\ell+}(\sigma) + i\,dS_{\ell+}(\sigma)|^2\rangle$, the first two statistical boundary conditions F_1 and F_2 for each wavenumber n when evaluated at positive (negative) frequency can be interpreted as the square of the amplitude of a westward (eastward) traveling wave at levels 1 and 2. These spectra at n = 2, 4, 5, 7 and 11 are plotted in Figs. 2 and 3, which show that there is much more energy associated with the wave motions in the 200-mb level than in 850-mb. Most of the energy in F_1 as well as in F_2 belong to the intermediate wavenumbers 5, 6, 7 and 8. Furthermore, the spectra for low wavenumbers 1 to 4 have larger magnitude at positive frequency than at negative frequency, and the opposite is true for the higher wavenumber spectra. In other words, the waves of low zonal wavenumbers at 30°N are moving relatively more westward than

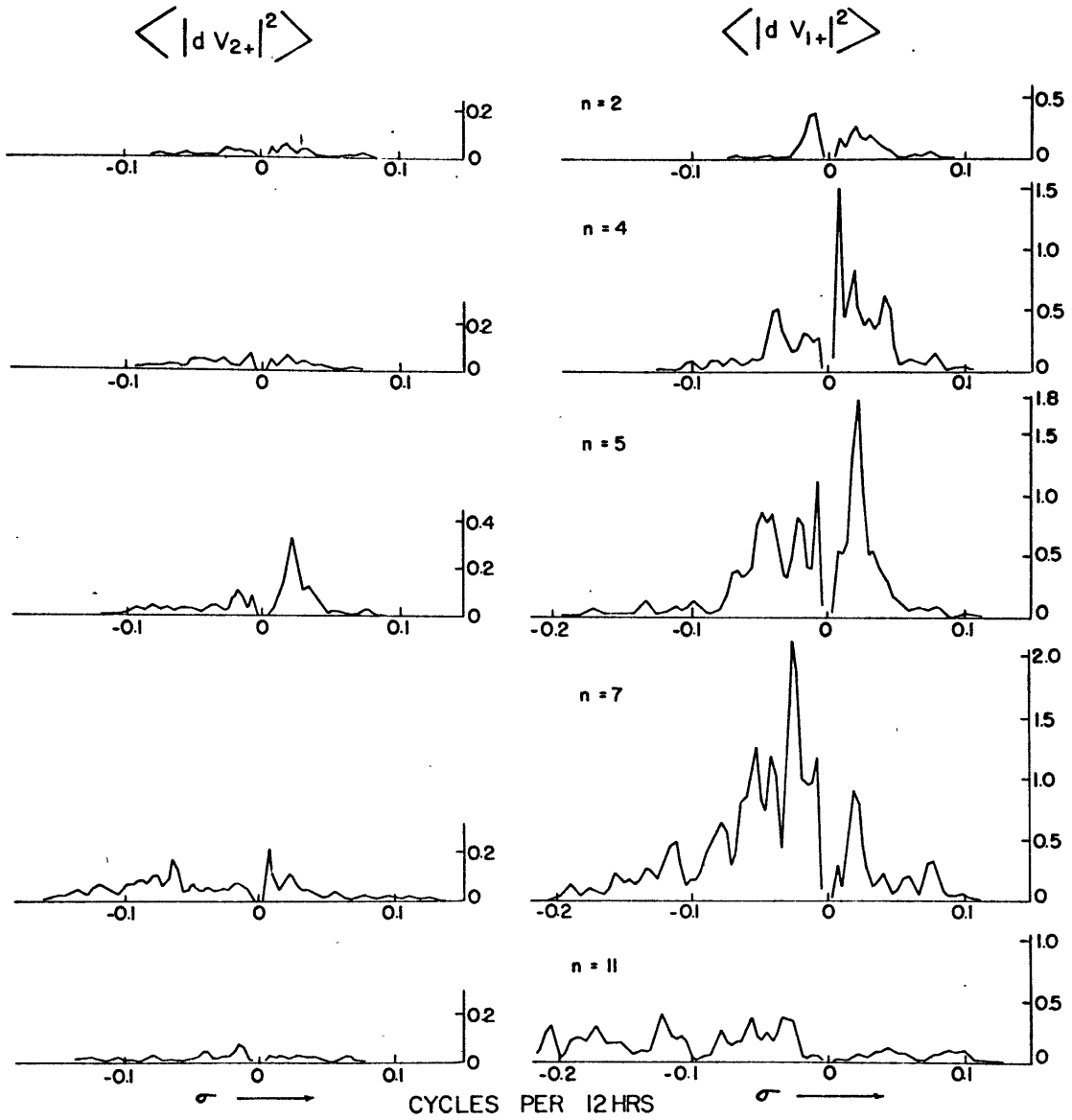

Fig. 2. $F_2 \equiv \langle |dV_{2+}|^2 \rangle$ in m^2 sec^{-2} for a frequency interval $(270)^{-1}$ cycles per 12 hrs centered at σ shown

Fig. 3. $F_1 \equiv \langle |dV_{1+}|^2 \rangle$ in m^2 sec^{-2} for a frequency interval $(270)^{-1}$ cycles per 12 hrs centered at σ shown

(for wavenumbers n = 2,4,5,7,11)

those of high wavenumbers. This is a well-known characteristic of the Rossby waves.

F_3 and F_4 can be interpreted as a measure of the relative phase between an upper level wave and a similar wave at lower level. This is perhaps best illustrated with a simple example. Consider two westward moving waves of different amplitude and phase but identical frequency σ_0 and wave number n

$$v_{1+} = A_1 \cos(nx + \sigma_0 t + \chi_1)$$
$$= \mathcal{C}_1(t) \cos nx + \mathcal{S}_1(t) \sin nx$$
$$v_{2+} = A_2 \cos(nx + \sigma_0 t + \chi_2)$$
$$= \mathcal{C}_2(t) \cos nx + \mathcal{S}_2(t) \sin nx$$

where

$$\mathcal{C}_l(t) = A_l \cos(\sigma_0 t + \chi_l)$$
$$\mathcal{S}_l(t) = -A_l \sin(\sigma_0 t + \chi_l)$$

Then by using the definitions in (4.6), we obtain

$$F_1 \equiv \langle |dV_{1+}|^2 \rangle = A_1^2$$
$$F_2 \equiv \langle |dV_{2+}|^2 \rangle = A_2^2$$
$$F_3 + i F_3 \equiv \langle dV_{1+} dV_{2+}^* \rangle = A_1 A_2 \left[\cos(\chi_2 - \chi_1) - i \sin(\chi_2 - \chi_1)\right]$$

Thus F_4/F_3 is a measure of the relative phase of the two waves, whereas F_1 and F_2 are their squared amplitudes. It should be noted that the absolute phase of each wave has no effect on F_1, F_2, F_3 and F_4. This should be so because our statistical forcings should not depend on the information about the absolute phase of v_{lt}.

5. Determination of the fundamental solutions

We now return to the problem of determining the four pairs of fundamental solutions which are to satisfy the same differential equations, (3.10), but have the four different sets of boundary conditions summarized in Table 3. The differential operators L_j in (3.10) have variable coefficients and have no simple relationships among themselves. It is virtually impossible to obtain the fundamental solutions in analytic form. We shall therefore solve them numerically. But in order to establish a complete picture of the fundamental solutions, we must numerically integrate (3.10) for a sufficiently dense combination of wavenumbers and frequencies. Otherwise certain combinations of ν and σ which give strong response might be overlooked. It is therefore a very practical matter that we require at least some broad notions about how the fundamental solutions vary in the wavenumber-frequency domain. We might gain such information if we could find a special case in which analytic solutions for (3.10) can be obtained. Not only could they serve as a guide for making an adequate and efficient scanning over the frequency scale, but also would shed considerable light on some intrinsic characteristics of the system. Fortunately there exists such a special case. The discussion in this section therefore consists of two parts. The first part is the analysis for this special case, which reveals the conditions under which resonance could occur. The second part describes the numerical scheme used to solve for the fundamental solutions in the general case.

5.1 Special case

Upon close examination of the four differential operators, L_i, we find that they reduce to remarkably simple forms when all the dissipative coefficients and the basic shear vanish. Hence the special case under consideration is a two-layer non-dissipative model with a barotropic basic state. When $\alpha = \beta = \gamma = 0$ and $\Lambda = 0$, we find

$$L_1 = -L_4 = \left(\frac{s^3}{n^2} - 2s\bar{\epsilon}\right)\frac{d^2}{dy^2} - \left[\frac{s^2}{n} + \left(\frac{1}{n} - s\right)2(n^2\bar{\epsilon} - s^2)\right] + sy^2$$

$$L_2 = -L_3 = \frac{s^3}{n^2}\frac{d^2}{dy^2} + \frac{s^2}{n} - sy^2 \qquad (5.1)$$

The symmetry among the operators now enables us to combine the two coupled equations in (3.10) into two uncoupled equations:

$$\left(\frac{d^2}{dy^2} + \frac{n}{s} - n^2\right)\left\{\hat{V}_1^i + \hat{V}_2^i\right\} = 0 \qquad (5.2)$$

$$\left(\frac{d^2}{dy^2} + \left(\frac{s^2}{\bar{\epsilon}} + \frac{n}{s} - n^2\right) - \frac{y^2}{\bar{\epsilon}}\right)\left\{\hat{V}_1^i - \hat{V}_2^i\right\} = 0 \qquad (5.3)$$

In this special case $(\hat{V}_1^i + \hat{V}_2^i)$ and $(\hat{V}_1^i - \hat{V}_2^i)$ can clearly be identified as the barotropic and the baroclinic components respectively.

Knowing the separate boundary conditions of $\hat{V}_1^i$ and $\hat{V}_2^i$ as summarized in Table 3, we can readily obtain them for $\hat{V}_1^i \pm \hat{V}_2^i$, which are given in Table 4.

	y = 0		y = Y	
j	$\hat{V}_1^j + \hat{V}_2^j$	$\hat{V}_1^j - \hat{V}_2^j$	$\hat{V}_1^j + \hat{V}_2^j$	$\hat{V}_1^j - \hat{V}_2^j$
1	d/dy = 0	d/dy = 0	0.5	0.5
2	d/dy = 0	d/dy = 0	0.5	-0.5
3	0	0	0.5	0.5
4	0	0	0.5	-0.5

Table 4.

Barotropic component

The barotropic component is governed by (5.2) which has sinusoidal solutions as follows.

$$j = 1, 2 \qquad \hat{V}_1^j + \hat{V}_2^j = \frac{1}{2} \frac{\cos \sqrt{\frac{n}{s} - n^2}\, y}{\cos \sqrt{\frac{n}{s} - n^2}\, Y}$$

$$j = 3, 4 \qquad \hat{V}_1^j + \hat{V}_2^j = \frac{1}{2} \frac{\sin \sqrt{\frac{n}{s} - n^2}\, y}{\sin \sqrt{\frac{n}{s} - n^2}\, Y} \qquad (5.4)$$

The barotropic component therefore becomes infinite whenever

$$\left(\frac{n}{s} - n^2\right)^{\frac{1}{2}} Y = \frac{m\pi}{2}, \qquad m = \pm 1, \pm 2, \cdots \qquad (5.5)$$

In terms of dimensional parameters, (5.5) is equivalent to

$$\sigma_{resonance} = \frac{2\Omega n}{\left(\frac{m\pi}{2Y}\right)^2 + n^2} - \frac{\bar{U} n}{a} \qquad (5.6)$$

These frequencies can therefore be called resonant frequencies associated with the barotropic mode. They correspond to barotropic Rossby waves in a channel $|y| \leq Y$. For each wavenumber n there are an infinite number of barotropic resonant frequencies, and $\sigma_{resonance}$ is a monotonically decreasing function of $|m|$. The upper and lower bounds are $\sigma\,(m=\pm 1)$ and $\sigma\,(m=\pm\infty)$ respectively. The distribution of these barotropic resonant modes is shown by the dashed curves in Fig. 4.

Baroclinic component

The baroclinic component is governed by (5.3). Its solutions are known to be parabolic cylinder functions. Let us first transform (5.3) into a standard form by using a new independent variable z defined by $z = \left(\frac{4}{\bar{\epsilon}}\right)^{\frac{1}{4}} y$

$$\left(\frac{d^2}{dz^2} - \left(\frac{1}{4}z^2 + \Gamma\right)\right)\left\{\hat{V}_1^j - \hat{V}_2^j\right\} = 0 \tag{5.8}$$

where $$\Gamma = \frac{-1}{2\sqrt{\bar{\epsilon}}}\left(\Delta^2 + \frac{n}{\Delta}\bar{\epsilon} - n^2\bar{\epsilon}\right) \tag{5.8a}$$

$$\Delta = \sigma + n\bar{u}$$

The two independent solutions of (5.8) are well-known and can be given in terms of confluent hypergeometric function ${}_1F_1(a,b,x)$.

The even solution is:

$$m^{I}(z;\Gamma) = e^{-\frac{1}{4}z^2}\,{}_1F_1\left(\tfrac{1}{2}\Gamma + \tfrac{1}{4}, \tfrac{1}{2}, \tfrac{1}{2}z^2\right)$$

The odd solution is: (5.9)

$$m^{II}(z;\Gamma) = z\,e^{-\frac{1}{4}z^2}\,{}_1F_1\left(\tfrac{1}{2}\Gamma + \tfrac{3}{4}, \tfrac{3}{2}, \tfrac{1}{2}z^2\right)$$

When the boundary conditions are incorporated, we obtain

$$\hat{V}_1^1 - \hat{V}_2^1 = -(\hat{V}_1^2 - \hat{V}_2^2) = \frac{1}{2}\,\frac{m^I(z;\Gamma)}{m^I(z_+;\Gamma)} \tag{5.10}$$

$$\hat{V}_1^3 - \hat{V}_2^3 = -(\hat{V}_1^4 - \hat{V}_2^4) = \frac{1}{2}\,\frac{m^{II}(z;\Gamma)}{m^{II}(z_+;\Gamma)}$$

Hence the baroclinic component also becomes infinite whenever

$$m^I(z_+;\Gamma) = 0 \qquad \text{or} \qquad m^{II}(z_+;\Gamma) = 0$$

Since $e^{-\frac{1}{4}z_+^2}$ and z_+ are positive quantities, this is equivalent to <u>either</u> of the two conditions

$$,F_1\left(\tfrac{1}{2}\Gamma+\tfrac{1}{4}\,,\ \tfrac{1}{2}\,,\ \tfrac{1}{2}z_+^2\right) = 0$$

$$,F_1\left(\tfrac{1}{2}\Gamma+\tfrac{3}{4},\ \tfrac{3}{2}\,,\ \tfrac{1}{2}z_+^2\right) = 0 \tag{5.11}$$

It should be noted that z_+ only depends on the static stability and the latitude of the northern boundary, whereas Γ as shown in (5.8a) is a cubic function of frequency. Hence the problem of determining the baroclinic resonant frequencies for each wavenumber consists of two parts. We must first determine all values of Γ that satisfy (5.11). Having done that we then solve for the three roots of σ associated with each of those values of Γ. There is however no established procedure whereby one can determine all values of a parameter which makes

a confluent hypergeometric function zero when the other parameter and the variable are held fixed. Nor is there any existing mathematical table of confluent hypergeometric function that covers the relevant range of the parameters in this study. Fortunately it is possible to devise a simple graphical method to determine the values of Γ with a sufficient accuracy. This method is based upon two general properties of confluent hypergeometric function in regards to its zeros, and also upon the relation between it and the error function. The rationale behind this graphical method is given in Appendix B. The resulting baroclinic resonant frequencies are shown in Fig. 4 by the solid curves.

One distinct feature of Fig. 4 is that the resonant modes in this special case fall into three groups. Only one group of them is bounded within an upper and a lower bound, and are characterized by their small frequency. They include all the barotropic modes and one third of the baroclinic modes. These are barotropic and baroclinic Rossby waves moving slowly westward with respect to the basic current. The other two groups of resonant modes are characterized by large positive and negative frequency. These are internal gravity-inertia waves which can travel both eastward and westward at relatively high speed.

5.2 General case

We now consider the problem of getting the fundamental solutions when the friction and cooling coefficients, and the basic shear are incorporated. As noted before we must resort to a numerical method to solve the governing equations (3.10). Several attempts using different

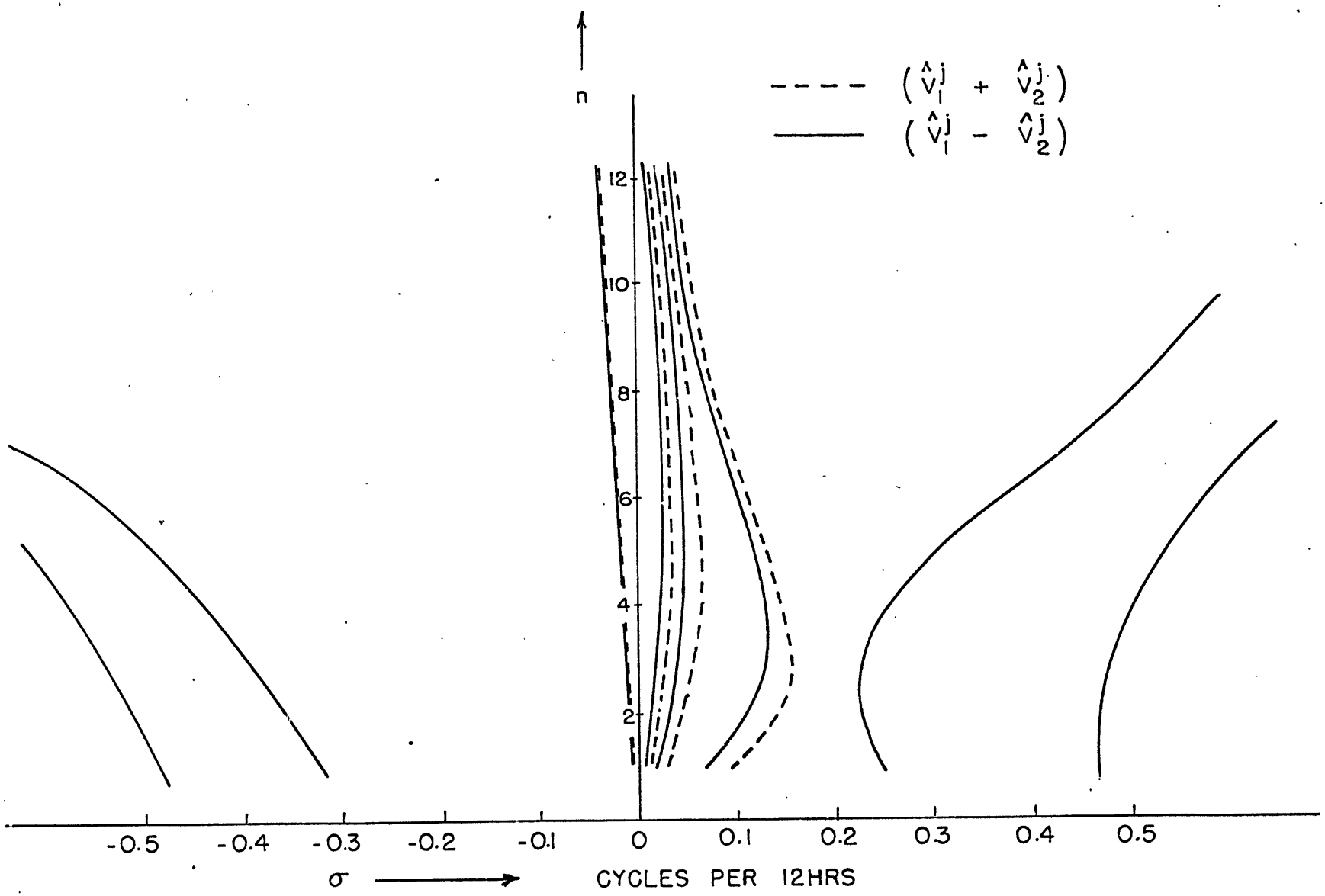

FIG. 4 RESONANT MODES IN SPECIAL CASE

direct transformations of (3.10) into a finite-difference form gave poor results; the numerical solutions for $\hat{V}_\ell^j$ and the associated solutions for $\hat{U}_\ell^j$ and $\hat{P}_\ell^j$ via (3.11) so obtained invariably did not match the prescribed boundary conditions in a reasonably smooth manner. Furthermore, when they were used to compute those second moment statistics representing energy conversions, large discrepancies in the total energy balance existed at several grid points near $y = Y$.

A more fundamental numerical scheme was therefore used. The unreduced spectral equations (3.8) were first written into a self-consistent centered-difference form. These six first-order difference equations were then reduced to two coupled second-order equations in exactly the same way as the differential equations (3.8) were reduced to (3.10). These two difference equations governing $\hat{V}_1^j$ and $\hat{V}_2^j$ together with the boundary conditions constitute a system of simultaneous nonhomogeneous linear algebraic equations for $\hat{V}_\ell^j$ at the points of the finite-difference grid. This system was solved with the "Gauss elimination" method. This approach gave good results.

Fifty-one grid points, $k = 1,2,\ldots, 51$, were used to cover the latitude zone from equator to 30°N. The variables $\hat{U}_\ell^j$ and $\hat{P}_\ell^j$ are defined at the same grid points, whereas $\hat{V}_\ell^j$ are defined at points midway between the points for the former. For clarity we omit temporarily the symbol $\wedge$ for the dependent variables as well as the superscript j which distinguishes the four different sets of fundamental solutions, and instead use a new superscript k to denote the grid points. (The difference equations for the four sets of fundamental solutions are identical;

it is only the four sets of boundary values in Table 5 which distinguish them.) The finite difference notation is then

$$y^k = (k-1)\Delta = (k-1)\frac{Y}{50}$$

$$V^k = V \quad \text{at} \quad y = (k-1)\Delta$$

$$U^k,\ P^k = U,\ P \quad \text{at} \quad y = (k-\tfrac{1}{2})\Delta$$

The centered difference form of (3.9) is as follows.

$$(s+2n\Lambda-i\beta)U_1^k - \frac{i\Lambda}{\Delta}(V_1^{k-1}-V_1^k) + \frac{i}{2}y^{k+\frac{1}{2}}(V_1^{k+1}+V_1^k) + i\beta U_2^k = -nP_1^k$$

$$\frac{1}{2}y^k(U_1^k+U_1^{k-1}) + (s+n\Lambda-i\beta)iV_1^k - \beta V_2^k = -\frac{1}{\Delta}(P_1^k-P_1^{k-1})$$

$$-i\beta U_1^k + (s-2n\Lambda-i\alpha)U_2^k + \frac{i\Lambda}{2}(V_2^{k+1}-V_2^k) + \frac{i}{2}y^{k+\frac{1}{2}}(V_2^{k+1}+V_2^k) = -nP_2^k$$

(5.12)

$$\frac{1}{2}y^k(U_2^k+U_2^{k-1}) + (s-n\Lambda-i\alpha)iV_2^k - \beta V_1^k = -\frac{1}{\Delta}(P_2^k-P_2^{k-1})$$

$$nU_1^k + nU_2^k - \frac{i}{\Delta}(V_1^{k+1}-V_1^k+V_2^{k+1}-V_2^k) = 0$$

$$2n\bar{\epsilon}U_1^k - \frac{i2\bar{\epsilon}}{\Delta}(V_1^{k+1}-V_1^k) + \frac{i\Lambda}{2}y^{k+\frac{1}{2}}(V_1^{k+1}+V_1^k+V_2^{k+1}+V_2^k) = (s-i\gamma)(P_2^k-P_1^k)$$

We then perform the steps equivalent to those in Appendix A to eliminate U_ℓ^k and P_ℓ^k from (5.12). The resulting second-order difference equations are the counterpart of (3.10) and apply at k = 1 to 50.

$$p_1^k V_1^{k+1} + p_2^k V_1^k + p_3^k V_1^{k-1} + p_4^k V_2^{k+1} + p_5^k V_2^k + p_6^k V_2^{k-1} = 0$$

$$q_4^k V_1^{k+1} + q_5^k V_1^k + q_6^k V_1^{k-1} + q_1^k V_2^{k+1} + q_2^k V_2^k + q_3^k V_2^{k-1} = 0 \qquad (5.13)$$

$p_1^k, \ldots, q_6^k$ are functions of $\bar{\epsilon}$, s, λ, α, β, γ, n, Δ and y^k.

The boundary conditions giving V at $k = 0$ and $k = 51$ correspond to those in Table 4 and are stated in Table 5.

j =	1	2	3	4
V_1^0 =	V_1^2	V_1^2	$-V_1^2$	$-V_1^2$
V_2^0 =	V_2^2	V_2^2	$-V_2^2$	$-V_2^2$
V_1^{51} =	0.5	0	0.5	0
V_2^{51} =	0	0.5	0	0.5

Table 5.

(5.13) together with the boundary values in Table 5 can be put into a vector form

$$\underline{\underline{A}}^{(m)} \cdot \underline{V} = \underline{F}^{(m)} \qquad m = 1, 2 \qquad (5.14)$$

$m = 1$, even solutions

$m = 2$, odd solutions

$\underline{A}^{(m)}$ is a 100 x 100 matrix whose elements consist of $p_1^k, \cdots, g_6^k$, $\underline{V}$ is a 100 x 2 matrix containing even (odd) fundamental solutions V_ℓ^k, $\underline{\mathcal{F}}^{(m)}$ is a 100 x 2 matrix containing the even (odd) boundary conditions. Such a system can be easily solved with the Gauss elimination method; the subroutine "GELB" at the MIT Computation Center was used.

Finally we come to the problem of scanning through the frequency scale from $\sigma = -\frac{1}{2}$ to $\sigma = +\frac{1}{2}$ cycles/12hr. for each wavenumber. The wave number range is $n = 1$ to 12. In order to do so efficiently we make use of Fig. 4 as a guide. A very small frequency interval, $(2700)^{-1}$ cycles/12hrs, was used in the neighborhood of the resonant frequencies of the special case, and a larger frequency interval (as large as $(14)^{-1}$ cycles/12 hr) was used elsewhere. The small frequency interval is 1/20 of the frequency resolution in the input spectra. It should be noted that the resonant frequencies in the special case treated earlier have an accumulation point at $\sigma = -n\bar{u} = -n \cdot (.00322)$ as the north-south wavenumber increases in the Rossby modes. The small frequency interval $\delta_0 = (2700)^{-1}$ was small enough to show conclusively that this fine structure was smeared out in the general case by friction and baroclinicity. For purpose of comparison, the fundamental solutions were also computed numerically for the special case for wavenumber $n = 4$ by simply setting α, β, γ and Λ equal to zero in the computation of p^k and q^k in (5.13).

Properties of the general fundamental solutions

In view of the complicated dependence of the response functions of second moment statistics upon the fundamental solutions [see (3.21)], little would be gained from a close examination of the detailed structure of each of the $\hat{V}_\ell^j$. Therefore only one broad aspect of them will be discussed, namely the latitudinal sum of $|\hat{V}_1^j \pm \hat{V}_2^j|$. These quantities give a crude indication of the intensity of the integrated response of the "quasi-barotropic" and "quasi-baroclinic" components as a function of wavenumber and frequency.

We compare, for $n = 4$, the numerical results for integrated response with the barotropic and baroclinic resonant frequencies obtained analytically for the special case. The even and odd "quasi-barotropic" integrated response components, $\sum_y |\hat{V}_1^j + \hat{V}_2^j|$, are shown separately in two plots in Fig. 5. The solid curves are for the special case and the broken curves are for the general case. The short vertical arrows along the frequency axes locate the resonant barotropic frequencies at $n = 4$ determined analytically for the special case. Figure 6 does likewise for the "quasi-baroclinic" components $\sum_y |\hat{V}_1^j - \hat{V}_2^j|$.

The numerical results in the special case are identical for $j = 1,2$ and for $j = 3,4$ as in agreement with the analytic solutions (5.4) and (5.10). Only one set of solid curves is therefore necessary on each of the four diagrams in Figs. 6 and 5.

We first note that the theoretically deduced arrows agree well with the location of the corresponding numerically computed peaks of

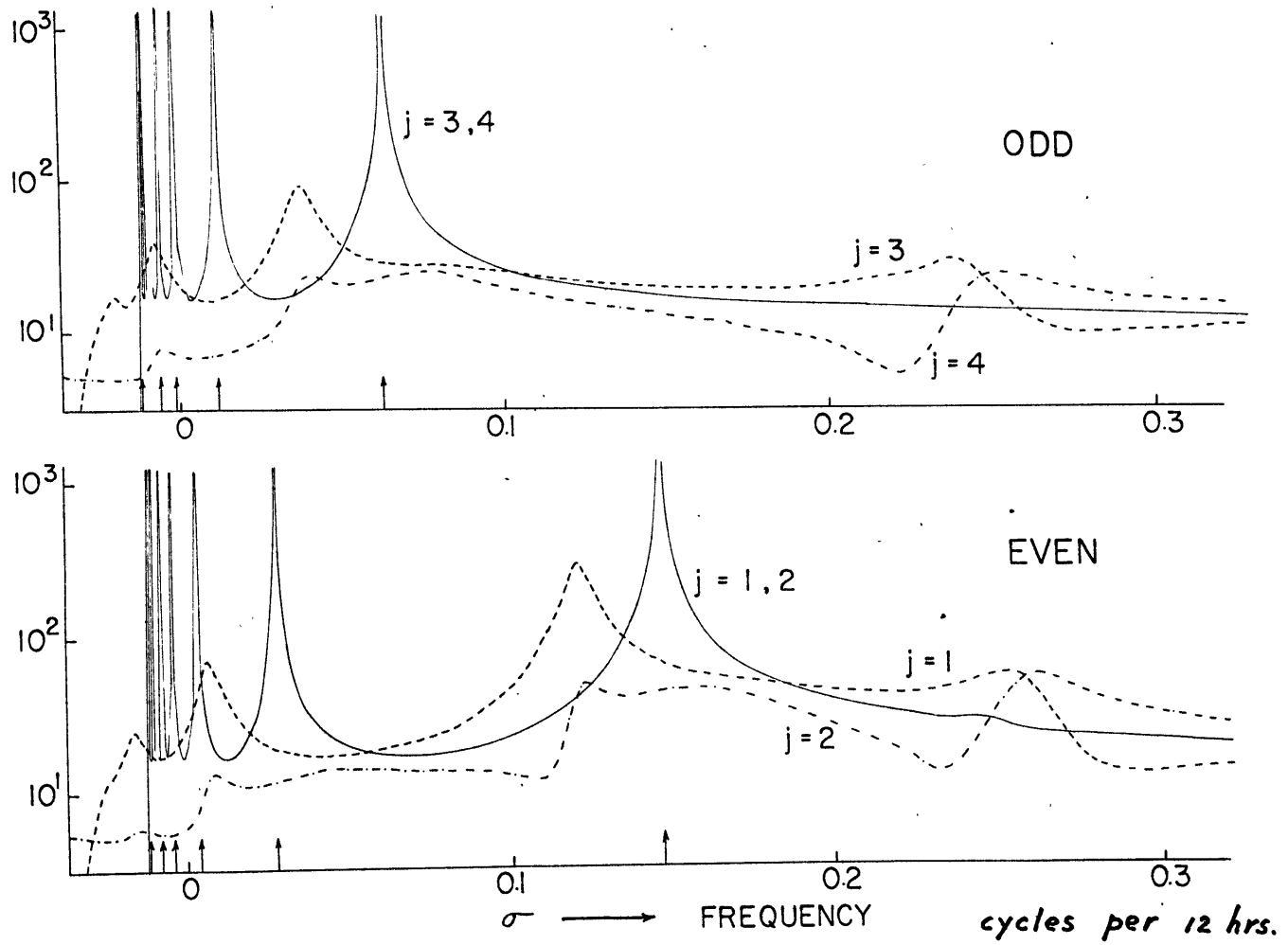

Fig. 5. $\sum_s |\hat{v}_1^{sj} + \hat{v}_2^{sj}|$, $j = 1, 2, 3, 4$ are latitudinal sum of the absolute value of the quasi-barotropic components of the fundamental solutions as a function of frequency for wavenumber n = 4.

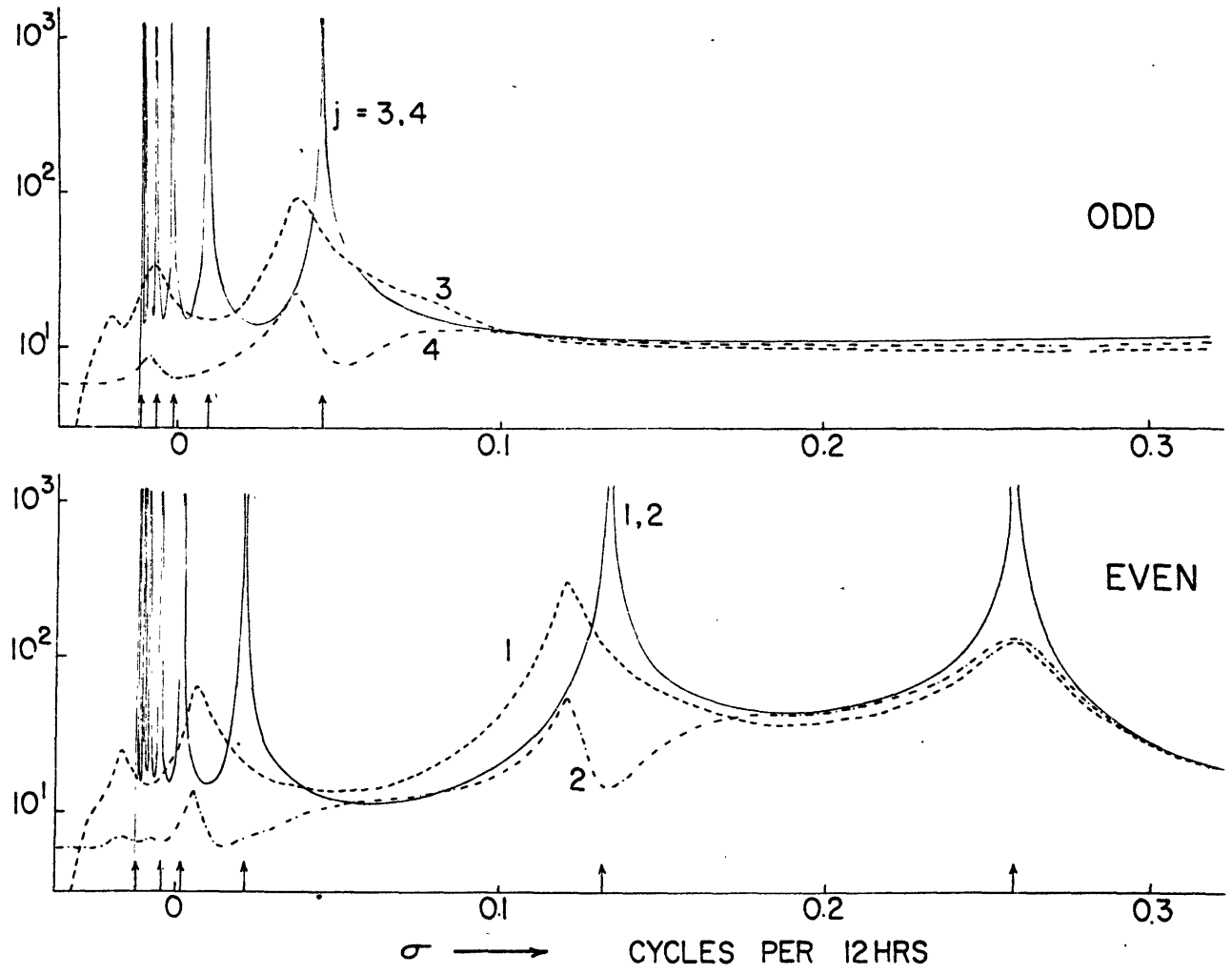

Fig. 6. $\Sigma |\hat{v}_1^j - \hat{v}_2^j|$, $j = 1, 2, 3, 4$ are latitudinal sum of the absolute value of the quasi-baroclinic components of the fundamental solutions as a function of frequency for wavenumber n = 4.

the solid curves on both Figs. 5 and 6. All solid peaks shown correspond to Rossby waves, except for the peak at $\sigma = .259$ in Fig. 6. This represents internal gravity wave of smallest positive σ at this wavenumber. The theoretical Rossby wave accumulation point at $\sigma = -4\bar{\mu} = -0.0129$ also checks. The quantitative agreements just described provide a welcome verification of the numerical method. (The behavior with y in the special case of the numerical values also agree well with the theoretical barotropic solutions.)

The broken curves have only three broad but well resolved peaks associated with the Rossby waves, and one peak associated with the said internal gravity wave. Damping due to dissipation is clearly dominant for those Rossby waves of high north-south wavenumbers located at very low frequencies. It is noted that the Rossby-wave peaks are shifted to smaller frequencies relative to their counterparts in the special case. Furthermore while the barotropic and baroclinic peaks of the latter are located at different frequencies, those broken peaks of the "quasi-barotropic" and "quasi-baroclinic" coincide. This indicates that the basic shear and the dissipative processes cause the previously separated barotropic and baroclinic components to interact with one another. As a result the sum and difference of the velocities at the upper and lower levels no longer represent the actual barotropic and baroclinic components. The internal gravity wave peak in Fig. 6 has no corresponding barotropic peak and the interaction should therefore be weak. This may account for the fact that there is hardly any shift of the broken peak relative to the solid peak and that some new secondary maximum peaks

appear in Fig. 5 near that frequency.

Finally it is of interest to examine how the fundamental solutions vary in the wavenumber-frequency space. As an example, we show one even solution of the "quasi-baroclinic" component, $\sum_y \left| \hat{V}_1' - \hat{V}_2' \right|$, in Fig. 7. The maximum has the same general pattern as the distribution of the resonant modes shown in Fig. 4. The most striking feature however is the location of maximum response around $n = 3$ at frequencies corresponding to the lowest latitudinal wave number of the Rossby waves and internal gravity waves. Even a small boundary forcing at such values of n and σ could then excite considerable response.

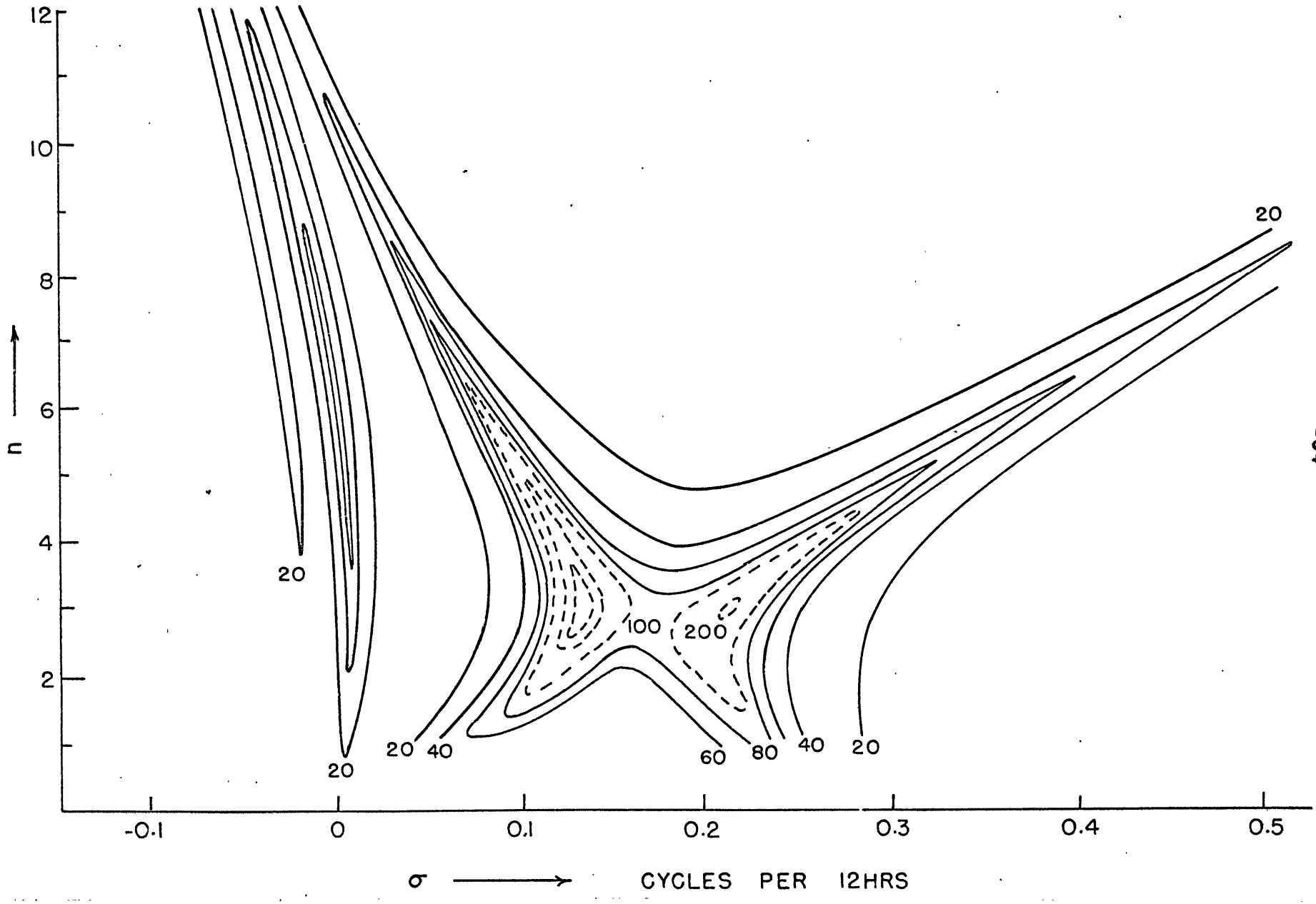

Fig. 7. Variation of $\sum_{*} |\vec{v}_1' - \vec{v}_2'|$ in the frequency-wavenumber domain.

6. The predicted statistics of the model

With the statistical boundary conditions obtained in Section 4 and the fundamental solutions in Section 5, we now can compute any variance or covariance by (4.8). Each of these statistics is either an even or an odd function of latitude y , because the basic state and the boundary forcings in the model are both symmetric with respect to the equator. As shown in (3.23) each statistic is equal to an integral over frequency σ and a sum over wavenumber n of a quantity, say X , which depends on n , σ , y , the boundary spectra and the basic state parameters. The decision has already been made to consider only n = 1 to 12. The elementary frequency interval δ used in the boundary spectra is $(270)^{-1}$ cycles per 12 hours and the resolution is 2δ . The frequency range we shall consider is $|\sigma| \leq \frac{1}{6}$, corresponding to a minimum period of 3 days. This limitation on σ is imposed by the nature of the boundary data, since this consisted of streamfunction analyses which are essentially based on the quasi-geostrophic theory.

The model statistics will generally be presented simply as functions of y . However in several cases the dependence of the integrand-summand "X" on n and σ will also be displayed. The integration over σ was performed by a trapezoidal sum, in which the frequency interval employed was small enough (generally equal to δ , in fact) to adequately sample the detailed behaviour with σ of the fundamental solutions and of the boundary spectra. The contribution from those

individual frequency intervals were then combined into 15 frequency bands of width $1/90 = 3\delta$ covering the range $\sigma = 0$ to $1/6$. These bands are centered at $\sigma = 1/180, 3/180, \ldots, 29/180$ cycles per 12 hours. They are wide enough to insure meaningful spectral resolution and yet narrow enough to show the distinct frequency dependence of the statistics.

6.1 Horizontal velocity statistics

Fig. 8 shows the square root of $\langle v_1^2 \rangle$ and $\langle v_2^2 \rangle$ as a function of latitude, as well as the observed values at 4 latitudes for the pressure levels 250 and 850 mbs. The latter were recently obtained from 5 years of data by Mr. John Kidson of the Planetary Circulations Project at Massachusetts Institute of Technology. The theoretical values predict too large $\langle v_1^2 \rangle$ and too small $\langle v_2^2 \rangle$ in the equatorial region. A larger value of the friction coefficient β might reduce this discrepancy. A more fundamental reason may be related to our choice of uniform zonal winds $\bar{u}_1$ and $\bar{u}_2$. The observed zonal wind shown in Table 2 is actually more easterly at low latitudes than the values used in the model. The analysis of Eliassen and Palm (1960) indicates that the southward wave energy flux in planetary waves is easier to propagate across a westerly current than an easterly current. Thus much of the excess $\langle v_1^2 \rangle$ at the equator in Fig. 8 might be reduced by incorporating a realistic latitudinal shear in $\bar{u}_1$. This point will be returned to in the summarizing Section 7.

Fig. 9 shows the same plot for the square root of $\langle u_\ell^2 \rangle$. Unfortunately, observational data for comparison is missing. The theo-

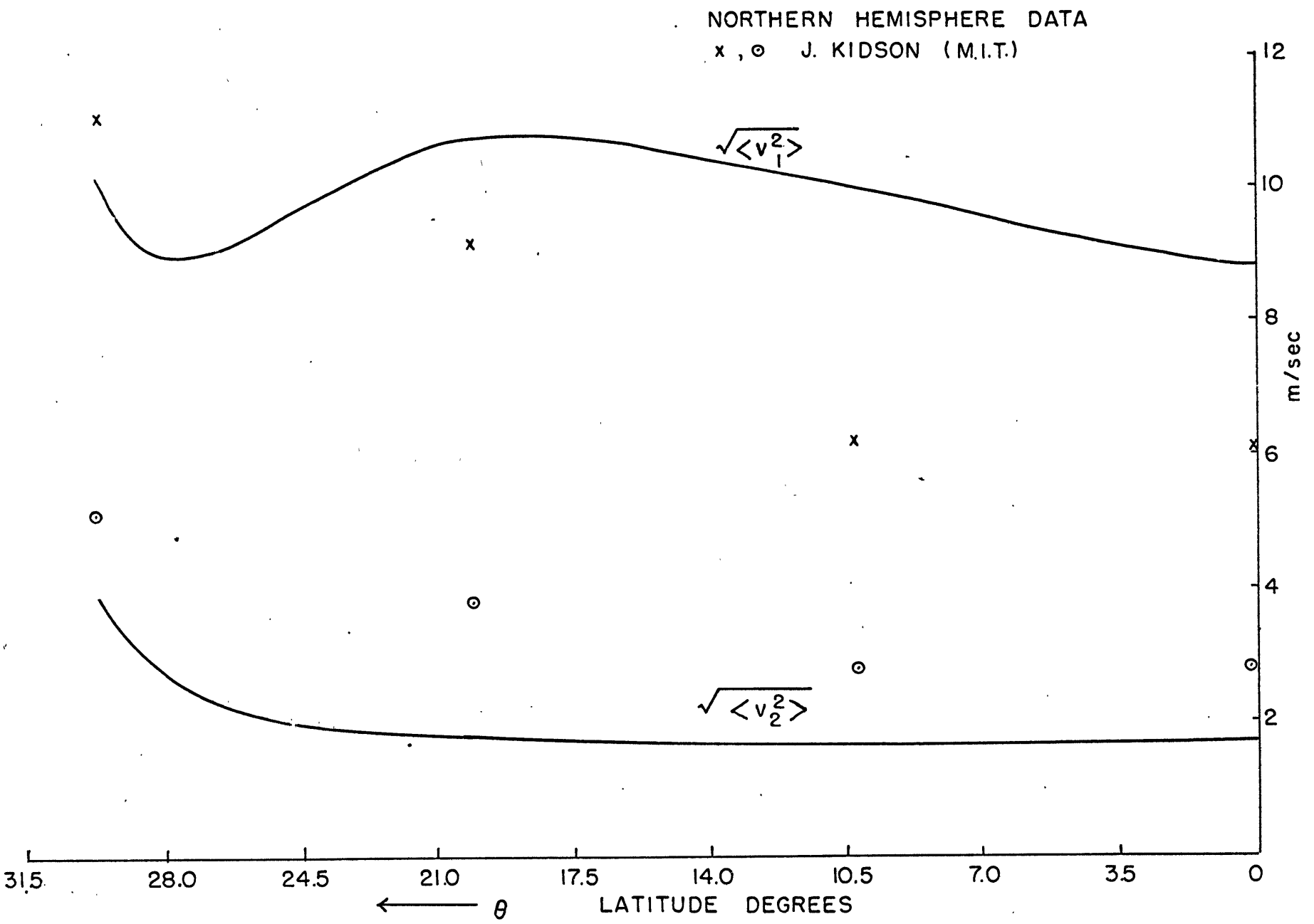

Fig. 8. $\sqrt{\langle v_1^2 \rangle}$ and $\sqrt{\langle v_2^2 \rangle}$ are standard deviation of the meridional velocity at 250-mb and at 750-mb level respectively.

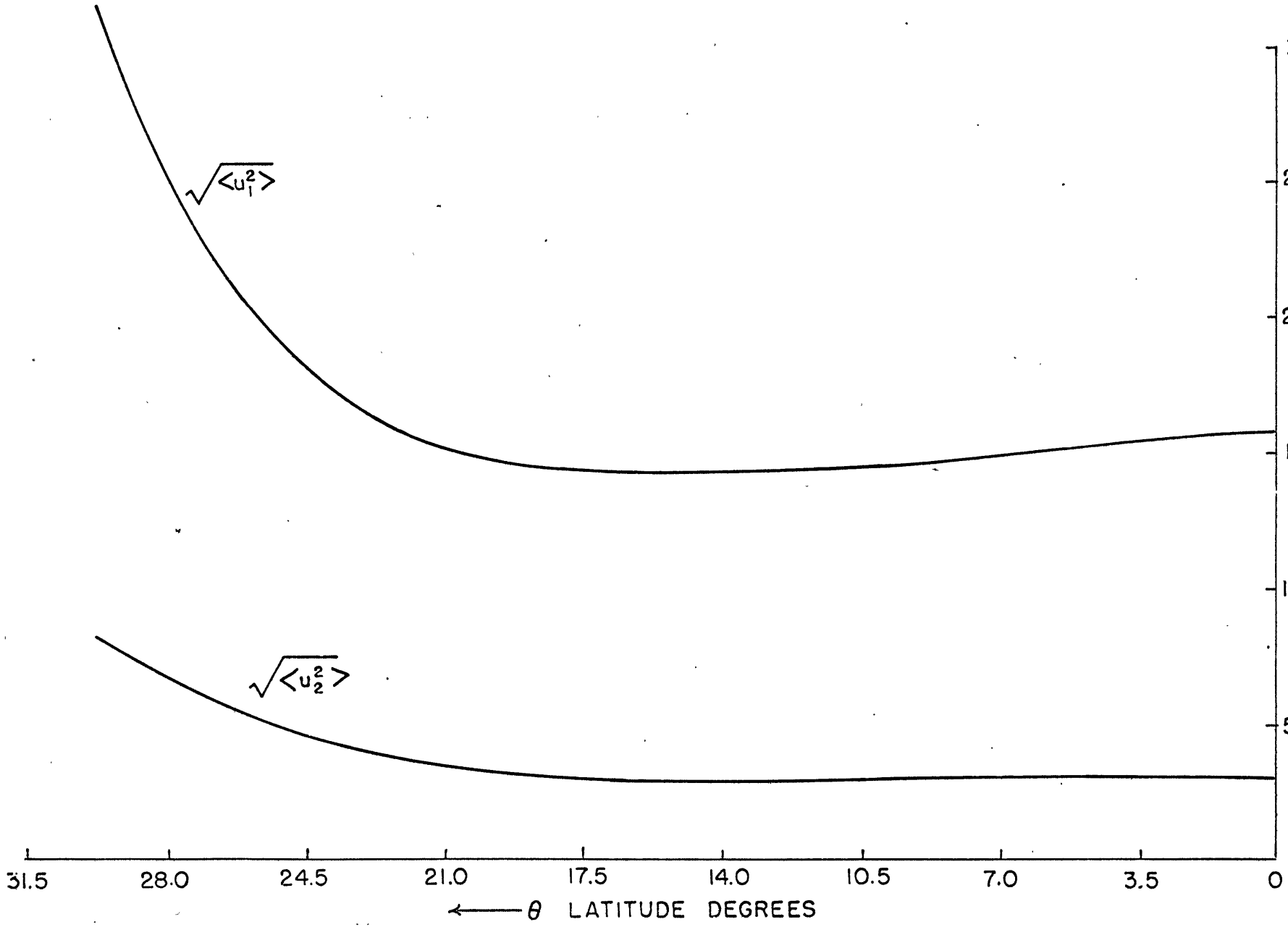

Fig. 9. $\sqrt{\langle u_1^2 \rangle}$ and $\sqrt{\langle u_2^2 \rangle}$ are standard deviation of the zonal velocity at 250-mb and at 750-mb level respectively.

retical values of $\langle u^2 \rangle$ are greater than $\langle v^2 \rangle$ at both levels throughout the model tropics. The values of $\langle u_2^2 \rangle$ appear to be somewhat too large, but are not unreasonable except near 30°N. This locally large $\langle u_1^2 \rangle$ may also be related to the use of uniform for the reason cited above. However by evidently overpredicting to some extent the upper level velocity variance, the model computation demonstrates that lateral coupling can easily account for much of the observed eddy kinetic energy in low latitudes.

The theoretical results in Figs. 8 and 9 also predict one other property of the asymmetrical motions. It is noted that both $\langle u_2^2 \rangle$ and $\langle v_2^2 \rangle$ decrease monotonically with latitude. $\langle u_1^2 \rangle$ decreases sharply from about (30 m sec^{-1})^2 at 30°N to about (15 m sec^{-1})^2 at 20°N, and then remains essentially constant to the equator. On the other hand, $\langle v_1^2 \rangle$ decreases only from about (10 m sec^{-1})^2 to about (9 m sec^{-1})^2 at the equator, with a weak undulation near 20°N. These features suggest that the variability of the two horizontal wind components at the lower level decrease with latitude in about the same way, whereas that of u_1 is quite different from that of v_1. The former decreases by only about 20%, and the latter by a factor of 4. In other words, the decrease with latitude of eddy kinetic energy at the upper level in the model is largely due to the decrease of $\langle u_1^2 \rangle$.

The extent of vertical coupling between the flows at the upper and lower levels may be measured statistically in terms of the correlation coefficient between u_1 and u_2, and between v_1 and v_2.

$$R_u = \frac{\langle u_1 u_2 \rangle}{(\langle u_1^2 \rangle \langle u_2^2 \rangle)^{1/2}} \quad ; \quad R_v = \frac{\langle v_1 v_2 \rangle}{(\langle v_1^2 \rangle \langle v_2^2 \rangle)^{1/2}}$$

R_u and R_v are shown in Fig. 10. They are generally small, less than 0.4, specially in the equatorial region of the model. This is quite consistent with the observations analysed by H. Riehl, which Charney cites in his 1963 paper as supporting his scale analysis result.

A different aspect of the velocity variances can be examined from a plot showing the contribution to their latitudinal sum from each wavenumber n and frequency band. This measure will indicate which are the dominant modes of the flow averaged over the region. Such statistics are shown in Figs. 11 and 12 for $\langle v_1^2 \rangle$ and $\langle u_1^2 \rangle$ respectively. (The corresponding plots for $\langle v_2^2 \rangle$ and $\langle u_2^2 \rangle$ are not presented because their small magnitudes relative to $\langle v_1^2 \rangle$ and $\langle u_1^2 \rangle$ respectively make any physical interpretation of detailed structure rather irrelevant.) Fig. 11 shows that most of the areal-integrated variance of $\langle v_1^2 \rangle$ is associated with wavenumbers 4 to 8 and in the frequency bands corresponding to period of 10 to 40 days. This prediction cannot be compared with the real tropical atmosphere because of lack of data. However it does not appear to be contradicted by any studies known to the writer. In Fig. 12 we also find overwhelming dominance by the low frequency modes, although it should be noted that the low wavenumbers in these low frequency bands are as significant as the intermediate wavenumbers which are dominant in Fig. 11. This differ-

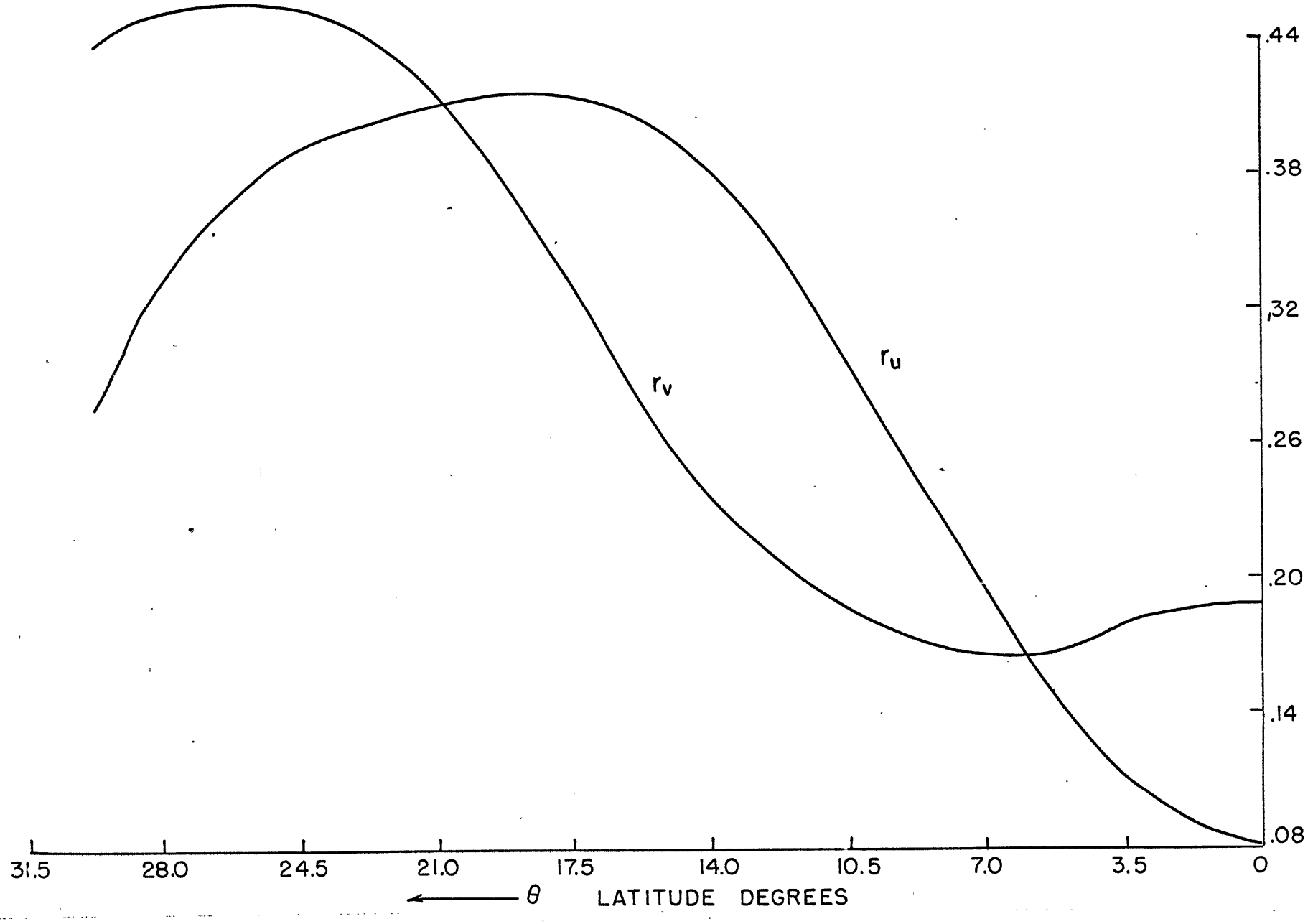

Fig. 10. r_u is correlation coefficient between the zonal velocity at 250-mb and at 750-mb levels, and r_v is correlation coefficient between the meridional velocity at 250-mb and at 750-mb levels.

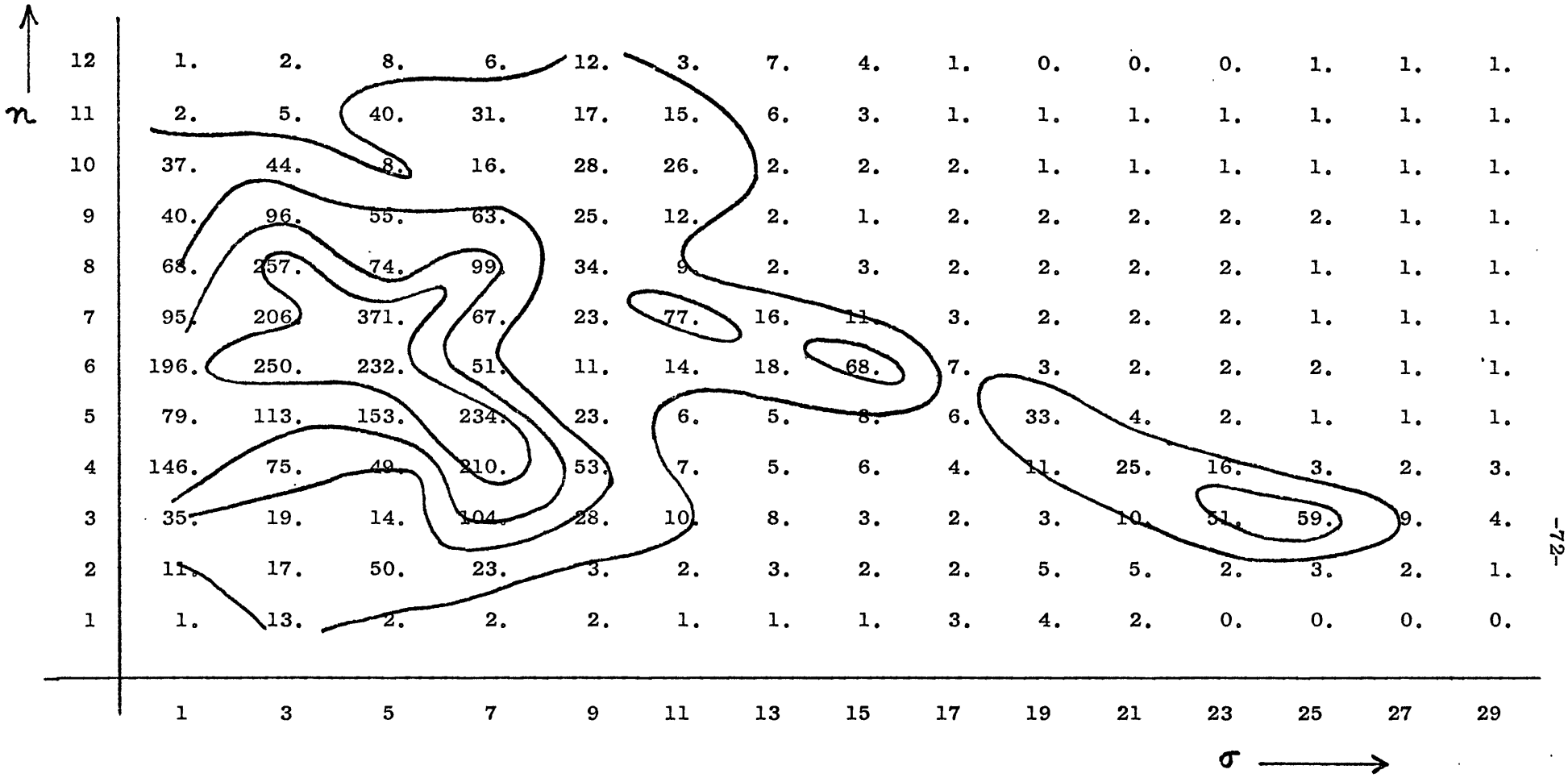

σ in $x(180)^{-1}$ cycles per 12 hours

Figure 11. $\sum_y \langle v_1^2 \rangle$ in wavenumber-frequency space.

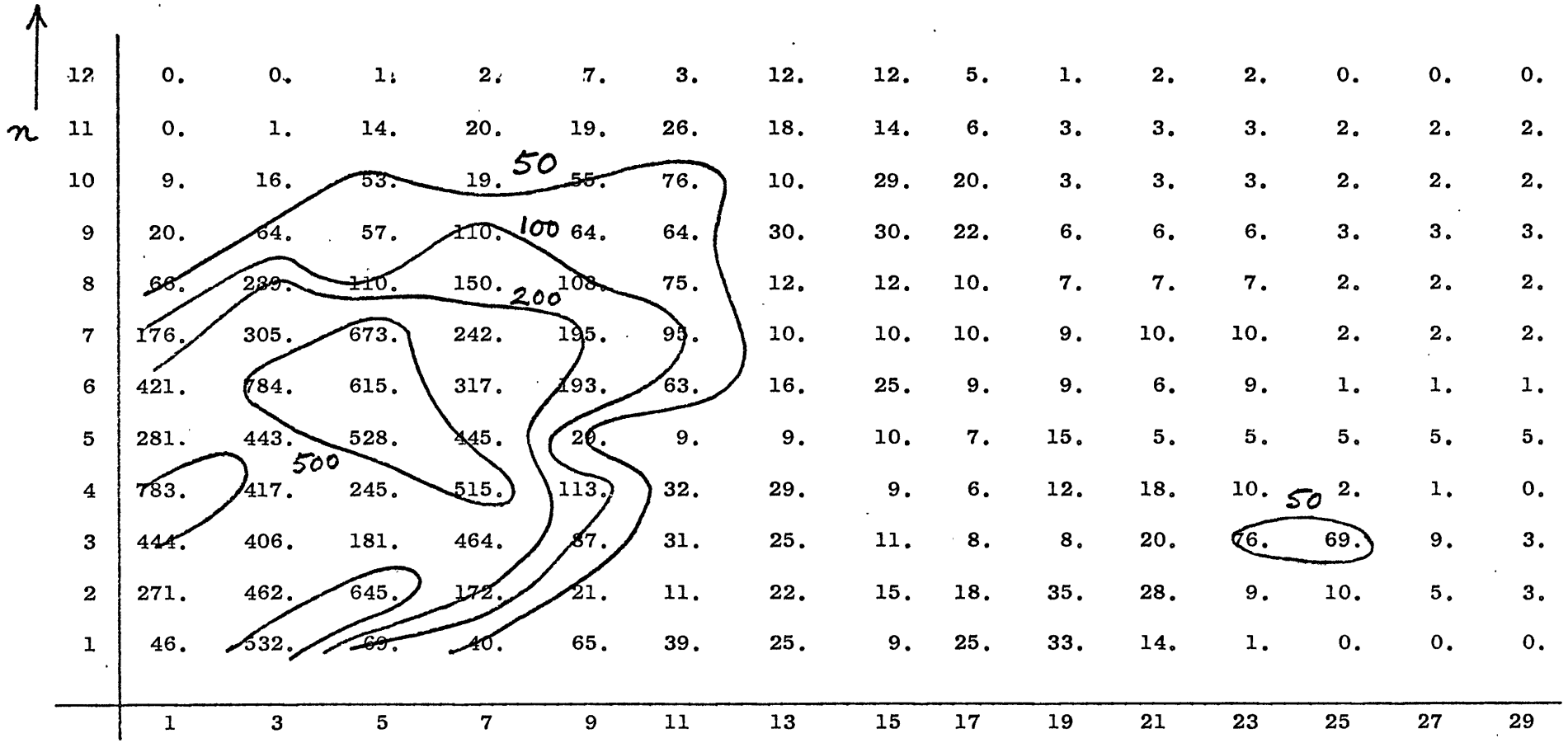

Figure 12. $\sum_{\gamma} \langle \mu_i^2 \rangle$ in wavenumber-frequency space.

ence in n dependence already suggests the horizontal non-divergent character of the flow, since v is proportional to n in non-divergent motion.

An additional feature in Fig. 11 which calls for consideration, is the narrow ridge extending towards the high frequency (around periods of 5 days) and low wavenumber region. There is no counterpart of this feature in Fig. 12. Yanai and Maruyama (1966) found rather regular short period oscillations of wind direction between 240° and 300° in the atmospheric layer between 18.3 km and 21.3 km over the central equatorial Pacific during March-July 1958. From vertical time section analyses they found that the observed wind oscillation is an indication of large-scale waves of period about 5 days propagating westward at a speed about 23 m sec^{-1}, and hence of wavelength about 10,000 km. The ridge in Fig. 11 mentioned above is also associated with disturbances of this wavelength and period. Although there is no stratospheric region as such in our model, its upper level might reflect some of the lower stratospheric features of the real atmosphere. It is therefore of special interest to determine the extent to which the motions associated with the ridge in Fig. 11 are concentrated over the equatorial region. We can readily do so by examining the ratio $\mathcal{R}$ = ($\langle v_1^2 \rangle$ at equator)/ (latitudinal average of $\langle v_1^2 \rangle$), on a wavenumber-frequency-band plot. The values of $\mathcal{R}$ shown in Fig. 13 reach a maximum of about 2.2 at n = 3 and σ = 1/9 cycles per 12 hours.

To show the actual latitudinal dependence of these motions,

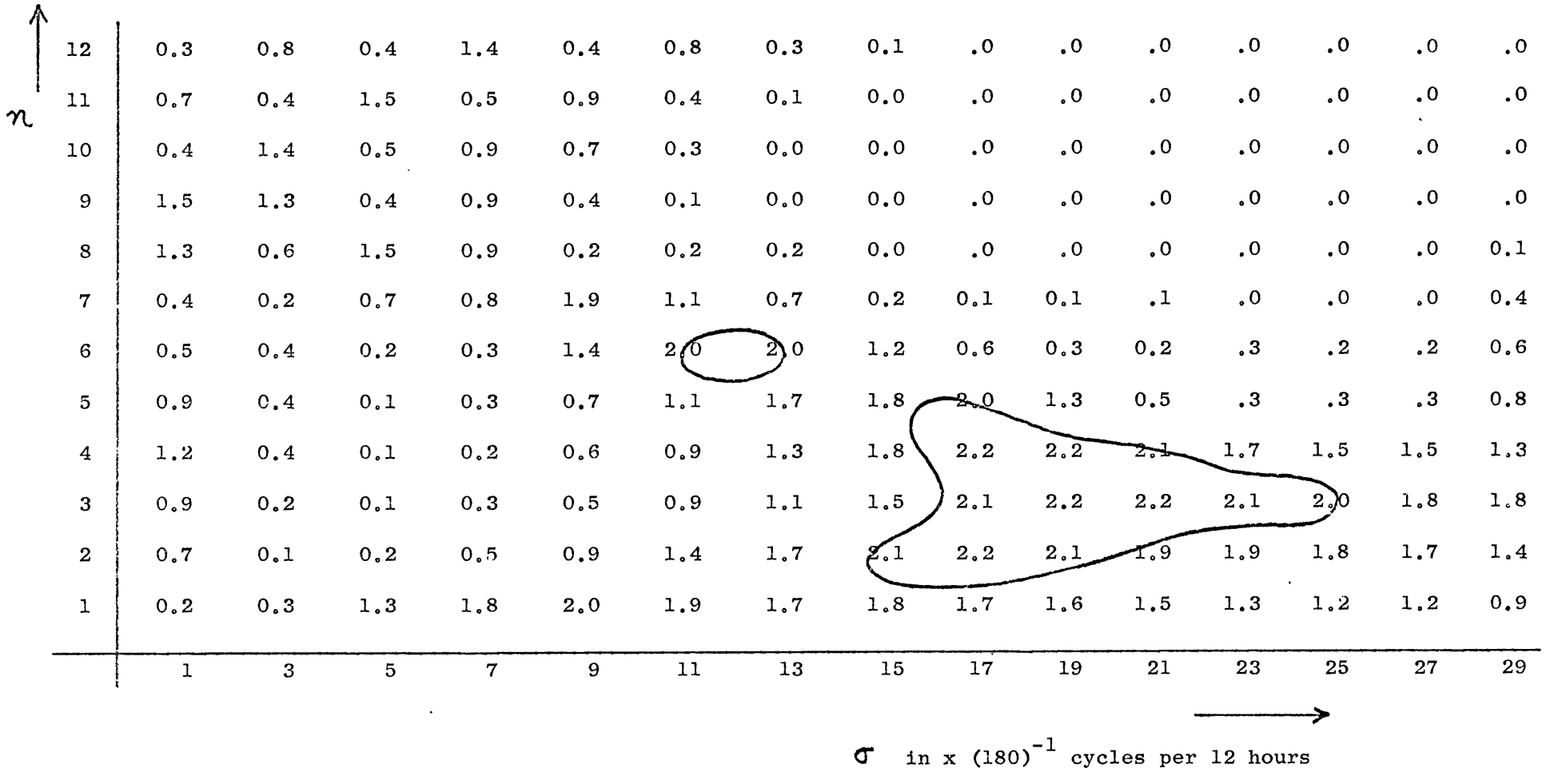

Figure 13. $\frac{(\text{. } \langle v_1^2 \rangle \text{ at equator})}{(\text{latitudinal average of } \langle v_1^2 \rangle)}$ in wave-frequency space.

$\langle v_1^2 \rangle$ for n = 5 and σ = 19/180 is plotted in Fig. 14. We see that this quantity drops by a factor of almost 5 from equator to 20°N. The latest report by Maruyama (1967) indicates that the observed waves are generally confined equatorward of 20°N. Furthermore the ridge in Fig. 11 evidently arises from the large values in the fundamental solutions (see Figs. 5 and 6) at those positive frequencies which are in the neighorhood of the internal and external Rossby waves of smallest latitudinal wavenumber which can be defined in a barotropic current. We may therefore conclude that the theoretical disturbances also have a westward propagation. In view of all these theoretical features, the dominant modes found at the equator of our model tropics appear to be the counterpart of the real phenomena reported by Yanai and Maruyama. If that is true, our computation suggests that such waves must occur quite often or else they would not contribute a sizeable variance. Furthermore since such waves in the model derive their energy from lateral forcing, their counterparts in the atmosphere may also be maintained in a similar manner.

Finally it is of some interest to examine the latitudinal dependence of two more detailed properties of $\langle v_1^2 \rangle$. Table 6 (i) shows at 4 latitudes (0, 10, 20 and 30°N) how the total contribution from 12 wavenumbers varies with frequency. Table 6(ii) shows at 4 latitudes how the total contribution from 15 frequency bands varies with wavenumber. As far as the frequency dependence is concerned, $\langle v_1^2 \rangle$ in the northern half of the model tropics has a maximum at period about 30 days and decreases monotonically with increasing frequency; whereas

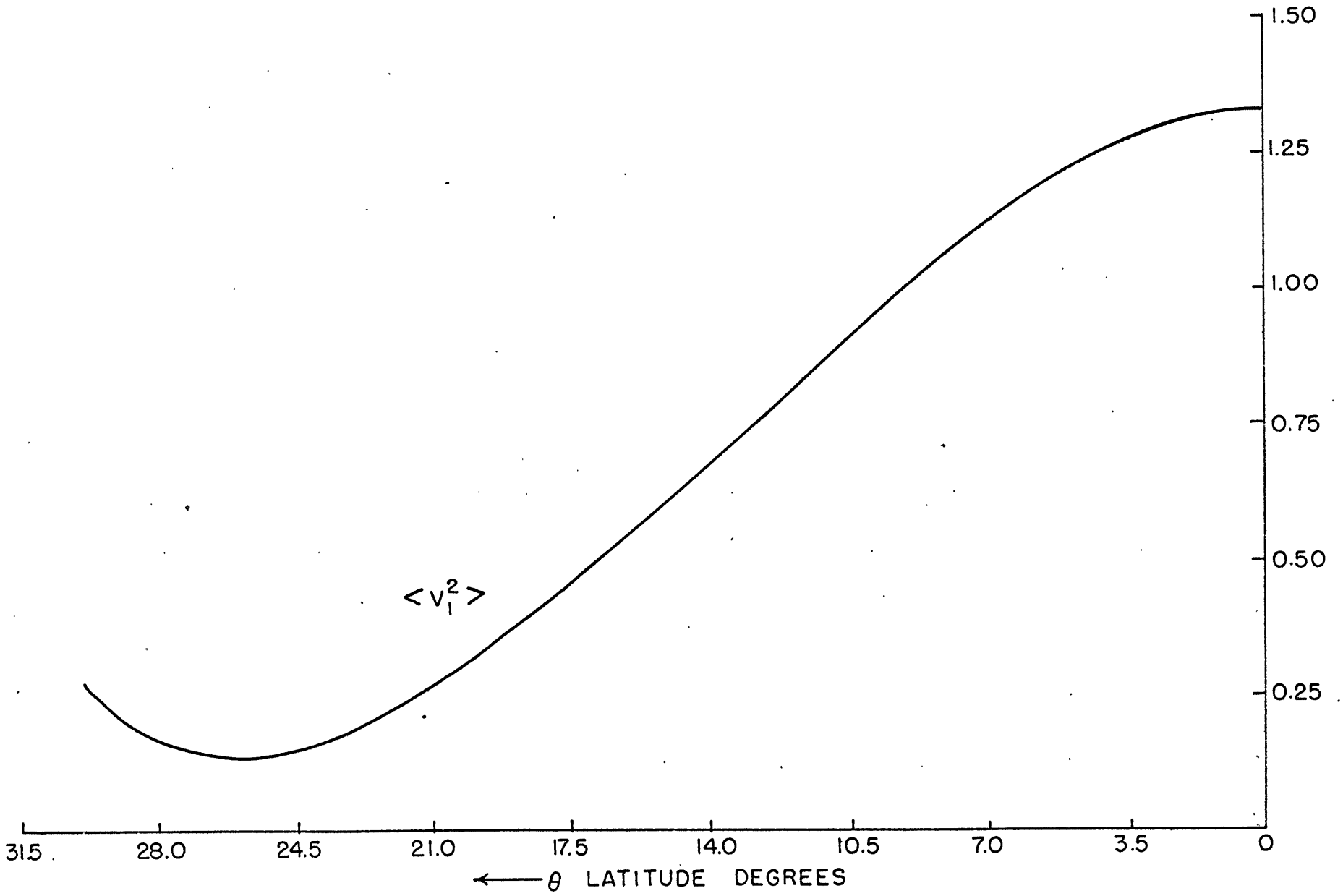

Fig. 14. Variance of meridional velocity at 250-mb level for n = 5 and σ = 19/180 cycles per 12 hours.

σ in $(180)^{-1}$ cycles per 12 hrs	0°N	10°N	20°N	30°N	(i)
1	19.4	6.8	22.0	8.0	
3	18.6	20.2	28.8	15.1	
5	8.3	27.0	26.1	12.9	
7	6.5	22.6	22.5	9.5	
9	3.1	4.9	5.9	7.6	
11	4.4	3.8	2.7	6.1	
13	1.7	1.4	1.1	4.0	
15	3.4	2.6	1.2	4.0	
17	.8	.6	.3	3.2	
19	2.3	1.7	.6	3.0	
21	1.9	1.3	.4	3.0	
23	3.0	2.1	.6	2.9	
25	2.8	2.0	.6	1.8	
27	.5	.4	.2	1.8	
29	.3	.2	.1	1.8	
Zonal Wavenumber	0°N	10°N	20°N	30°N	(ii)
1	.6	.8	.5	.4	
2	1.8	3.2	3.0	1.8	
3	7.8	8.9	7.1	3.7	
4	10.2	12.2	16.4	6.0	
5	8.0	16.0	16.1	9.8	
6	14.0	18.1	19.1	16.6	
7	11.3	19.2	21.6	14.5	
8	13.1	8.0	14.6	10.6	
9	5.8	5.1	7.0	9.3	
10	2.0	3.3	3.9	5.5	
11	1.9	2.0	2.9	4.2	
12	.7	.6	1.0	2.4	

Table 6. (i) $\langle v_i^2 \rangle$ summed over 12 wavenumbers at each frequency band of width 1/90 cycles per 12 hrs.

(ii) $\langle v_i^2 \rangle$ summed over 15 frequency bands for each wavenumber.

in the southern half of the model tropics it has a secondary maximum at periods about 5 days. The high frequency contributions to $\langle v_1^2 \rangle$ can be identified with the large-scale waves discussed previously in comparison with Yanai and Maruyama's observation. As far as the wavenumber dependence is concerned, $\langle v_1^2 \rangle$ at 30°N is mainly associated with wavenumbers from 5 to 9, whereas at lower latitudes it has significant contribution from more wavenumbers, particularly from the lower ones. Each of the corresponding results for $\langle u_1^2 \rangle$ does not qualitatively change with latitude and is therefore not presented. Most of the contributions to $\langle u_1^2 \rangle$ are associated with periods from 2 weeks to 40 days and with wavenumbers from 2 to 7. Observational values for these aspects of the statistics are missing, and no comparison can thus be made. However it should not be difficult to collect sufficient data for computing such statistics. In order to check the frequency dependence, we only need sufficiently long records of wind data at several stations located at or near the 3 internal latitudes. For checking the wavenumber dependence, on the other hand, we need good data coverage in longitude along those latitudes.

6.2 Variance of ω and temperature at the 500-mb level

Fig. 15 shows the theoretical value of the square root of $\langle \omega^2 \rangle$ at the 500-mb level of the model as a function of latitude. It drops from about 7×10^{-4} mb sec^{-1} at 30°N to about 2×10^{-4} mb sec^{-1} at 20°N and then decreases gradually to 1×10^{-4} mb sec^{-1} at the equator. This variation corresponds to a root mean square value of horizontal divergence

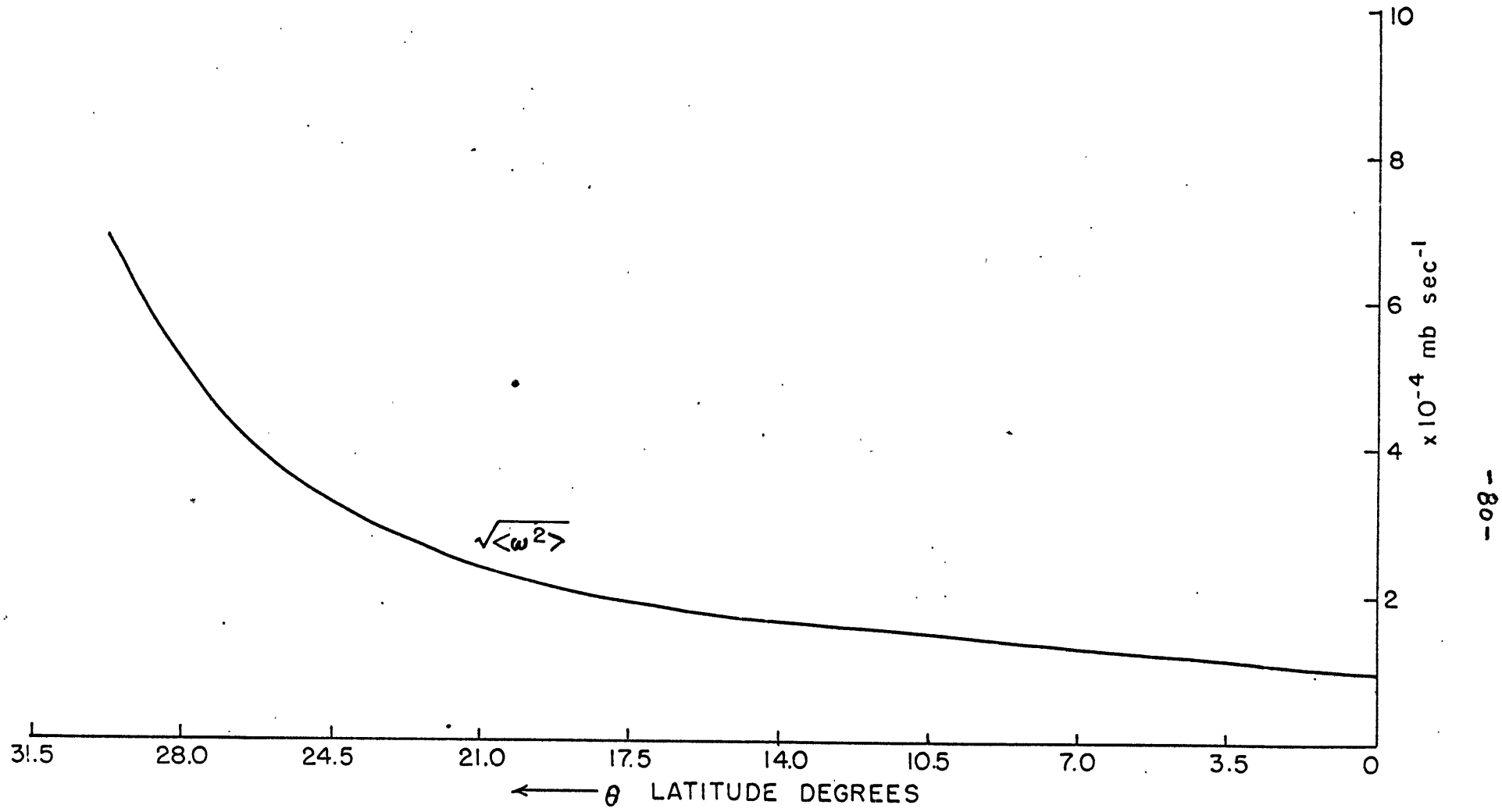

Fig. 15. Standard deviation of p-velocity ω at 500-mb level. $\sqrt{\langle \omega^2 \rangle}$

at either level of 1.4×10^{-6}, 0.4×10^{-6}, and 0.2×10^{-6} sec^{-1}. The value at $30^{o}N$ in the model is reasonable compared to the typical value in middle latitudes. Unfortunately there is no observed value for the tropical region. However the theoretical prediction of a decrease of horizontal divergence by a factor of 5 from subtropics to the tropics is again consistent with Charney's (1963) scale argument. The decrease of the Coriolis parameter requires smaller horizontal pressure and temperature gradients, and the approximately constant static stability is consistant with this only if ω decreases.

A small $\langle \omega^2 \rangle$ implies a small $\langle T^2 \rangle$ in the absence of local heating. Fig. 16 shows the latter as a function of latitude, together with the observed values collected by Peixoto (1960). The theoretical result does show a substantial decrease with latitude, and is therefore compatible with the result for $\langle \omega^2 \rangle$ mentioned above. The agreement between the observed value of $\langle T^2 \rangle$ and the theoretical values is very good, and thus leads one to believe that the theoretical value of $\langle \omega^2 \rangle$ should also be reasonably realistic. Since the variance of temperature is proportional to the eddy available potential energy, the theoretical result in Fig. 15 can then be interpreted as a decrease of eddy available potential energy with latitude in the model tropics. We may therefore expect only small energy conversions between the eddy available potential energy and the kinetic energy.

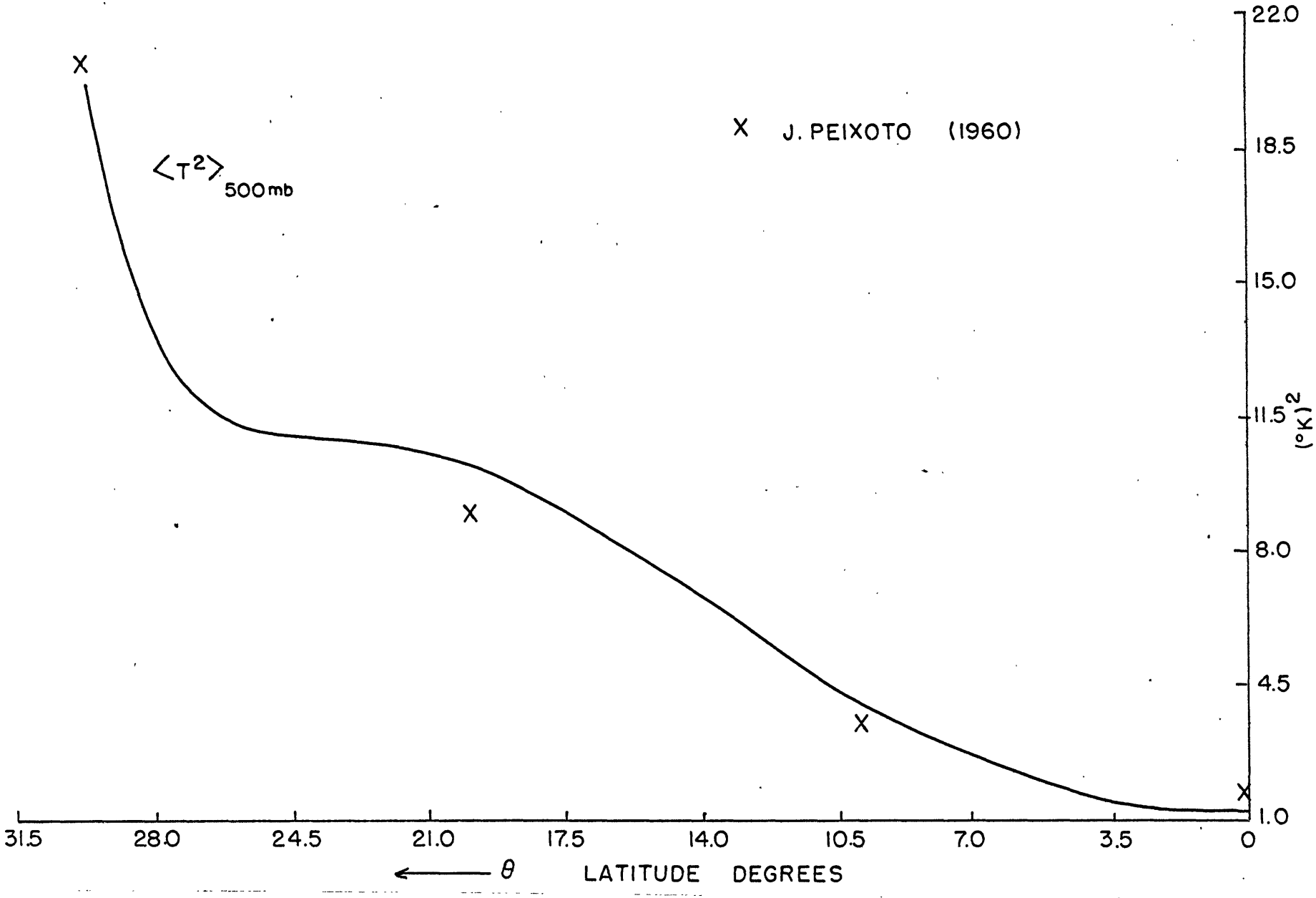

Fig. 16. Variance of temperature at 500-mb level. $\langle T^2 \rangle$.

6.3 Cross-latitude eddy fluxes of sensible heat, wave energy, and momentum

Fig. 17 shows $\frac{1}{R \ln 2} \left\langle \frac{v_1+v_2}{2}(\phi_1-\phi_2) \right\rangle$ where R is the gas constant for dry air, as a function of latitude. This is the eddy contribution to $\langle vT \rangle_{TOTAL}$ at 500 mb, in virtue of the hydrostatic approximation. The theoretical value is negative everywhere except near the northern boundary, with a maximum magnitude of about 0.7 ^{o}K m sec^{-1} at 20^{o}N. The observed values obtained by Kidson at M.I.T. and Peixoto (1960) are shown by circles and crosses respectively. The agreement between the theoretical and observed values is surprisingly good in view of the fact that this quantity has a very small magnitude. A negative value of $\langle vT \rangle$ means an equatorward flux of sensible heat by eddies which in turn represents a countergradient heat flux since the basic temperature gradient is poleward. Such a feature has also been reproduced in the numerical experiment by Smagorinsky, Manabe and Holloway (1965). It should be noted that a countergradient heat flux represents a rather severe constraint upon the energetics of the asymmetric motions in the model. This stems from the fact that it means a net conversion from eddy available potential energy to zonal available potential energy. Since radiation cooling is parameterized to destroy eddy available potential energy, it follows that the latter must be maintained by a net conversion from eddy kinetic energy. The latter in turn has to be replenished either by conversion from zonal kinetic energy or by an inflow of wave energy into the model tropics. All these aspects will be discussed in more detail later.

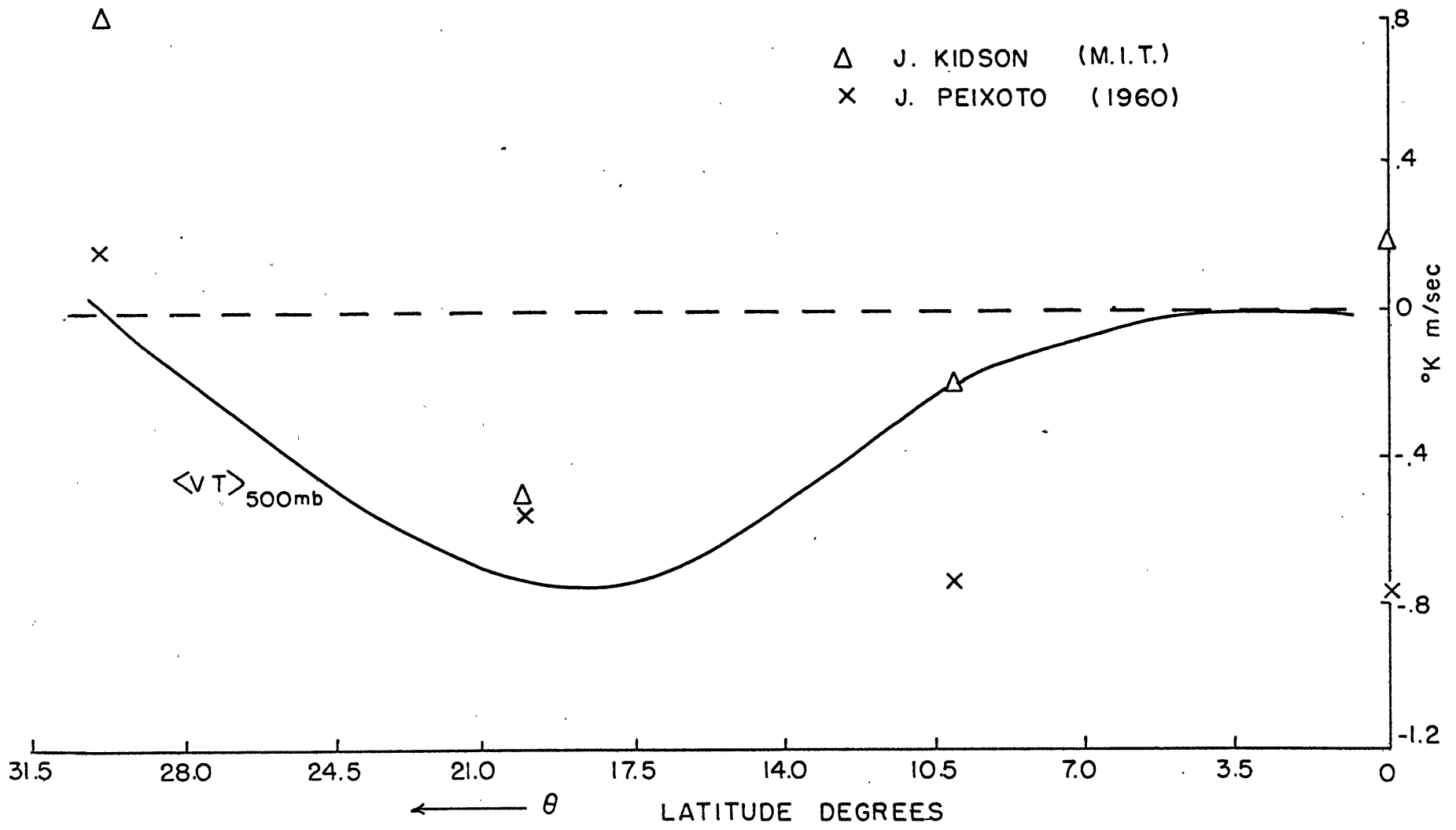

Fig. 17. Poleward eddy sensible heat flux per unit mass at 500-mb level, and observed values. $\langle vT \rangle$

Fig. 18 shows $\langle v_1 \phi_1 \rangle$ and $\langle v_2 \phi_2 \rangle$ as functions of latitude. These represent the poleward cross-latitude wave energy flux per unit mass in the model tropics at the 250-mb and 750-mb levels. The theoretical results are negative for both levels, increasing monotonically toward zero at the equator. The magnitude of $\langle v_1 \phi_1 \rangle$ is much larger than that of $\langle v_2 \phi_2 \rangle$. Such results imply a net equatorward flow of wave energy across the boundaries at $\pm 30^{\circ}$, primarily at the upper level. Thus the pressure work done on the model tropics by the lateral forcing at the two levels is equal to twice the value at 30°N, i.e. about 1600 $m^3 sec^{-3}$. There are no observed values to compare with this, although it is not at all unreasonable that this flux should be equatorward. Its magnitude in the model may be somewhat too large, since $\langle v_1^2 \rangle$ has been overpredicted. For the reason given in Section 6.1 we may expect some changes in this flux if a realistic lateral shear is added to the present basic current.

Fig. 19 shows the Reynolds stress terms $\langle u_1 v_1 \rangle$ and $\langle u_2 v_2 \rangle$ as functions of latitude. They are proportional to the poleward momentum flux by eddies at the 250- and 750-mb levels. They are positive at both levels, with $\langle u_1 v_1 \rangle$ much larger than $\langle u_2 v_2 \rangle$ except in the equatorial region where both decrease toward zero. The observed values obtained by Kidson at M.I.T. and Starr and White (1952, 1954) are also shown in Fig. 19. It is seen that while the theoretical result for $\langle u_2 v_2 \rangle$ agrees quite well with the observed value, that for $\langle u_1 v_1 \rangle$ is generally three times larger than the observed value. The exceptionally large value near 30°N is probably associated with the

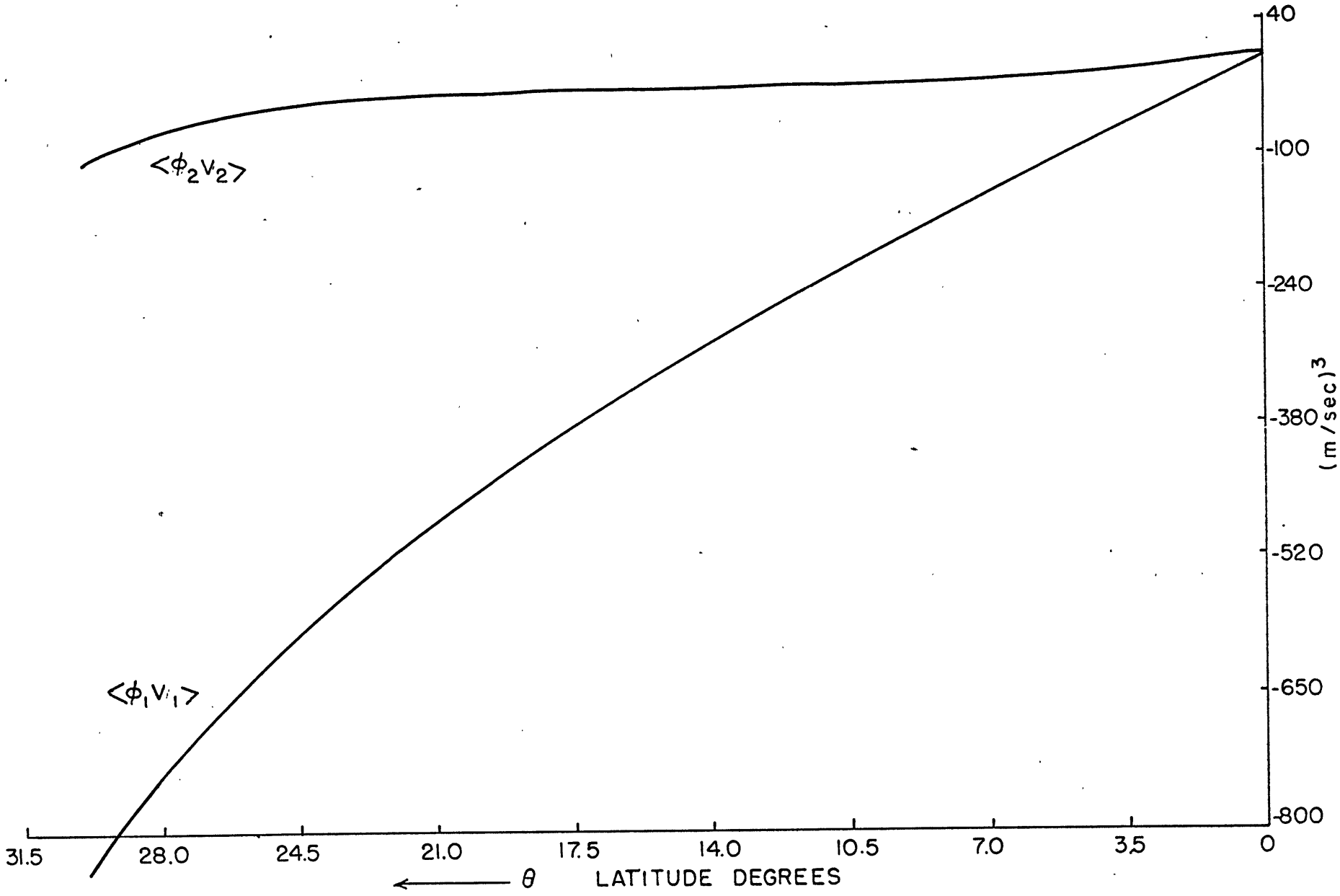

Fig. 18. Poleward wave energy flux per unit mass at 250-mb and 750-mb levels. $\langle v_1 \phi_1 \rangle$, $\langle v_2 \phi_2 \rangle$

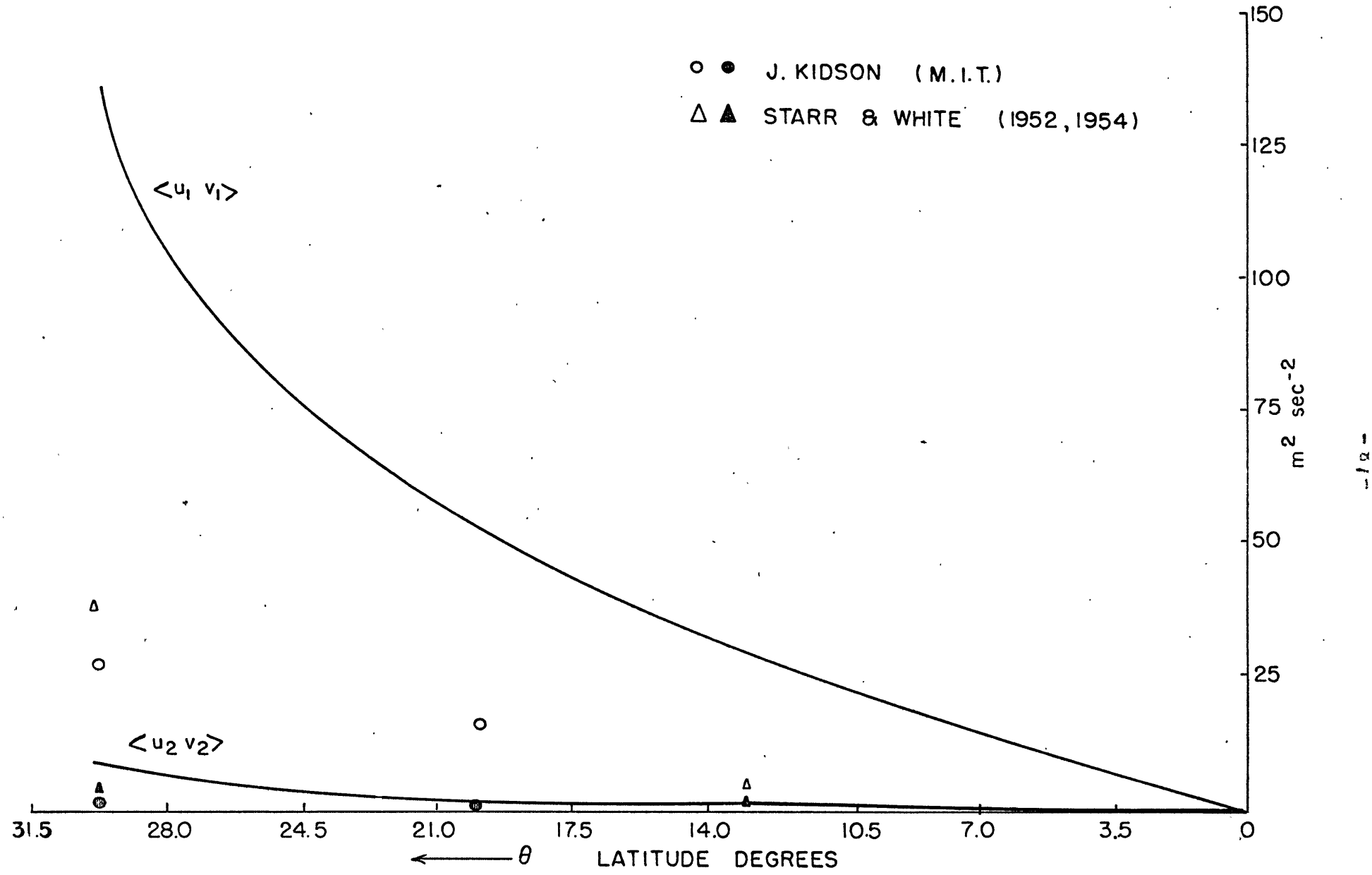

Fig. 19. Poleward momentum flux per unit mass at 250-mb and 750-mb levels. $\langle u_1 v_1 \rangle$, $\langle u_2 v_2 \rangle$

large value of $\langle u_1^2 \rangle$ in Fig. 9.

The general picture of equatorward wave energy flux, equatorward sensible heat flux and poleward momentum flux which has emerged from these calculations is consistent with the relation among these fluxes in stationary $(\sigma = 0)$ wave patterns which was deduced by Eliassen and Palm [1960; see their equation (10.5)], especially when the larger amplitudes in layer 1 of the model, with its positive $\bar{u}$, are considered.

6.4 Energetics of the asymmetric motions in the model tropics

The energetics of the disturbances are expressed mathematically by two equations, one describing the rate of change of eddy kinetic energy and the other the rate of change of eddy available potential energy. They are derived from (3.5) and are as follows:

$$\frac{\partial}{\partial t}(K_1+K_2) = -\left[(\bar{u}+\Lambda)\frac{\partial K_1}{\partial x} + (\bar{u}-\Lambda)\frac{\partial K_2}{\partial x}\right] \tag{6.1}$$

$$+ 2\Lambda(u_1+u_2)\omega - 2(\phi_1-\phi_2)\omega$$

$$- \left[\frac{\partial}{\partial x}(u_1\phi_1 + u_2\phi_2) + \frac{\partial}{\partial y}(v_1\phi_1 + v_2\phi_2)\right]$$

$$- 2\left[\alpha K_2 + \beta K_1 - \beta(u_1u_2 + v_1v_2)\right]$$

$$\frac{\partial}{\partial t} A = -\bar{u}\frac{\partial A}{\partial x} + \frac{\Lambda}{2\bar{\epsilon}} y (v_1+v_2)(\phi_1-\phi_2) \tag{6.2}$$

$$+ 2(\phi_1-\phi_2)\omega - 2\gamma A$$

where

$$K_1 = \frac{1}{2}(u_1^2 + v_1^2)$$

$$K_2 = \frac{1}{2}(u_2^2 + v_2^2)$$

$$A = \frac{1}{4\bar{\epsilon}}(\phi_1 - \phi_2)^2$$

$$\omega = -\frac{1}{2}\left(\frac{\partial u_1}{\partial x} + \frac{\partial v_1}{\partial y}\right)$$

The ensemble (and x-) average of these equations does not have the terms containing the time derivative and x-derivative:

$$0 = 2\Lambda\langle(u_1+u_2)\omega\rangle - 2\langle(\phi_1-\phi_2)\omega\rangle - \frac{d}{dy}\left[\langle v_1\phi_1\rangle + \langle v_2\phi_2\rangle\right]$$
$$- 2\left[\alpha\langle K_1\rangle + \beta\langle K_2\rangle - \beta\left(\langle u_1u_2\rangle + \langle v_1v_2\rangle\right)\right] \tag{6.3}$$

$$0 = \frac{\Lambda}{2\bar{\epsilon}}\gamma\langle(v_1+v_2)(\phi_1-\phi_2)\rangle + 2\langle(\phi_1-\phi_2)\omega\rangle - \frac{\gamma}{2\bar{\epsilon}}\langle(\phi_1-\phi_2)^2\rangle \tag{6.4}$$

Equations (6.3) and (6.4) have simple physical interpretation. The first two terms in (6.3) represent the net conversion from zonal kinetic energy and eddy available kinetic energy to eddy kinetic energy. The third term is the convergence of the wave energy flux, sometimes known as pressure work. The last term is the frictional dissipation. The first two terms of (6.4) represent the net conversion from the zonal available potential energy and eddy kinetic energy to eddy available potential energy. The third term is simply the destruction due to radiation. [A basic current

varying with y would introduce terms of the form $-\langle uv \rangle \frac{d\bar{u}}{dy}$.]

The numerical values of the four terms in (6.3) for our model tropics are shown in Fig. 20. The results indicate that the only supply of eddy kinetic energy in the model tropics is the pressure work, in other words through the equatorward flux of wave energy from the lateral boundaries. The other three terms are negative and hence represent sinks of eddy kinetic energy. The largest sink is the frictional dissipation. The conversion of eddy kinetic to eddy available potential energy is substantial between 13° and 25°N, whereas the conversion of eddy kinetic to zonal kinetic energy is very small everywhere. Hence the asymmetric disturbances in the model tropic have no internal source of eddy kinetic energy. The inflow of wave energy is more than enough to compensate for the frictional dissipation, with most of the residue converted to eddy available potential energy.

The numerical values of the three processes that constitute the eddy available potential energy balance are shown in Fig. 21. Here we find that its only positive source is the conversion from eddy kinetic energy. There is a small loss due to radiation and a larger loss from conversion to zonal available potential energy. The latter has a maximum at about 20°N. This is a necessary consequence of the equatorward eddy sensible heat flux found in subsection 6.3. This effect is sometimes dramatically referred to as a "refrigeration process," in the sense that the warmer part of the atmosphere is being warmed up by the advection of enthalpy by the motions. However the values in Figs. 20 and 21 show

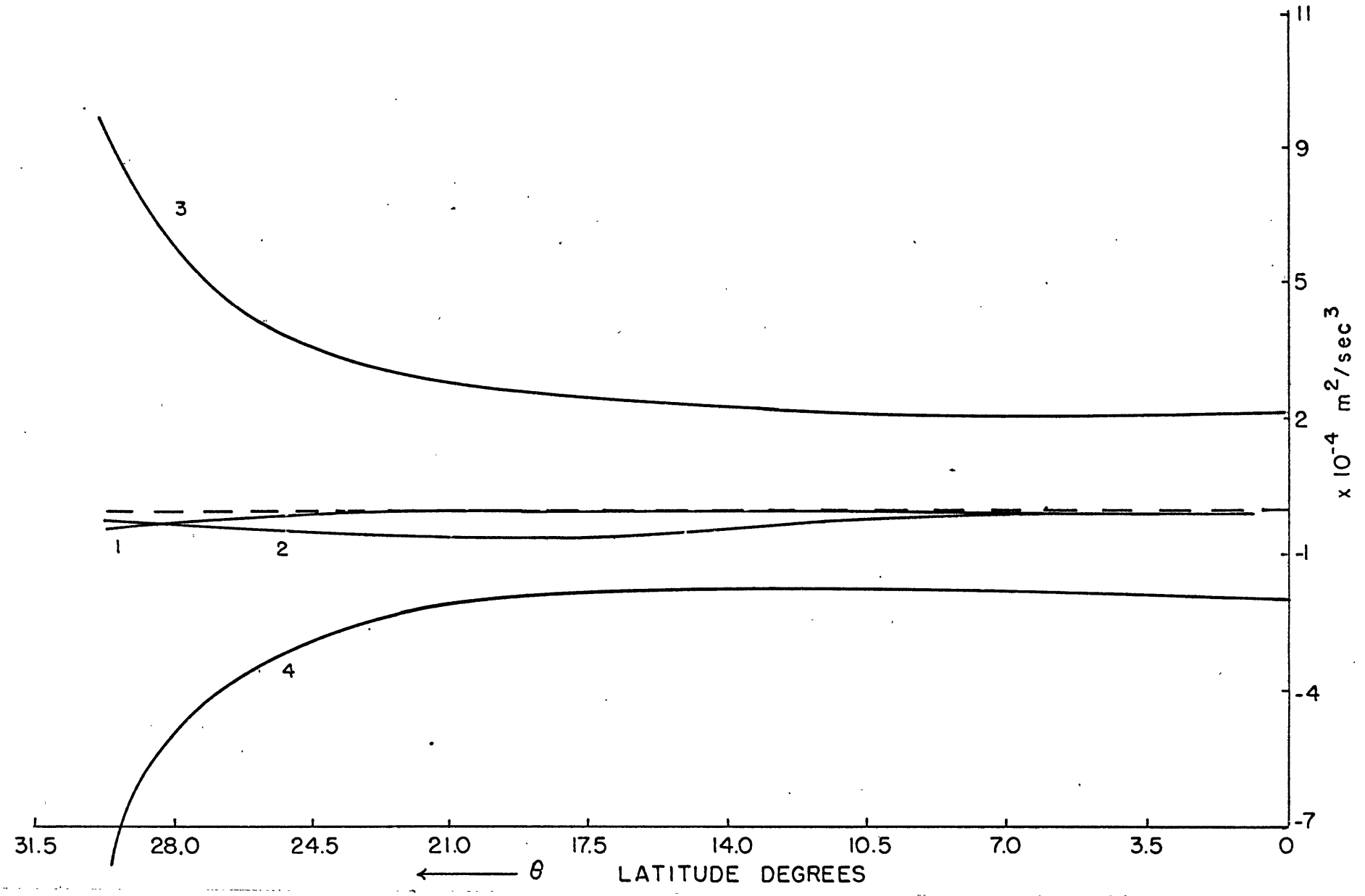

Fig. 20. Eddy kinetic energy (EKE) balance:

1. conversion from zonal kinetic energy to EKE,
2. conversion from eddy available potential energy to EKE,
3. pressure work, and
4. frictional dissipation.

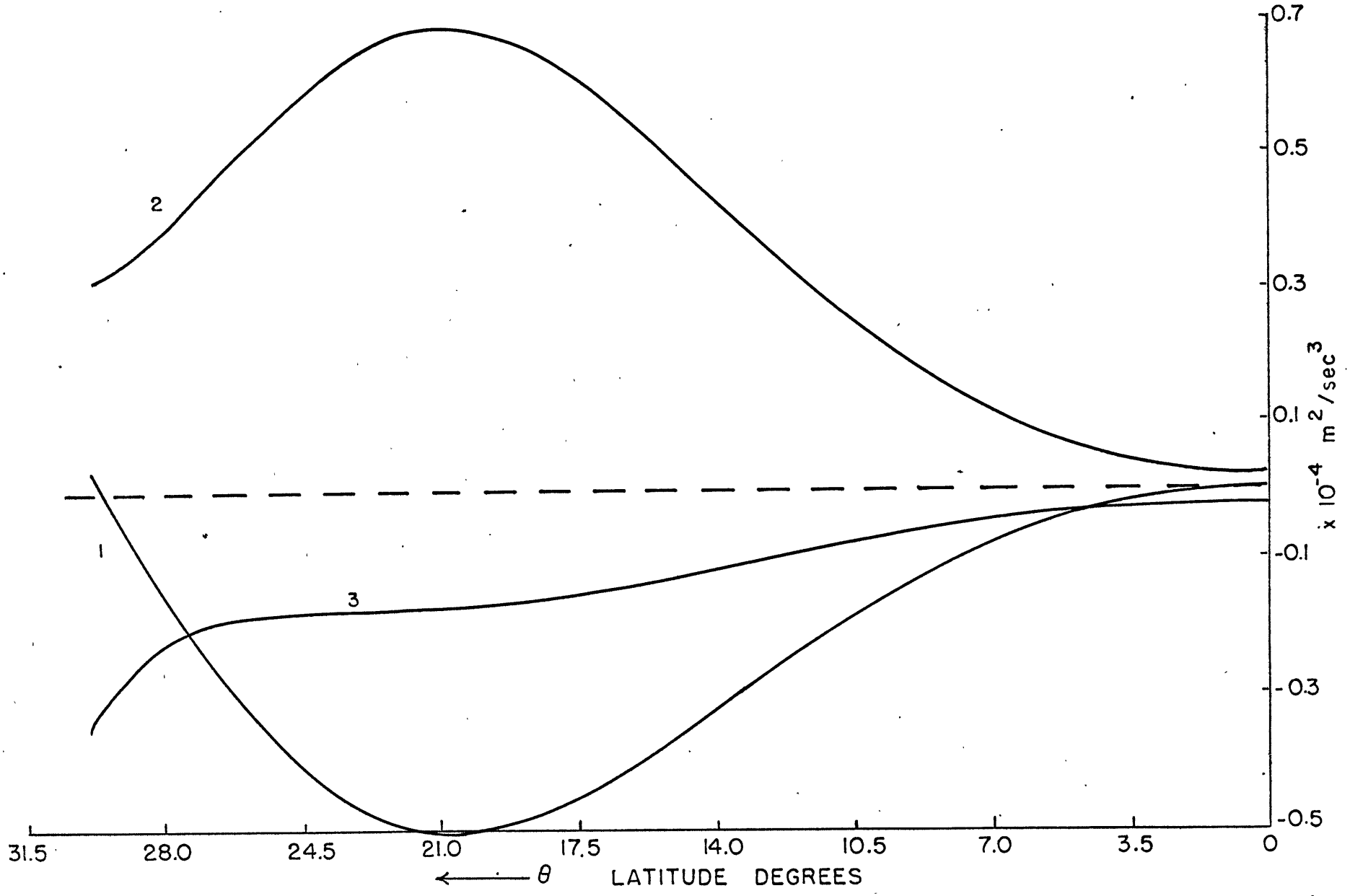

Fig. 21. Eddy available potential energy (EAPE) balance:

1. conversion from zonal available potential energy to EAPE,
2. conversion from eddy kinetic energy to EAPE, and
3. radiational loss.

that the amount of energy involved is small and that the refrigeration process is an inefficient one. As far as the asymmetric motions in the model tropic are concerned, their energetics may be summarized schematically in Fig. 22. This is an incomplete description of the energetics of

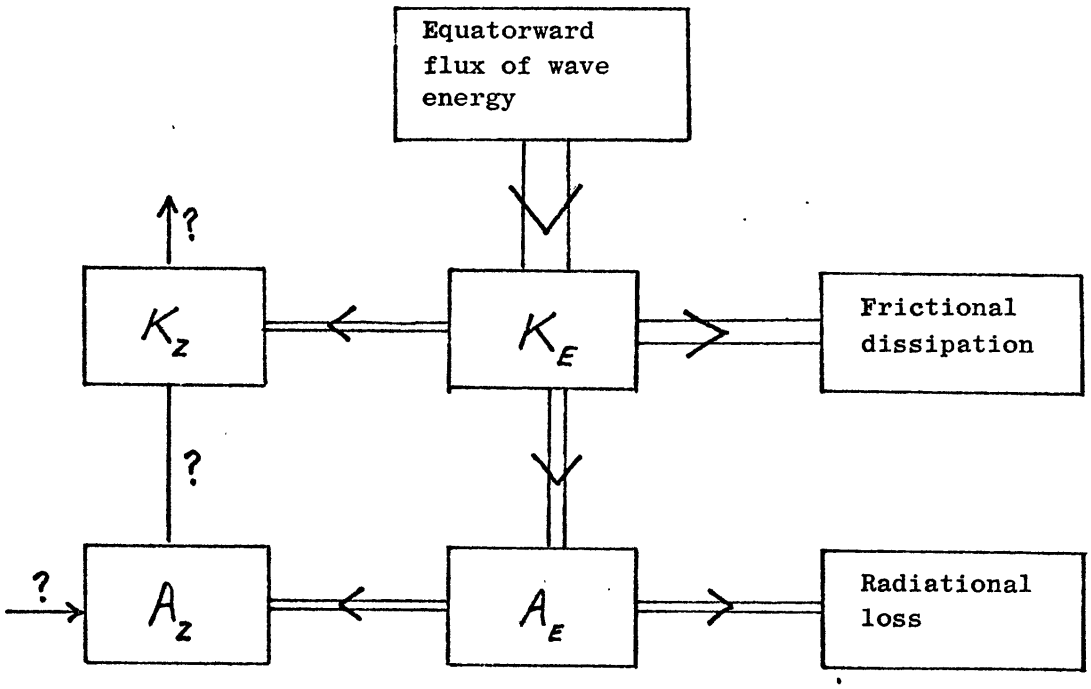

Figure 22. Energetics of the model tropic

the model tropics because it does not include the energetics of the zonally averaged circulation. But this is all the information that one can deduce from this model as it stands.

Now let us compare the theoretical results described above with the corresponding results obtained in other studies. Analysis of the energetics of tropical motions is sketchy; the handicap arising from the scattered data and the usual inability to determine the vertical

velocity reliably. If we want to check our theoretical results, we may however compare these with the computer-generated climatological data based upon a presumably realistic general circulation model. The obvious difficulty is that small-scale processes and condensation processes are only crudely incorporated in the existing models. Thus a comparison between the results from two crude models may not mean very much. The most sophisticated general circulation model thus far is the one designed by the Geophysical Fluid Dynamics Laboratory group under the direction of J. Smagorinsky in Washington, D.C. In the paper by Manabe and Smagorinsky (1967), the energetics for low latitudes in a dry and a wet numerical model are presented. They found that the results in the two cases were quite different. For example, while the conversion between eddy kinetic energy and eddy available potential energy is very small in the dry model, there is a strong conversion from the latter to the former in the wet model. But they also found in the wet model an unrealistically large conversion from zonal kinetic energy to eddy kinetic energy. They nevertheless conclude that the conversion of eddy available potential energy generated by the heat of condensation represents a realistic source of eddy kinetic energy in the tropics of their wet model. If condensation is indeed the main source of eddy kinetic energy in the real tropics, any dry model such as this one would be inappropriate. It is however conceivable that since precipitation tends to be concentrated along narrow regions in the tropics (as suggested by satellite cloud pictures), the release of latent heat by and large mainly affects the zonally averaged motions and has only minor effects upon the asymmetric motions over the

rest of the tropics. The intensity of the large-scale tropical eddies could then, as in the present model, depend upon the baroclinic activities in higher latitudes, and their presence in the tropics has only a secondary effect upon the mean state.

As a conclusion to this presentation of the predicted energetics it is important to emphasize again that the computed wave energy flux was into the tropics from the boundaries. (This was true not only for the ensemble average $\langle v_\ell \phi_\ell \rangle$ but was true at all σ for all n.) This result is consistant with our braod approach that the tropical eddy motions are primarily a response of the dynamically stable tropics to the unstable baroclinic processes in higher latitudes. If the model tropics had been dynamically unstable, on the other hand, statistical boundary forcing of the type used here could have resulted in an <u>outward</u> wave energy flux.

7. Concluding remarks

The prominent features of the statistical properties of the laterally-driven stochastic motions in the model tropics have been summarized in the Abstract. It was noted that the theoretical statistics are in general compatible with our limited knowledge about the eddy motions in the tropical atmosphere. In particular, the temperature variance and sensible heat flux are in good agreement with the observed values. But on the other hand, the variance of the meridional velocity and the poleward momentum flux at the upper level are overpredicted. It was suggested in Section 6 that one plausible reason for getting unrealistic results is our neglect of horizontal shear in the basic zonal currents in the model.

A brief heuristic discussion is now given about the effects of a basic horizontal shear in a simple case. Let us consider an inviscid, incompressible, homogeneous layer on a β-plane between $|y| \leq Y$. A basic current $\bar{u}$ is given, and the perturbations are then governed by

$$\frac{\partial u}{\partial x} + \frac{\partial v}{\partial y} = 0 \tag{7.1}$$

$$\left(\frac{\partial}{\partial t} + \bar{u}\frac{\partial}{\partial x}\right)\left(\frac{\partial v}{\partial x} - \frac{\partial u}{\partial y}\right) + B v = 0$$

where

$$\bar{u} = \bar{u}(y)$$

$$B = \beta - \frac{d^2\bar{u}}{dy^2}, \qquad \beta = \frac{df}{dy}$$

Plane wave solutions exist for (7.1)

$$u = Re\left\{ U e^{i(kx-\omega t)} \right\} \qquad k > 0$$
$$v = Re\left\{ V e^{i(kx-\omega t)} \right\} \qquad \infty > \omega > -\infty$$

The amplitude functions U and V are then governed by

$$U = \frac{i}{k}\frac{dV}{dy} \tag{7.2}$$

$$\frac{d^2V}{dy^2} + G(y)\,V = 0 \tag{7.3}$$

where

$$G(y) = \frac{B(y)}{\bar{u}(y) - \frac{\omega}{k}} - k^2$$

A somewhat realistic wind profile is a parabolic type

i.e. $\bar{u} = a + by^2$; $a<0$, $b>0$

Let us consider a profile where $2b$ is smaller than β . Then B becomes a positive constant. Then $G(y)$ is positive when $\bar{u}$, $\frac{\omega}{k}$ and $\frac{B}{k^2}$ are such that $0 < (\bar{u} - \frac{\omega}{k}) < \frac{B}{k^2}$ and is negative outside this range. It is clear from (7.3) that for the region where $G(y)$ is positive, V has oscillatory-like solutions, otherwise V has exponential-like solutions. Oscillatory

solutions mean cross-latitude wave propagation, and whether or not the amplitude increases equatcrward depends upon the variation of $G(y)$ with latitude. Exponential solutions imply reflection of wave by the basic current. Since equation (7.3) has the form of the time independent Schroedinger equation describing the wave function of a particle moving in a potential field, all the well-known conclusions about the behavior of the wave function in the presence of a simple potential barrier, or potential step-jump can be applied to the solution of V here. For a more realistic basic current, such as a parabolic profile, we probably have to use WKBJ solutions and long-wave approximation (Morse and Fashbach, 1953 pp. 1088-1095) in order to deduce the asymptotic properties of the solutions. However we can make a heuristic statement about the different effects of a parabolic basic current on forcing motions of eastward or westward phase propagation. The following diagrams show a schematic relative magnitude among $\frac{\beta}{k^2}$, $\bar{u}$, $\bar{u} - \frac{\omega}{k}$.

Waves of eastward phase propagation

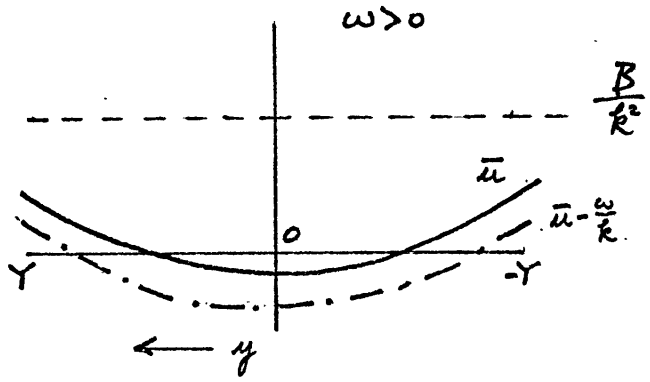

Waves of westward phase propagation

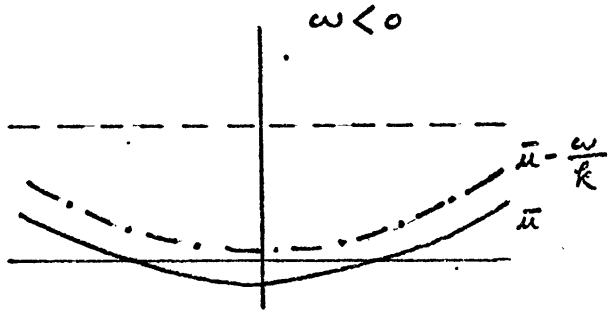

We can see that the condition for cross-latitude propagation

$$0 < \bar{u} - \frac{\omega}{k} < \frac{\beta}{k^2}$$

is in general more likely met by waves of westward phase propagation than those of eastward propagation. For short latitudinal wavelength, the amplitude V according to the WKBJ solution is then proportional to $G^{-\frac{1}{2}}$. The role of the basic current is then to permit only waves of certain ω and k combinations to propagate equatorward. The variation of $\bar{u}(y)$ makes this screening for different waves occur at different latitudes. As a result, one may expect a gradual variation with latitude of the velocity variances.

Although firm conclusions cannot be made from these qualitative arguments about effect on the statistical properties if a basic horizontal shear is incorporated in our model, the results presented in this thesis are encouraging enough to warrant further exploration.

Appendix A

This appendix shows the procedure of reducing the six spectral equations in (3.9) to two coupled equations in (3.10). We first eliminate dP_1 between the first and second equations of (3.9), dP_2 between the third and fourth equations, and $(dP_2 - dP_1)$ from the first, third and sixth equations. The result, together with the fifth equation of (3.9) is

$$
\begin{aligned}
&N_1\{dU_1\} + N_2\{dU_2\} + N_3\{dV_1\} + \beta n\, dV_2 = 0 \\
&N_2\{dU_1\} + N_4\{dU_2\} + \beta n\, dV_1 + N_5\{dV_2\} = 0 \\
&B_1\, dU_1 + B_2\, dU_2 + N_6\{dV_1\} + N_7\{dV_2\} = 0 \\
&n\, dU_1 + n\, dU_2 - iD\{dV_1\} - iD\{dV_2\} = 0
\end{aligned}
\qquad \text{(A.1)}
$$

The new symbols are

$$
\begin{aligned}
D &= d/dy \\
N_1 &= (s + 2n\Lambda - i\beta)D - ny \\
N_2 &= i\beta D \\
N_3 &= -i\left[D(\Lambda D - y) + n(s + n\Lambda - i\beta)\right] \\
N_4 &= (s - 2n\Lambda - i\alpha)D - ny \\
N_5 &= i\left[D(\Lambda D + y) - n(s - n\Lambda - i\alpha)\right]
\end{aligned}
$$

$$N_6 = i\left[\left((s-i\gamma)\Lambda - 2n\bar{\epsilon}\right)D - (s-i\gamma-n\Lambda)y\right]$$

$$N_7 = i\left[(s-i\gamma)\Lambda D + (s-i\gamma+n\Lambda)y\right]$$

$$B_1 = 2\bar{\epsilon}n^2 - (s-i\gamma)(s+2n\Lambda-i2\beta)$$

$$B_2 = (s-i\gamma)(s-2n\Lambda-i(\alpha+\beta))$$

We next eliminate dU_1 from the four equations in (A.1)

$$n(N_2-N_1)\{dU_2\} + (nN_3 + iN_1D)\{dV_1\} + (n^2\beta+iN_1D)\{dV_2\} = 0$$

$$n(N_4-N_2)\{dU_2\} + (n^2\beta + iN_2D)\{dV_1\} + (nN_5+iN_2D)\{dV_2\} = 0 \qquad \text{(A.2)}$$

$$n(B_1-B_2)\,dU_2 - (nN_6+iB_1D)\{dV_1\} - (nN_7+iB_1D)\{dV_2\} = 0$$

Finally we can eliminate dU_2 from the three equations in (A.2):

$$L_1\{dV_1\} + L_2\{dV_2\} = 0$$

$$L_3\{dV_1\} + L_4\{dV_2\} = 0 \qquad \text{(A.3)}$$

L_j (j = 1,2,3,4) are four second-order differential operators in y:

$$L_j = a_j\frac{d^2}{dy^2} + b_j\, y\frac{d}{dy} + c_j + d_j\, y^2$$

where a_j, b_j, c_j and d_j are functions of the parameters defined as follows.

Define

$$B_3 = i\beta$$

$$f_1 = s + 2n\Lambda -$$

$$f_2 = -n\Lambda$$

$$f_3 = \frac{1}{n} - s - n\Lambda$$

$$f_4 = n\Lambda(s - i$$

$$f_5 = -s + n\Lambda +$$

Then we can write

$$a_1 = \frac{1}{n^2}[f_1($$

$$a_2 = \frac{1}{n^2}[f_1($$

$$a_3 = \frac{1}{n^2}[g_1($$

$$a_4 = \frac{1}{n^2}[g_1($$

$$b_1 = \frac{1}{n}[f_5$$

$$b_2 = \frac{1}{n}[g_5$$

$$b_3 = \frac{1}{n}[f_5$$

$$b_4 = \frac{1}{n}[g_5$$

Define

$$B_3 = i\beta$$

$$f_1 = s + 2n\Lambda - i\beta \qquad g_1 = s - 2n\Lambda - i\alpha$$

$$f_2 = -n\Lambda \qquad g_2 = n\Lambda$$

$$f_3 = \frac{1}{n} - s - n\Lambda + i\beta \qquad g_3 = \frac{1}{n} - s + n\Lambda + i\alpha$$

$$f_4 = n\Lambda(s - i\alpha) - 2n^2\bar{\epsilon} \qquad g_4 = n\Lambda(s - i\alpha)$$

$$f_5 = -s + n\Lambda + i\alpha \qquad g_5 = s + n\Lambda - i\alpha$$

Then we can write

$$a_1 = \frac{1}{n^2}\left[f_1(f_4 + B_2) - (B_1 - B_2)f_2 - B_3(f_4 + B_1)\right]$$

$$a_2 = \frac{1}{n^2}\left[f_1(g_4 + B_2) - B_3(g_4 + B_1)\right]$$

$$a_3 = \frac{1}{n^2}\left[g_1(f_4 + B_1) - B_3(f_4 + B_2)\right]$$

$$a_4 = \frac{1}{n^2}\left[g_1(g_4 + B_1) + (B_1 - B_2)g_2 - B_3(g_4 + B_2)\right] \qquad \text{(A.4)}$$

$$b_1 = \frac{1}{n}\left[f_5(f_1 - B_3) - f_4 - B_1\right]$$

$$b_2 = \frac{1}{n}\left[g_5(f_1 - B_3) - g_4 - B_2\right]$$

$$b_3 = \frac{1}{n}\left[f_5(g_1 - B_3) - f_4 - B_1\right]$$

$$b_4 = \frac{1}{n}\left[g_5(g_1 - B_3) - g_4 - B_2\right]$$

$$c_1 = \frac{1}{n} f_5 (f_1 - B_3) - (B_1 - B_2) f_3$$

$$c_2 = \frac{1}{n} f_1 g_5 + B_3 \left(B_1 - B_2 - \frac{g_5}{n}\right)$$

$$c_3 = \frac{1}{n} g_1 f_5 + B_3 \left(-B_1 + B_2 - \frac{f_5}{n}\right)$$

$$c_4 = \frac{1}{n} g_5 (g_1 - B_3) + (B_1 - B_2) g_3$$

$$d_1 = d_3 = -f_5$$

$$d_2 = d_4 = -g_5$$

dU_2 is given in terms of dV_1 and dV_2 by the third equation of (A.2),

$$dU_2 = M_1\{dV_1\} + M_2\{dV_2\}$$

$$M_1 = \frac{1}{n(B_1 - B_2)} (n N_6 + i B_1 D) \quad ; \quad M_2 = \frac{1}{n(B_1 - B_2)} (n N_7 + i B_1 D) \tag{A.5}$$

and the fourth equation of (A.1) then gives dU_1 in terms of dU_2, dV_1 and dV_2 :

$$dU_1 = A_1 dU_2 + M_3\{dV_1\} + M_4\{dV_2\} \tag{A.6}$$

$$A_1 = -1 \quad ; \quad M_3 = \frac{i}{n} D \quad ; \quad M_4 = \frac{i}{n} D$$

Finally we obtain dP_1 and dP_2 from the first and third equations of (3.9):

$$dP_1 = A_2 dU_1 + A_3 dU_2 + M_5\{dV_1\} \tag{A.7}$$

$$A_2 = \frac{-1}{n} (\Lambda + 2n\Lambda - i\beta) \quad ; \quad A_3 = -\frac{i\beta}{n} \quad ;$$

$$M_5 = \frac{i}{n} (\Lambda D - y)$$

$$dP_2 = A_3\, dU_1 + A_4\, dU_2 + M_6\{dV_2\}$$

$$A_4 = \frac{-1}{n}(\Delta - 2n\Lambda - i\alpha)$$

$$M_6 = \frac{-i}{n}(\Lambda D + y) \qquad \text{(A.8)}$$

Equations (A.3) to (A.8) constitute the complete set of differential equations and kinematic relations in our model. They are referred to in (3.10) and (3.11) of Section 3.

Appendix B

A graphical method is deviced to determine the values of Γ that satisfy

$$\text{either} \quad {}_1F_1\left(\tfrac{1}{2}\Gamma+\tfrac{1}{4}, \tfrac{1}{2}, \tfrac{1}{2}z_+^2\right) = 0$$

$$\text{or} \quad {}_1F_1\left(\tfrac{1}{2}\Gamma+\tfrac{3}{4}, \tfrac{3}{2}, \tfrac{1}{2}z_+^2\right) = 0 \qquad \text{(B.1)}$$

where ${}_1F_1(a,b,x)$ is confluent hypergeometric function. This graphical method is partly based upon two properties of this function concerning the distribution of its zeros, which are stated as follows. (Ref. Slater, 1960).

(1) ${}_1F_1(a,b,x) \geq 1$ for $x \geq 0$, $b > 0$, $a > 0$

(2) ${}_1F_1(a,b,x)$ has k zeros when

$x > 0$, $b > 0$, $a = -k+\eta < 0$ where $0 < \eta < 1$

According to the first property, (B.1) clearly cannot be satisfied if $\Gamma \geq -\frac{1}{2}$. The second property enables us to foretell the number of values of Γ within a given range, $\Gamma_0 \leq \Gamma < -\frac{1}{2}$, that satisfy (B.1) for a given z_+.

It is also known that, for any positive integer m, we have the relations:

$$
{}_1F_1\left(-m, \tfrac{1}{2}, \tfrac{1}{2}z^2\right) = \frac{m!}{(2m)!}\left(-\tfrac{1}{2}\right)^{-m} He_{2m}(z)
$$

$$
{}_1F_1\left(-m, \tfrac{3}{2}, \tfrac{1}{2}z^2\right) = \frac{m!}{(2m+1)!}\left(-\tfrac{1}{2}\right)^{-m} He_{2m+1}(z) \qquad \text{(B.2)}
$$

$$
He_m(z) = (-1)^m \sqrt{2\pi}\, e^{\frac{z^2}{2}}\, \mathcal{E}^{(m)}(z)
$$

where

$He_m(z)$ is the Hermite polynomial of degree m

$\mathcal{E}^{(m)}(z) \equiv \dfrac{d^m}{dz^m}\left(\dfrac{1}{\sqrt{2\pi}}\, e^{-\frac{z^2}{2}}\right)$ is the $(m+1)^{\text{th}}$ derivative of the "error function". Therefore the zeros of $\mathcal{E}^{(2m)}(z)$ coincide with those of ${}_1F_1\left(-m, \tfrac{1}{2}, \tfrac{1}{2}z^2\right)$, and the zeros of $\mathcal{E}^{(2m+1)}(z)$ coincide with those of ${}_1F_1\left(-m, \tfrac{3}{2}, \tfrac{1}{2}z^2\right)$.

Fortunately the zeros of $\mathcal{E}^{(k)}$, $k = 1, 2, \cdots, 20$ can be found in the mathematical table, Harvard, 23 (1952). We now make use of these known zeros to device a graphical method to determine the first several zeros of ${}_1F_1\left(\tfrac{1}{2}\Gamma + \tfrac{1}{4}, \tfrac{1}{2}, \tfrac{1}{2}z_+^2\right)$ and of ${}_1F_1\left(\tfrac{1}{2}\Gamma + \tfrac{3}{4}, \tfrac{3}{2}, \tfrac{1}{2}z_+^2\right)$. In particular, we use the zeros for $k = 2, 4, \cdots, 20$ in determining the former and those for $k = 1, 3, \cdots, 19$ the latter.

A family of curves are drawn in Fig. 23 linking the zeros of the derivative of even orders of the "error function". These curves can be thought of as the loci of the zeros of ${}_1F_1(a, \frac{1}{2}, \frac{1}{2}\zeta^2)$. This interpretation is verified by the fact that the least positive zeros of this function at thirteen values of a , obtained from Slater (1960), fall onto the first curve. Each curve is drawn asymptotically towards an upper bound at a negative integer, so that the property (2) cited above concerning the number of zeros is not violated. Now suppose a value of ζ_+ is given as represented by the dotted line. The zeros of ${}_1F_1(a, \frac{1}{2}, \frac{1}{2}\zeta_+^2)$ are then the intersecting points between the dotted line and the family of curves. From the value of a of those points we can easily determine the associated values of Γ . Fig. 24 is a similar plot for determining the values of Γ that make ${}_1F_1(\frac{1}{2}\Gamma + \frac{3}{4}, \frac{3}{2}, \frac{1}{2}\zeta_+^2)$ equal to zero. ζ_+ is equal to 2.91 in our model tropics.

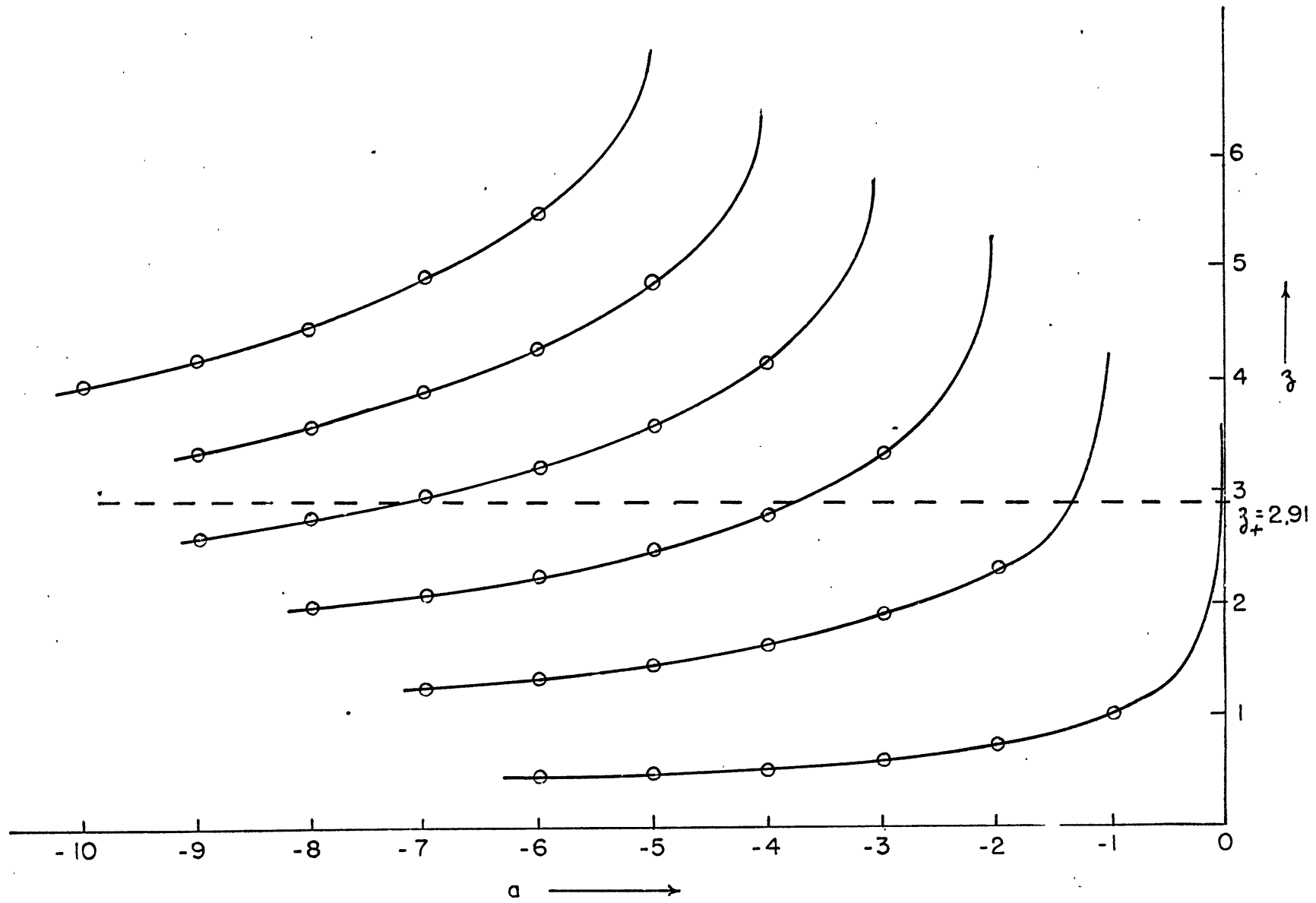

Fig. 23. Loci of the zeros of confluent hypergeometric function, ${}_1F_1(a, 1/2, \frac{1}{2}z^2)$
o zeros of $(2m)^{th}$ derivatives of the error function when a = -m.

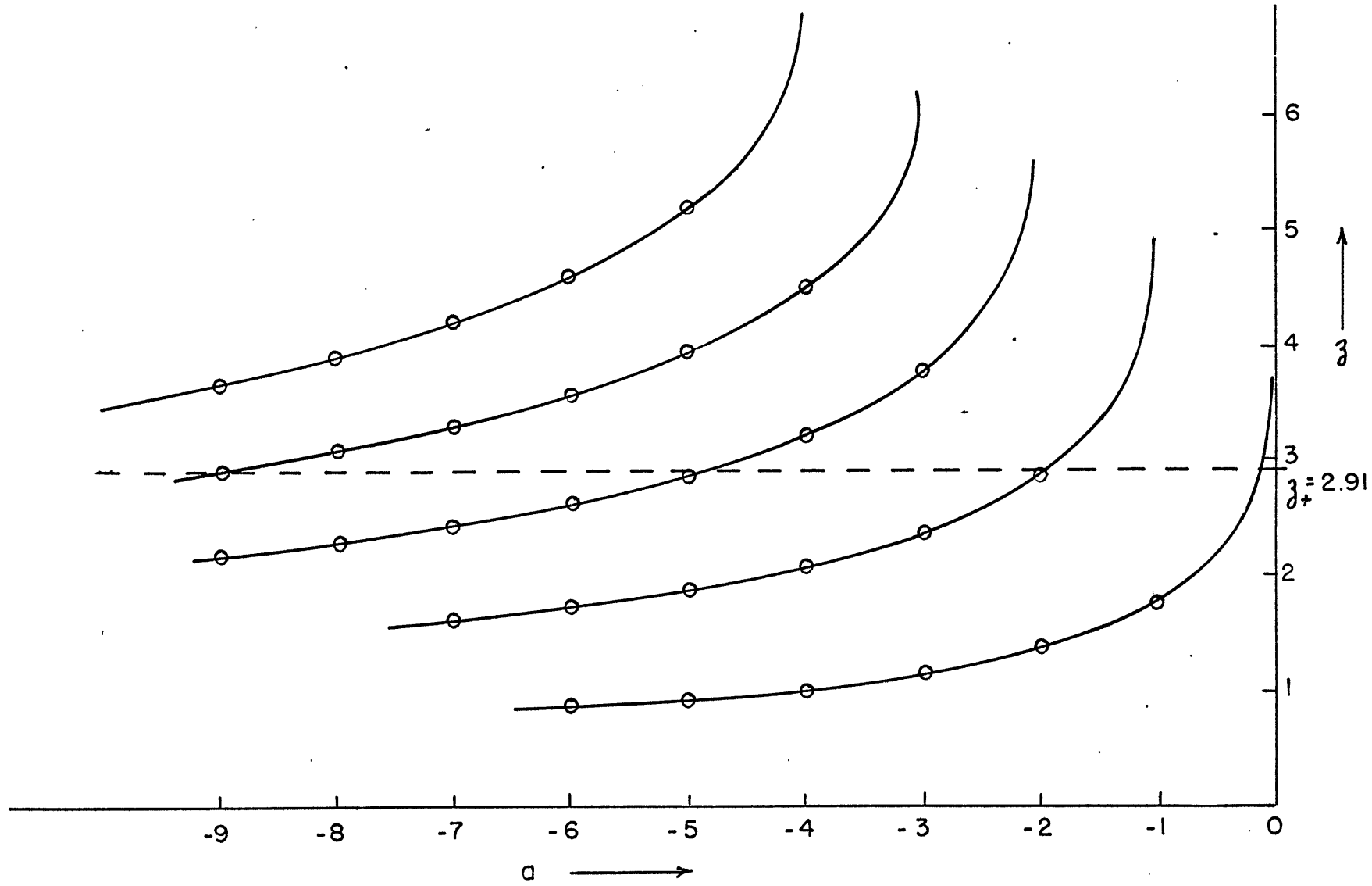

Fig. 24. Loci of the zeros of confluent hypergeometric function, ${}_1F_1(a, 3/2, \frac{1}{2}z^2)$
o zeros of $(2m+1)^{th}$ derivatives of the error function when a = -m.

Appendix C

A band-pass recursive filter is designed for filtering the discrete time series of the spatial Fourier components of the streamfunction at 30^{o}N discussed in Section 4. By filtering a time series recursively, we mean that each output point of the filtered sequence is computed as a weighted sum of the input points plus a weighted sum of previously computed output points. This is an alternative technique to the usual digital convolution, and is found in most cases significantly more efficient than the latter, Shanks (1967).

This recursive technique is based on the Z-transform representation of the convolution operation on a discrete time series.

$$Y(z) = F(z)\,X(z) \tag{C.1}$$

where

$$X(z) = x_0 + x_1 z + \cdots + x_M z^M$$

$$F(z) = f_0 + f_1 z + \cdots + f_N z^N$$

$$Y(z) = y_0 + y_1 z + \cdots + y_{N+M} z^{N+M}$$

They are the corresponding Z-transforms of the following sequences:

$\{x_0, x_1, \cdots, x_M\}$ input series

$\{f_0, f_1, \cdots, f_N\}$ filter weighting function

$\{y_0, y_1, \cdots, y_{N+M}\}$ output series

Z can be thought of as a delay operator. We specifically consider filters whose Z-transform is a rational function of Z. In other words, $F(z)$ is expressible as a ratio of two polynomials in .

$$F(z) = \frac{A(z)}{B(z)} = \frac{a_0 + a_1 z + \cdots + a_N z^N}{b_0 + b_1 z + \cdots + b_M z^M}$$

The amplitude and phase response of the digital filter can be determined by evaluating $F(z)$ at the unit circle in the Z-plane, i.e. at $|z| = 1.0$, (Treitel and Robinson, 1964). Values of z along the unit circle correspond to values of real frequency. In particular, $Z = 1.0 + i\,0.0$ corresponds to zero frequency and $Z = -1.0 + i\,0.0$ to the Nyquist frequency ω_N. Frequencies linearly distributed between zero and ω_N correspond to points linearly distributed on the upper half of the unit circle. Hence we can control the behavior of the filter by choosing the number and the location of the zeros and poles of $F(z)$.

The time series in our study have a sampling interval of 12 hours, and should have at least a strong annual component. Hence we need a filter that can eliminate the components of a period shorter than 1 day or longer than half a year. The simplest recursive filter that has such properties is one that has two zeros, one at $Z = 1.0 + i\,0.0$ and the other at $Z = -1.0 + i\,0.0$. In order to have as small attenuation as possible for the intermediate components, we need add at least two poles outside the unit circle on the real axis of the Z-plane. Such a simple filter is used in this study. It is shown in Fig. 25.

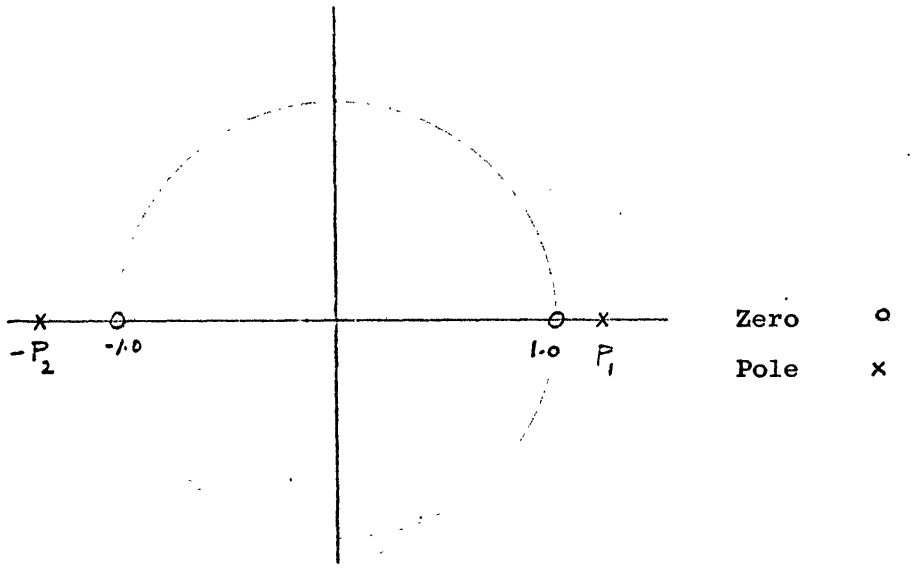

Figure 25. Z -plane.

$$F(z) = \frac{(1-z)(1+z)}{(P_1-z)(P_2+z)}$$

where

$$\alpha_1 = \frac{1}{P_1}$$

$$\alpha_2 = \frac{1}{P_2}$$

$$= \alpha_1 \alpha_2 (1-z^2)\left[1+(\alpha_1-\alpha_2)z - \alpha_1\alpha_2 z^2\right]^{-1}$$

The amplitude response of the filter can be computed by

$$\left| \frac{\alpha_1 \alpha_2 (1-z^2)}{1+(\alpha_1-\alpha_2)z - \alpha_1\alpha_2 z^2} \right| \quad \text{at} \quad |z| = 1.0 \qquad \text{(C.3)}$$

A filtering operation introduces a phase change to the input series as well as the amplitude attenuation given by (C.3). One way to insure zero phase change is to filter the time series first with a time-forward operation and then to filter the subsequent series with a time-reversed operation. The recursion equation for time-forward filtering with a rational filter specified by (C.2) is:

$$y_n = \alpha_1\alpha_2\left(x_n - x_{n-2} + \left(\frac{1}{\alpha_2} - \frac{1}{\alpha_1}\right)y_{n-1} + y_{n-2}\right) \qquad \text{(C.4)}$$

The corresponding equation for a time-reversed filtering is

$$y_n = \alpha_1\alpha_2\left(x_n - x_{n+2} + \left(\frac{1}{\alpha_2} - \frac{1}{\alpha_1}\right)y_{n+1} + y_{n+2}\right) \qquad \text{(C.5)}$$

The net effect of filtering a series first with (C.3) and then with (C.4) is to introduce zero phase and an amplitude attenuation equal to the square of (C.3). α_1 and α_2 used in the filter for this study are chosen to be 0.938 and 0.917 respectively. The power response as a result of our filtering procedure is shown in Fig. 26. It is seen that the attenuation factor is about 0.7 between frequency range from 0.03 to 0.3, and has a fairly sharp cut-off beyond these limits.

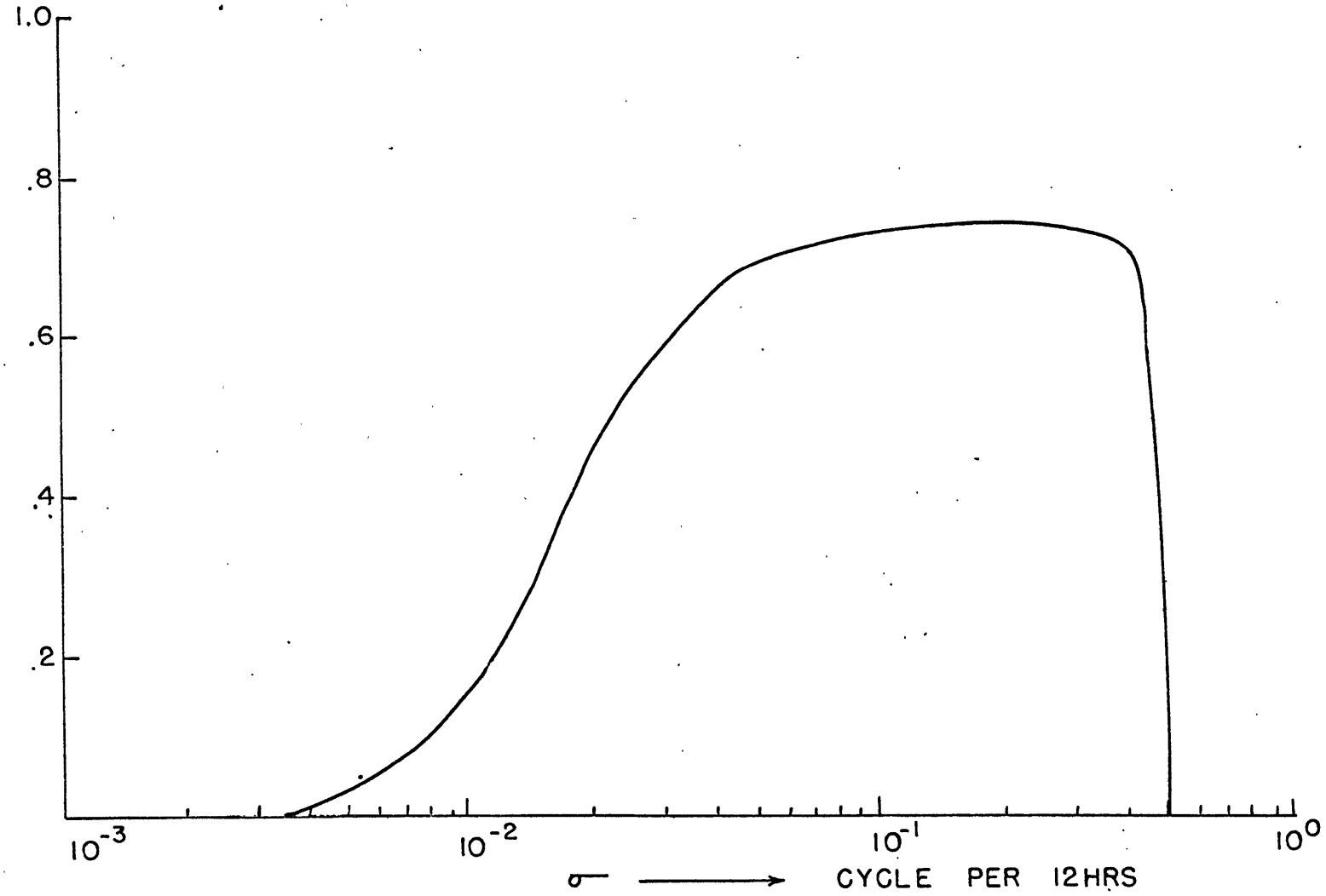

Fig. 26. Power response of the prefiltering operation.

Appendix D

This appendix gives a complete listing of the statistical boundary conditions F_j , j = 1,2,3,4 for n = 1 to 12 and each frequency interval δ centered at σ in unit of δ . ($\delta = (270)^{-1}$ cycles per 12 hrs.)

n = 1

σ	F_1	F_2	F_3	F_4
	0.0004082	0.0001037	0.0001028	-0.0001074
	0.0002790	0.0000744	0.0000397	-0.0001153
	0.0002929	0.0000487	0.0000732	-0.0000342
	0.0003378	0.0000577	0.0000822	0.0000649
	0.0002611	0.0000602	0.0000012	0.0000654
-40	0.0002697	0.0001571	-0.0000912	0.0001566
	0.0008228	0.0002597	-0.0000980	0.0002083
	0.0014501	0.0002307	-0.0000502	-0.0001819
	0.0016901	0.0002208	0.0000320	-0.0003565
	0.0016069	0.0001611	0.0001766	-0.0000581
	0.0010906	0.0001488	0.0002225	-0.0000591
	0.0006955	0.0002815	0.0001429	-0.0000219
	0.0007370	0.0003698	0.0001414	0.0001644
	0.0005110	0.0003346	0.0001725	0.0000281
	0.0005020	0.0001672	0.0000741	-0.0000798
-30	0.0009107	0.0000661	0.0000673	-0.0000928
	0.0015033	0.0001395	-0.0000900	-0.0001173
	0.0022565	0.0001730	-0.0004402	-0.0001205
	0.0021181	0.0001761	-0.0001506	-0.0001790
	0.0014666	0.0003000	0.0001907	-0.0000312
	0.0020593	0.0004164	0.0003030	0.0001621
	0.0030254	0.0003321	0.0005226	0.0000566
	0.0024065	0.0002515	0.0004338	0.0000242
	0.0017551	0.0002986	0.0005092	0.0000968
	0.0018542	0.0004677	0.0007539	-0.0000998
-20	0.0019595	0.0007619	0.0005649	-0.0006666
	0.0021044	0.0007716	0.0001367	-0.0010812
	0.0014410	0.0005620	0.0000914	-0.0007939
	0.0006846	0.0007238	0.0003772	-0.0000452
	0.0036748	0.0009138	0.0006641	0.0000091
	0.0071035	0.0008633	0.0002277	-0.0005368
	0.0070128	0.0016216	-0.0021267	-0.0003958
	0.0064308	0.0031969	-0.0030622	-0.0006008
	0.0077346	0.0037309	-0.0012584	-0.0024229
	0.0094331	0.0026869	-0.0011223	-0.0031514
-10	0.0093932	0.0036647	-0.0015507	-0.0041631
	0.0141521	0.0056072	-0.0000778	-0.0075474
	0.0161299	0.0036210	0.0014928	-0.0063248

(continued for n = 1)

σ	F_1	F_2	F_3	F_4
	0.0132542	0.0012310	0.0027236	-0.0011264
	0.0159017	0.0019242	0.0019562	0.0007613
	0.0328297	0.0049163	0.0019512	0.0056849
	0.0763931	0.0109705	-0.0023230	0.0144665
	0.1107836	0.0171414	-0.0195093	0.0122734
	0.1108156	0.0184036	-0.0265523	0.0016354
-1	0.0033889	0.0003322	0.0006485	0.0000485
+1	0.0018902	0.0002374	-0.0003255	-0.0005831
	0.0236955	0.0059697	0.0037228	-0.0039381
	0.0598030	0.0124657	0.0198476	0.0148831
	0.0920421	0.0125664	0.0207233	0.0177901
	0.0642671	0.0051743	0.0073638	0.0056084
	0.0215897	0.0016710	0.0012941	0.0008827
	0.0086567	0.0034127	0.0024076	0.0032594
	0.0055240	0.0076611	0.0030998	0.0030881
	0.0071486	0.0103702	0.0046151	0.0044176
10	0.0132773	0.0068795	0.0034761	0.0048900
	0.0233402	0.0039750	0.0052710	0.0032274
	0.0257128	0.0041339	0.0089151	0.0037232
	0.0139498	0.0021234	0.0044100	0.0026161
	0.0026631	0.0006887	0.0001851	0.0011202
	0.0032631	0.0018921	0.0011147	0.0008482
	0.0053397	0.0033486	0.0032101	-0.0006813
	0.0082854	0.0034561	0.0048634	-0.0007752
	0.0068358	0.0019268	0.0034744	0.0001968
	0.0035704	0.0010437	0.0015847	0.0004258
20	0.0018136	0.0015635	0.0008140	0.0006238
	0.0012225	0.0015212	0.0001532	0.0005819
	0.0019570	0.0015218	0.0003936	-0.0006675
	0.0024354	0.0019974	0.0007688	-0.0017809
	0.0019369	0.0016932	0.0008885	-0.0011220
	0.0043948	0.0022279	0.0027531	-0.0001194
	0.0077713	0.0029270	0.0044894	-0.0002153
	0.0068551	0.0030055	0.0042693	-0.0004393
	0.0069234	0.0036668	0.0048587	-0.0003028
	0.0075795	0.0036860	0.0050379	0.0000124
30	0.0066127	0.0029749	0.0040428	0.0007418
	0.0070071	0.0018821	0.0029621	0.0007480
	0.0052375	0.0006359	0.0010871	0.0001250
	0.0018432	0.0003386	0.0002166	0.0000436
	0.0006528	0.0004618	0.0004301	0.0001618
	0.0004483	0.0002529	0.0001799	0.0001326
	0.0003462	0.0002701	0.0001100	0.0001200
	0.0004562	0.0004604	0.0003333	0.0001278
	0.0007094	0.0002743	0.0002994	0.0000983
	0.0009149	0.0000754	0.0001675	0.0001416
40	0.0004843	0.0000660	0.0000548	0.0001128
	0.0005737	0.0000692	0.0000842	-0.0000384
	0.0012894	0.0001097	0.0001241	-0.0001999
	0.0013577	0.0001410	0.0000203	-0.0002968
	0.0010770	0.0000973	0.0000433	-0.0002416
	0.0006645	0.0000865	0.0000198	-0.0000822

n = 2

σ	F_1	F_2	F_3	F_4
	0.0043133	0.0007632	0.0013394	-0.0009030
	0.0035825	0.0005720	0.0010919	-0.0001526
	0.0037345	0.0004266	0.0005502	-0.0001678
	0.0045222	0.0003759	0.0000533	-0.0008273
	0.0025914	0.0004208	-0.0002276	-0.0005881
-40	0.0012073	0.0006533	-0.0001374	-0.0002408
	0.0026706	0.0007490	0.0007829	-0.0004694
	0.0037889	0.0006773	0.0012958	-0.0007640
	0.0028979	0.0005134	0.0004343	-0.0008870
	0.0023734	0.0003920	-0.0000869	-0.0008345
	0.0016650	0.0001906	0.0000535	-0.0003368
	0.0033914	0.0004212	0.0000191	0.0011151
	0.0063837	0.0009264	0.0000562	0.0020278
	0.0042772	0.0006951	0.0001129	0.0009077
	0.0013457	0.0005229	-0.0001394	0.0000896
-30	0.0005306	0.0009033	-0.0000850	0.0000696
	0.0003991	0.0011071	-0.0000697	-0.0000900
	0.0022612	0.0009149	-0.0003888	0.0003477
	0.0059573	0.0010813	0.0007262	0.0000689
	0.0103647	0.0017123	0.0027251	-0.0001266
	0.0141651	0.0014712	0.0028561	0.0016268
	0.0118228	0.0012568	0.0014289	0.0016521
	0.0094229	0.0017301	0.0004509	-0.0011860
	0.0123786	0.0012874	0.0004842	-0.0028298
	0.0094969	0.0007436	0.0006362	-0.0011603
-20	0.0052378	0.0042787	-0.0005573	0.0031404
	0.0167140	0.0118541	0.0011837	-0.0015287
	0.0276394	0.0124848	0.0046066	-0.0113400
	0.0166924	0.0057579	0.0014406	-0.0082453
	0.0102577	0.0045414	-0.0016102	0.0008371
	0.0153366	0.0124051	0.0028422	0.0022388
	0.0143313	0.0159873	0.0094847	-0.0047037
	0.0203935	0.0148409	0.0098376	-0.0070964
	0.0280177	0.0077387	0.0010412	-0.0039572
	0.0187511	0.0104291	-0.0077347	-0.0010563
-10	0.0114453	0.0108012	-0.0055606	0.0035460
	0.0140120	0.0080020	0.0000872	0.0018313
	0.0154437	0.0229801	0.0069063	-0.0072230

(continued for n = 2)

σ	F_1	F_2	F_3	F_4
	0.0640051	0.0420226	0.0022375	-0.0021072
	0.1174847	0.0340002	-0.0195051	0.0138955
	0.1935304	0.0261327	-0.0064714	0.0425119
	0.3623350	0.0297035	0.0287821	0.0835390
	0.3750870	0.0227492	0.0299288	0.0785360
	0.2010797	0.0266350	0.0157854	0.0494938
-1	0.0009124	0.0024216	0.0003942	0.0036383
+1	0.0091356	0.0038988	0.0035180	-0.0025298
	0.1731645	0.0447742	0.0225540	-0.0305512
	0.0931658	0.0189935	0.0007669	-0.0128243
	0.2065821	0.0430845	0.0772885	-0.0230089
	0.2744877	0.0572557	0.1192474	-0.0251076
	0.1741999	0.0306013	0.0591564	-0.0190076
	0.1552579	0.0174006	0.0200857	0.0007405
	0.1975466	0.0332012	0.0440358	0.0293479
	0.1623617	0.0348938	0.0601340	0.0202152
10	0.1091060	0.0153351	0.0362701	0.0052850
	0.0965867	0.0053804	0.0196613	0.0058952
	0.0728565	0.0082900	0.0174464	0.0000705
	0.0254742	0.0082917	0.0053288	0.0001293
	0.0086751	0.0046121	0.0001102	0.0035735
	0.0104816	0.0036159	0.0038318	0.0036478
	0.0230820	0.0085536	0.0123600	0.0061527
	0.0327595	0.0125716	0.0144752	0.0092754
	0.0204488	0.0097515	0.0051073	0.0073367
	0.0362715	0.0136382	0.0177516	0.0011036
20	0.0045594	0.0208058	0.0363408	-0.0013324
	0.0371988	0.0116086	0.0203676	0.0006596
	0.0077675	0.0019009	0.0013792	-0.0003029
	0.0074457	0.0019317	-0.0010520	-0.0023181
	0.0080240	0.0033639	0.0022935	-0.0008616
	0.0109025	0.0040288	0.0060543	0.0012614
	0.0091971	0.0021977	0.0040649	0.0012517
	0.0054440	0.0008363	0.0018027	0.0001789
	0.0061165	0.0013654	0.0014660	-0.0003749
	0.0058498	0.0015509	0.0005034	-0.0002821
30	0.0052336	0.0009941	0.0007798	-0.0005579
	0.0055409	0.0010882	0.0019353	-0.0003954
	0.0052679	0.0016185	0.0025957	0.0003526
	0.0057572	0.0017905	0.0030851	-0.0001746
	0.0061462	0.0020054	0.0032135	-0.0008082
	0.0045600	0.0017160	0.0024266	-0.0003070
	0.0063841	0.0019115	0.0033147	0.0000046
	0.0086126	0.0026787	0.0046915	0.0003192
	0.0070773	0.0026513	0.0040824	0.0001883
	0.0057032	0.0020803	0.0031114	-0.0007737
40	0.0044637	0.0011066	0.0017760	-0.0004702
	0.0037411	0.0004308	0.0007543	0.0005141
	0.0032840	0.0004333	0.0006413	0.0001314
	0.0037107	0.0010408	0.0014948	-0.0008899
	0.0037965	0.0013970	0.0019223	-0.0011650
	0.0019965	0.0009443	0.0008364	-0.0004600

n = 3

σ	F_1	F_2	F_3	F_4
	0.0100069	0.0009988	0.0015160	0.0004968
	C.C129823	0.C0C5592	0.0010788	0.0000378
	C.C1C4629	0.0007051	0.0016107	-0.0000862
	0.C0922C5	0.0011160	0.0029034	0.0007289
	0.C092733	0.C013369	0.0030275	0.0016637
-40	0.C078347	0.0019471	0.0023298	0.0020090
	0.0089580	0.0017740	0.0009451	0.0010038
	0.0134135	C.0006952	0.0008828	0.0001349
	C.C102661	C.C003C88	0.0013835	0.C002076
	0.C035746	0.0006679	0.0010866	0.0005526
	C.0029274	0.0010564	0.0010401	0.0012807
	0.0071791	0.0013115	0.0017407	0.0023853
	C.0110641	C.C012045	0.0019689	0.0022457
	C.C118129	0.0010078	0.0020906	0.0009513
	C.C299549	0.0012936	0.0025112	0.0032954
-30	C.C469192	0.0011559	0.0016096	0.0054975
	0.0312077	0.0004932	0.0013106	0.0021743
	0.0380839	0.0011527	-0.0031513	-0.0021634
	0.0548463	C.0028191	-0.0084027	-0.0031823
	C.C315498	0.0027233	-0.0032473	-0.0013191
	C.C154130	0.0011259	0.0015651	-0.0007411
	0.C172236	0.0005302	0.0010343	-0.0018870
	0.0386293	0.0025725	0.0082323	-0.0029585
	0.C621697	0.0060755	0.0118997	-0.0000880
	C.0450610	0.0107366	-0.0034832	0.0017142
-20	0.0441706	0.C176007	-0.0244165	-0.0044480
	C.C981786	0.0225265	-0.0382980	-0.0191919
	0.1194906	0.0187843	-0.0310213	-0.0246363
	0.C778260	0.0113041	-0.0031058	-0.0027006
	0.0622447	0.0090539	0.0141281	0.0164220
	C.0590817	0.0217906	0.0068346	0.0174654
	0.0554776	0.0343367	-0.0087031	0.0153780
	0.0901690	0.0187658	-0.0152643	0.0104712
	C.1243490	0.0224162	-0.0392880	0.0067357
	C.1139653	0.0527114	-0.0660929	0.0110440
-10	0.0559398	0.0510481	-0.0399058	0.0049005
	0.1459312	0.C321083	-0.0090831	0.0123330
	C.3712181	0.0204460	-0.0216936	0.0324369

(continued for n = 3)

σ	F_1	F_2	F_3	F_4
	0.4385338	0.0197322	-0.0089820	0.0210857
	0.4080425	0.0235871	0.0340996	0.0093286
	0.3657684	0.0154593	0.0280490	0.0019949
	0.3661293	0.0356577	0.0641620	0.0331572
	0.5092314	0.0946435	0.1729507	0.1130235
	0.6199688	0.1193572	0.1850469	0.1400580
-1	0.0135147	0.0011841	-0.0002555	0.0016991
+1	0.0167686	0.0037679	0.0050094	0.0058665
	0.2499962	0.0390196	0.0653638	0.0531330
	0.1088966	0.0155996	0.0274094	0.0061816
	0.0344995	0.0129750	0.0108772	-0.0040656
	0.0080322	0.0162822	-0.0029040	-0.0058564
	0.0123698	0.0189395	-0.0039425	-0.0055510
	0.0658091	0.0143697	-0.0042646	0.0051430
	0.1519495	0.0254079	0.0064249	-0.0088543
	0.2124847	0.0525820	0.0622116	-0.0337048
10	0.2915936	0.0613877	0.1214989	-0.0156446
	0.3178229	0.0428827	0.1097589	-0.0010258
	0.1849803	0.0162065	0.0416564	-0.0047691
	0.1884053	0.0221442	0.0533054	-0.0050099
	0.2967710	0.0391802	0.1011410	-0.0048237
	0.1629407	0.0219239	0.0520613	0.0037321
	0.0680454	0.0132170	0.0220809	0.0181297
	0.1245823	0.0244644	0.0470408	0.0209104
	0.1057149	0.0193278	0.0399242	0.0030464
	0.1012464	0.0144078	0.0322069	0.0069925
20	0.1193964	0.0165247	0.0338611	0.0254587
	0.0660442	0.0117597	0.0190179	0.0183397
	0.0202392	0.0107651	0.0057969	0.0074331
	0.0107058	0.0098193	-0.0004925	0.0021685
	0.0070189	0.0068024	0.0018282	-0.0023529
	0.0164502	0.0071479	0.0067583	-0.0022233
	0.0191119	0.0041486	0.0017341	0.0006005
	0.0093187	0.0023843	-0.0027089	0.0008963
	0.0122177	0.0045177	0.0008934	-0.0018928
	0.0223469	0.0057330	0.0067300	-0.0009052
30	0.0217184	0.0065275	0.0083370	0.0045968
	0.0172236	0.0062495	0.0071169	0.0061957
	0.0218502	0.0064039	0.0095248	0.0022451
	0.0326048	0.0082280	0.0144934	0.0014744
	0.0225778	0.0062392	0.0098731	0.0035713
	0.0089196	0.0026258	0.0035653	0.0029883
	0.0114237	0.0023112	0.0046222	0.0016389
	0.0135674	0.0034755	0.0065445	0.0006698
	0.0118912	0.0041793	0.0069701	-0.0000322
	0.0079480	0.0029923	0.0046773	-0.0004837
40	0.0087566	0.0013281	0.0028338	-0.0010818
	0.0113767	0.0009032	0.0025157	-0.0011869
	0.0061568	0.0010016	0.0010056	-0.0011964
	0.0029409	0.0011063	0.0004805	-0.0008549
	0.0056640	0.0007814	0.0008392	-0.0001937
	0.0059662	0.0003248	0.0000356	-0.0000955

n = 4

τ	F_1	F_2	F_3	F_4
	C.C208C93	0.0015435	0.0004272	-0.0019851
	C.C203735	0.0011292	-0.0022072	-0.0003164
	0.02CC363	0.0003932	-0.0013207	0.0000814
	0.0211961	0.0016777	0.0017110	-0.0003514
	0.0127832	0.0031609	0.0024657	-0.0008340
-40	C.0051541	0.0019381	0.0016304	0.0000077
	C.C08CC38	0.0009595	0.0010459	0.0019133
	C.C093061	0.0015176	0.0007589	0.0030987
	0.0081879	0.0018860	-0.0000463	0.0026798
	C.C161020	0.0014736	-0.0010065	0.0026652
	0.03112C6	0.0017315	0.0020715	0.C017402
	C.C314866	0.0029228	0.0036323	-0.0013364
	C.C229C18	0.0027609	0.0004553	-0.0004794
	0.0172264	0.0039806	0.0001677	0.0006912
	0.0098151	0.0082117	-0.0020133	-0.CC26195
-30	C.0131SC2	0.0086887	-0.0070707	-0.0040251
	C.C377633	0.0041175	-0.0060265	-0.0019196
	C.C726961	0.0011701	0.0022633	-0.0013529
	C.C884554	0.0081419	-0.0015298	0.0049675
	C.0607558	0.0184396	-0.0152539	0.0136882
	C.C197416	0.0145226	-0.0115638	0.0087202
	0.03506C1	0.0090386	-0.0088043	0.0121426
	0.0957958	0.0118448	-0.0183393	C.0271499
	C.0952597	0.0130898	-0.0158194	0.0237142
	C.C4C3258	C.0141531	-0.0090609	0.0099680
-20	C.0621313	0.0133485	-0.0206134	0.0018834
	0.1118540	0.0136896	-0.0285998	0.0059535
	C.C851226	C.C2C3269	-0.0079558	0.0234722
	C.C516546	0.0201552	0.0081120	0.0278579
	C.C654655	0.0122519	0.0001149	0.0230909
	0.0952365	0.0110379	0.0015477	0.0255593
	0.0941984	C.0301247	0.0328448	0.0139942
	C.1135232	0.C448975	0.0491842	-0.0018665
	0.2591949	0.0400936	-0.0053006	0.0374110
	C.4843357	0.0428769	-0.0269667	0.C893001
-10	C.5015784	0.0366132	0.0239487	0.0705524
	C.339684C	0.0284662	0.0293359	0.0644400
	0.2501429	C.0411742	0.0110989	0.0810893

(continued for n = 4)

τ	F_1	F_2	F_3	F_4
	0.1620340	0.0478320	0.0045458	0.0316267
	0.1778986	0.0297639	0.0041100	-0.0241137
	0.3103475	0.0126382	0.0061528	-0.0386300
	0.3171718	0.0211107	0.0039796	-0.0435971
	0.2455684	0.0401256	0.0395552	-0.0095802
	0.2746372	0.0715252	0.1116011	0.0735373
-1	0.0161528	0.0044827	0.0060415	0.0044837
+1	0.1127254	0.0043368	0.0107605	-0.0089720
	1.3052349	0.0482478	0.0702407	-0.1360554
	0.4295196	0.0143347	-0.0006004	-0.0440800
	0.6379909	0.0371797	0.1279608	0.0054999
	0.8274178	0.0637391	0.2184348	0.0285528
	0.5068209	0.0414437	0.1151690	0.0204920
	0.3759848	0.0192067	0.0482480	-0.0035076
	0.4422497	0.0350145	0.1000999	0.0109204
	0.3509238	0.0389826	0.0950042	0.0342143
10	0.3948090	0.0201443	0.0612007	0.0185926
	0.6247522	0.0205296	0.1007056	-0.0072723
	0.5327705	0.0246103	0.1023804	-0.0211135
	0.1978238	0.0109238	0.0327862	-0.0153733
	0.0549273	0.0049298	0.0063111	-0.0059593
	0.0791286	0.0078611	0.0189587	-0.0078951
	0.1073489	0.0067509	0.0185311	-0.0134145
	0.0910752	0.0093919	0.0144584	-0.0014529
	0.0747066	0.0135624	0.0157736	0.0143785
	0.0484019	0.0088497	0.0080896	0.0066049
20	0.0878738	0.0073028	0.0171510	0.0035622
	0.1450130	0.0099480	0.0339329	0.0063315
	0.0729390	0.0095857	0.0192927	0.0042792
	0.0078347	0.0141359	0.0076302	0.0035927
	0.0211241	0.0183857	0.0111380	-0.0072253
	0.0352122	0.0150506	0.0061815	-0.0162348
	0.0352146	0.0104066	0.0036551	-0.0073029
	0.0307089	0.0076915	0.0095672	0.0004319
	0.0354764	0.0054786	0.0124655	-0.0027347
	0.0508855	0.0061020	0.0164128	-0.0045496
30	0.0422431	0.0088682	0.0161857	-0.0030981
	0.0151036	0.0097813	0.0085582	-0.0022498
	0.0068053	0.0105626	0.0073552	-0.0007331
	0.0077461	0.0118199	0.0092720	-0.0002775
	0.0046168	0.0085245	0.0060190	-0.0001412
	0.0023791	0.0043184	0.0028613	0.0004265
	0.0032892	0.0032560	0.0025986	-0.0007539
	0.0051164	0.0023642	0.0009497	-0.0005279
	0.0054604	0.0025176	-0.0003441	0.0010016
	0.0055283	0.0026904	0.0003326	0.0006891
40	0.0079855	0.0011202	0.0001922	0.0000779
	0.0074134	0.0003315	0.0000400	0.0002114
	0.0097688	0.0007044	0.0015067	0.0000339
	0.0158674	0.0007346	0.0026154	-0.0009103
	0.0169461	0.0034077	0.0054979	-0.0031434
	0.0145065	0.0062276	0.0075410	-0.0039137

n = 5

σ	F_1	F_2	F_3	F_4
	C.C516458	0.0071132	0.0128601	0.0102828
	C.C361138	0.0043283	0.0005799	0.0089010
	C.0289766	0.0085869	-0.0054521	0.0108967
	0.0228424	0.0185301	-0.0025896	0.0170173
	C.0197772	0.0217053	-0.0017435	C.0187896
-40	C.C243439	0.0143822	-0.0009274	0.0148078
	C.C249876	0.0057725	-0.0004962	0.0067662
	C.C249878	0.0039050	-0.0049753	0.0048514
	C.0762987	0.0045726	-0.0029754	0.0100062
	C.1355381	0.0053843	-0.0013482	0.0118121
	C.0870829	0.0087893	-0.0052765	0.0027614
	C.0308268	0.0126498	-0.0023352	0.0028479
	C.0384435	0.0122202	-0.0043217	C.0107611
	C.C406526	C.0101582	-0.0089329	-0.C012331
	C.C635684	0.0131492	-0.0009053	-0.0006207
-30	C.C885033	0.0148288	0.0048210	0.0203178
	C.0550193	0.0095847	0.0003341	0.0165121
	C.0736259	0.0111930	-0.0202120	-0.0036263
	C.1368210	0.C184012	-0.0379383	-0.0182655
	C.1191524	0.0235547	-0.0313388	-0.0095931
	C.0735234	0.0341637	-0.0316588	0.0172015
	0.0397552	0.0322722	-0.0238074	0.0182219
	C.C367807	0.0299771	-0.0124328	0.0189098
	C.C587998	0.0440400	-0.0092948	0.0326375
	C.C734321	C.C379568	0.0167797	0.0170203
-20	C.1678267	0.0297511	0.0173573	-0.0364711
	0.3595089	0.C362075	-0.0272793	-0.0885667
	C.3911456	0.0229782	-0.0444310	-0.0709843
	C.3378839	0.0228445	-0.0333265	0.0326285
	C.3478497	0.0375847	-0.0291001	0.1037113
	0.4075668	0.0333632	0.0404493	0.0727577
	C.7654624	C.0300668	0.1237147	0.0283211
	C.8854462	0.0180985	0.0928584	-0.0068977
	0.7734053	0.0137428	0.0813832	-0.0496479
	C.8437124	0.0299270	0.0913689	-0.0820154
-10	C.6356115	0.0451526	0.0262291	-0.C150215
	C.3656250	0.0462096	0.0049834	0.0833547
	C.3007492	0.0307602	0.0462347	0.0528743
	C.5015937	0.0270970	0.0482947	0.0208591

(continued for n = 5)

σ	F_1	F_2	F_3	F_4
	0.8385475	0.0700216	-0.0130792	0.1368354
	0.7696544	0.1183457	-0.0271726	0.2484761
	0.4220398	0.0824041	0.0224367	0.1689794
	0.3912867	0.0343192	0.0768901	0.0701150
	1.1209822	0.0891245	0.2623639	0.1017241
-1	0.0963453	0.0073417	0.0249295	0.0028264
+1	0.0239640	0.0025831	-0.0039951	0.0061762
	0.5576141	0.0281751	-0.0511133	0.0653620
	0.5274341	0.0854334	0.1243434	0.0021087
	0.6354640	0.1357263	0.2458715	0.0473770
	1.3987188	0.2454424	0.5393121	0.1621848
	1.6004847	0.3219408	0.7151770	0.2073480
	1.0165720	0.2032601	0.4086496	0.1582634
	0.5077449	0.1091276	0.2018693	0.1070156
	0.5512758	0.1225431	0.2429723	0.0479210
10	0.4357473	0.1035607	0.1638955	0.0237797
	0.3426399	0.0669826	0.0163822	0.0703627
	0.2747215	0.0339868	-0.0467599	0.0623280
	0.1665533	0.0165723	-0.0053561	0.0288788
	0.1210093	0.0224168	0.0373217	0.0322681
	0.0869139	0.0217311	0.0287401	0.0254537
	0.0572407	0.0113193	0.0112042	0.0172487
	0.0676133	0.0048751	0.0058780	0.0065413
	0.0787068	0.0043400	0.0060244	-0.0097903
	0.0672625	0.0110836	0.0135647	-0.0060843
20	0.0564665	0.0247363	0.0296498	0.0081939
	0.0767633	0.0275783	0.0368776	0.0035785
	0.0791108	0.0126868	0.0195916	-0.0041697
	0.0376275	0.0046866	0.0027725	0.0009695
	0.0077472	0.0062276	0.0021855	0.0037104
	0.0080000	0.0042002	0.0024190	0.0030816
	0.0098002	0.0013966	0.0000175	0.0024861
	0.0130509	0.0026932	0.0034034	0.0022763
	0.0257154	0.0076877	0.0129790	0.0021095
	0.0285406	0.0093336	0.0138583	-0.0019466
30	0.0151699	0.0055092	0.0037427	-0.0039233
	0.0074495	0.0024397	-0.0023857	-0.0002308
	0.0067619	0.0025616	-0.0027714	0.0020184
	0.0041409	0.0038088	-0.0025153	-0.0000195
	0.0042285	0.0044455	-0.0011213	-0.0000733
	0.0067941	0.0035654	-0.0004068	0.0025974
	0.0055066	0.0018345	-0.0010825	0.0017815
	0.0039969	0.0011686	0.0001470	-0.0004482
	0.0041878	0.0019908	0.0017107	-0.0001775
	0.0039144	0.0035542	-0.0003328	-0.0003774
40	0.0063897	0.0039273	-0.0030437	-0.0016658
	0.0110980	0.0023474	-0.0021707	-0.0021628
	0.0125112	0.0012121	-0.0002107	-0.0020571
	0.0083989	0.0006875	-0.0002816	-0.0006952
	0.0109230	0.0007648	0.0017522	-0.0001754
	0.0176280	0.0013394	0.0044691	-0.0003745

n = 6

τ	F_1	F_2	F_3	F_4
	C.C265C27	0.0065928	-0.0061140	-0.0047758
	0.0411226	0.0061277	-0.0070423	0.0063462
	C.0511502	0.0091279	-0.0020194	0.0158195
	C.0465756	0.0148504	0.0046830	0.0189143
	C.0318374	0.0181053	0.0015487	0.0171652
-40	C.0292912	0.0095578	0.0035643	0.0079084
	C.0702396	0.0043015	0.0126584	0.0091326
	C.1145262	0.0079371	0.0083256	0.0192955
	C.1803818	0.0088797	-0.0184956	0.0212917
	C.2342215	0.0076584	-0.0273076	0.0130152
	C.1446880	0.0081648	-0.0052726	0.0010992
	0.1034074	0.0165328	0.0109228	0.0262177
	C.1602087	0.0328021	0.0160446	0.0646010
	C.1265940	0.0435115	0.0188892	0.0343503
	0.1883073	0.0406865	0.0390947	0.0026605
-30	C.2784092	0.0312033	0.0430982	0.0249048
	0.2168092	0.0192215	0.0044120	0.0122116
	C.2229003	0.0079516	-0.0099405	-0.0051695
	C.2031320	0.0041387	0.0007148	0.0120789
	C.0783628	0.0068214	0.0074408	0.0088180
	C.0582674	0.0253849	-0.0086764	0.0082584
	C.0902560	0.0487523	-0.0426806	0.0293628
	0.0693647	C.0603811	-0.0184714	0.0230652
	0.0535250	0.0553414	0.0218584	-0.0015075
	0.0607961	0.0444233	-0.0017947	0.0111405
-20	C.3243285	0.0467491	0.0071631	0.0214214
	C.6426947	0.0363648	0.0512495	0.0196371
	0.9688158	0.0429324	-0.0350471	0.1350352
	1.2648954	0.0759251	-0.1249153	0.2637072
	1.1115322	0.0894457	-0.0126041	0.2714956
	1.1491795	0.1069942	0.1647555	0.2940059
	1.3114614	0.1086173	0.2255651	0.1982314
	1.3501434	0.0784635	0.1937513	0.0639901
	1.1699152	0.0543474	0.1308368	0.1023808
	C.8831007	C.0624085	0.0435905	0.1872057
-10	C.8596999	0.0989878	0.0060781	0.2504660
	1.1694775	0.1945665	0.2522603	0.3100058
	1.5470867	0.2695131	0.5057089	0.3536306
	1.1615067	C.2027737	0.4021185	0.2119637

(continued for n = 6)

σ	F_1	F_2	F_3	F_4
	C.7772461	0.1393059	0.3088899	0.0576237
	1.2458744	0.1691735	0.3202408	0.2392810
	1.9816494	0.2282059	0.3376560	0.5315983
	2.0139761	0.2235729	0.3992167	0.4306557
	2.3395100	0.2042565	0.6102957	0.1338025
-1	C.2082686	0.0151314	0.0469014	0.0164465
+1	C.2401466	0.0057429	0.0280566	0.0222496
	3.0395575	0.0715601	0.3650544	0.2613319
	1.1143465	0.0332383	0.1322417	0.1123749
	0.7481701	0.0364724	0.1086796	0.0359403
	C.7817564	0.0759984	0.1953527	-C.0101903
	C.7545481	0.1154040	0.2751064	0.0014941
	C.6203286	0.1033760	0.2432886	-0.0012274
	0.2920489	0.0629914	0.1081805	0.0004958
	C.1109673	0.0423576	0.0239855	0.0067083
10	C.1075863	C.0398049	0.0255194	-0.0271239
	0.0869826	0.0325929	0.0118524	-0.0331332
	C.0875176	0.0252968	-0.0038373	-0.0155707
	C.0723433	0.0218764	0.0138919	-0.0114356
	C.0642728	0.0152408	0.0276999	-C.0063024
	C.0865856	C.0204741	0.0265329	-0.0153212
	C.1752225	0.0376804	0.0503018	-0.0331316
	C.2447453	0.0385899	0.0715528	-0.0250172
	C.1304330	0.0194554	0.0290027	-0.0064820
	C.0276704	0.0076479	-0.0005995	-0.0026455
20	0.0757335	0.0248409	0.0375187	-0.0030516
	0.1142357	0.0426863	0.0626265	0.0038398
	0.0618697	0.0238620	0.0275810	0.0079383
	C.0303268	0.0042658	0.0003073	0.0075835
	C.0442516	0.0030917	0.0031646	0.0091956
	C.0247154	0.0016411	0.0010150	0.0056567
	C.0049911	0.0030633	-0.0016154	0.0011346
	C.0183405	0.0060599	0.0020475	-0.0024749
	0.0381570	0.0067811	0.0103739	-0.0060004
	C.0397441	0.0088866	0.0167685	-0.0026218
30	C.0310738	0.0107804	0.0160195	0.0001157
	C.0236264	0.0072162	0.0077987	-0.0034140
	C.0194261	0.0021973	0.0020139	-0.0040323
	C.0119639	0.0008447	0.0009183	-0.0010704
	C.0095518	C.0011666	-0.0000762	0.0005919
	C.0182535	0.0024923	0.0023655	-0.0005947
	C.0219659	C.0068749	0.0095678	-0.0015302
	0.0196900	0.0083913	0.0111886	0.0015508
	C.0135278	0.0053281	0.0053045	0.0042221
	0.0179466	0.0052377	0.0066501	0.0015308
40	C.0334949	0.0057003	0.0116605	-0.0020194
	C.0364256	0.0027831	0.0078202	-0.0020086
	C.0268730	C.0009743	0.0028779	-0.0017341
	C.0182435	0.0010590	0.0009859	-0.0007999
	0.0134199	0.0010969	-0.0009093	0.0001027
	0.0061451	0.0018917	-0.0006172	-C.0001767

n = 7

σ	F_1	F_2	F_3	F_4
	0.0586633	0.0194300	0.0121118	0.0272297
	C.0520657	0.0132943	0.0123987	C.0157399
	C.1112713	0.0033786	0.0088199	0.0044746
	C.2265313	0.0045383	0.0070982	0.0223880
	0.2028400	0.0114611	-0.0008488	0.0362596
-40	C.1480084	0.0173619	-0.0246916	0.0315787
	0.1790206	0.0226261	-0.0265029	0.0308433
	C.1313224	0.0233786	0.0084636	0.0164105
	C.1520115	0.0355343	0.0350211	0.0386507
	C.2711849	0.0493031	0.0468402	0.0863469
	0.2567731	0.0334697	0.0447294	0.0674729
	C.1828774	0.0223124	0.0402100	0.0419902
	C.2285139	C.0459797	0.0415110	0.0835963
	C.3328418	0.0668710	0.0447089	0.1297235
	C.4522716	0.0604861	0.1050649	0.0828877
-30	C.4949628	0.0506403	0.1388073	0.0078580
	C.2631678	0.0351125	0.0535835	-0.0087241
	C.1163061	0.0267858	-0.0265326	0.0174798
	C.1862390	0.0452152	-0.0239503	0.0490863
	C.1789779	0.0632146	0.0278973	0.0670763
	C.2490169	0.0656532	0.0359494	0.1081684
	0.3878624	0.0807026	0.0382247	0.1505927
	C.4669319	0.0828552	C.0886889	0.0869143
	C.5740316	0.0676516	0.1372854	-0.0035158
	0.6581036	0.0993280	0.1588538	0.0848305
-20	C.5624002	0.1093342	0.0802062	0.1817394
	C.2844578	0.0536584	-0.0182806	0.0960296
	C.2927373	0.0817490	0.1076651	-0.0201015
	C.8133921	0.1697949	0.2325616	-0.0029368
	C.8528947	0.1282028	0.0769014	0.0885410
	1.0528755	0.0392819	0.0446289	0.0463391
	1.2828321	0.0459481	0.1434829	0.0249138
	C.8378224	C.0700966	0.0930498	0.1137202
	0.7397532	0.0485985	0.0987975	0.0985436
	1.2019062	0.0444887	0.2083670	0.0662721
-10	1.0354900	0.0561335	0.2043563	0.0777647
	C.4267890	0.0418670	0.0982620	0.0450527
	0.9770216	0.0428518	0.1527494	0.0901476
	2.1480293	0.0511801	0.2544917	0.1801680

(continued for n = 7)

σ	F_1	F_2	F_3	F_4
	1.8448915	0.0498216	0.1960620	0.1073765
	1.0172377	0.0693412	0.1620961	0.0382862
	0.9587866	0.0767619	0.1745026	0.1006715
	0.9607270	0.0599111	0.1523411	0.0923854
	1.1969070	0.0501162	0.1552721	0.0194765
-1	0.0851113	0.0006073	0.0043065	0.0033812
+1	0.0233456	0.0150497	0.0180267	-0.0029377
	0.3042992	0.2219651	0.2130496	-0.0782616
	0.1014303	0.0853345	0.0525925	-0.0359550
	0.4732520	0.0458933	0.1005726	0.0341453
	0.9139737	0.0781372	0.2294168	0.1021178
	0.7963682	0.1135876	0.2595173	0.1248584
	0.4647368	0.0913163	0.1644203	0.1020848
	0.2542526	0.0495580	0.0611506	0.0455528
	0.1200768	0.0452496	0.0375302	-0.0154665
10	0.1591523	0.0483161	0.0598003	-0.0359555
	0.2384517	0.0342529	0.0646855	-0.0172313
	0.1392581	0.0229374	0.0360002	0.0086133
	0.0515358	0.0179711	0.0130272	0.0185360
	0.0886939	0.0253401	0.0281257	0.0150427
	0.1767164	0.0410124	0.0657061	-0.0119427
	0.2065451	0.0342645	0.0658423	-0.0354341
	0.1090174	0.0168576	0.0311104	-0.0132999
	0.0435392	0.0106102	0.0135814	0.0086241
	0.1450566	0.0118540	0.0345826	0.0010783
20	0.3014423	0.0200702	0.0735685	-0.0190458
	0.3229800	0.0254155	0.0817641	-0.0168473
	0.2105182	0.0213508	0.0580632	0.0075809
	0.0850456	0.0117913	0.0243228	0.0114291
	0.0382500	0.0152702	0.0133504	0.0068325
	0.0389730	0.0277515	0.0236102	0.0001886
	0.0464773	0.0203364	0.0200411	-0.0072273
	0.0509708	0.0071350	0.0094144	0.0012312
	0.0290054	0.0129965	0.0086222	0.0060435
	0.0128128	0.0202282	0.0092407	-0.0005976
30	0.0140123	0.0120742	0.0048812	-0.0027536
	0.0628879	0.0044900	0.0086877	0.0009430
	0.1080485	0.0050533	0.0140627	0.0037590
	0.0615756	0.0057985	0.0077760	0.0026395
	0.0179204	0.0038016	0.0021258	-0.0014204
	0.0118845	0.0017647	0.0022605	-0.0022041
	0.0041707	0.0026035	0.0029129	-0.0008023
	0.0054396	0.0055024	0.0011283	-0.0001749
	0.0074580	0.0063071	-0.0018067	0.0013576
	0.0132655	0.0040890	-0.0013325	0.0038781
40	0.0219457	0.0025188	-0.0013270	0.0060004
	0.0218050	0.0021859	-0.0008622	0.0059651
	0.0161577	0.0021550	0.0020999	0.0041069
	0.0100426	0.0021536	0.0012509	0.0023924
	0.0072129	0.0017180	-0.0014393	0.0017328
	0.0080678	0.0008839	-0.0006257	0.0001033

n = 8

σ	F_1	F_2	F_3	F_4
	0.2395639	0.0205016	0.0370708	0.0496809
	C.2219090	C.C205779	C.0193934	0.0434805
	C.C9015&C	C.0204543	0.0067494	0.0242104
	C.C717846	0.0553105	0.0295969	0.0468886
	C.1910301	0.0894931	0.0606329	C.C809788
-40	C.2189173	0.C464779	0.0443331	0.045442C
	0.1039032	0.0086691	0.0135008	0.0135527
	C.3638167	0.0356537	0.0935294	0.0346182
	C.6666493	0.0697933	0.1741471	0.0377383
	0.3277575	0.0693765	0.0881960	0.0195362
	0.0545100	0.0613947	-0.0122269	0.0384013
	C.1151258	0.0619487	-0.0336249	0.0481103
	C.1349255	0.0607735	-0.0526467	0.0152316
	C.1425712	0.0612762	-0.0780436	0.0102715
	C.2968996	0.0764570	0.0401680	0.0154624
-30	C.5164003	0.0954853	0.1880691	-0.0091901
	C.6681765	0.1020087	0.1478367	0.0797018
	C.7126565	0.1314245	0.1145273	0.2088377
	C.5961181	0.1221508	0.1363777	0.1651063
	C.5426612	0.0883489	0.1353600	0.1162262
	C.3906069	0.0797793	0.1269933	0.C835876
	C.1922967	0.0444340	0.0748735	0.0275203
	C.2116084	0.0274969	0.0228868	-0.0147275
	0.2143655	0.0481710	0.0176416	-0.0635817
	C.3500738	0.0758812	0.0982503	C.C105979
-20	C.5301503	0.C843937	0.1557092	0.1039140
	C.3517222	0.0561348	0.0917557	0.0422757
	C.3301651	0.0386209	0.0753483	-0.0046684
	0.4345732	C.0319850	0.0854806	0.0248801
	C.5539731	0.0218657	0.0420440	-0.0304131
	C.7286586	0.0168131	0.0149947	-0.0864431
	C.5364411	0.0233147	-0.0103121	-0.0862858
	C.5243971	C.0429626	0.0107587	-0.0958161
	C.6014397	0.0436941	0.0839818	-0.0363991
	C.5973824	0.C281692	0.0998399	0.0454435
-10	C.7643058	0.0210926	0.0972136	0.0568316
	C.6765605	C.0242619	0.0596358	0.0196413
	C.4973974	0.0523353	0.0138882	-0.0637015
	C.4465489	0.0869087	0.0826631	-0.0883543

(continued for n = 8)

σ	F_1	F_2	F_3	F_4
	C.4288361	0.C808036	0.1484967	-0.0321214
	C.6497380	0.0813593	0.1741014	-0.0990433
	1.0593138	0.1087932	0.2303588	-0.2278222
	1.2092209	0.1279672	0.2940799	-0.2050316
	1.1542225	0.2054413	0.4128666	-0.1716098
-1	C.C442503	C.0139962	0.0210399	-0.0119129
+1	C.C146696	0.0073223	0.0074667	-0.0053013
	C.1711746	0.1325335	0.0891780	-0.0928475
	0.0842826	0.0707695	0.0228238	-0.0624451
	0.3511247	0.0722458	0.0110934	C.0731499
	C.5136310	0.0951493	0.0387750	0.1571206
	0.3500599	0.1255599	0.1240838	0.0559161
	C.3626552	0.1268770	0.1670024	-0.0418960
	0.4183351	0.0756536	0.0754166	-C.0243591
	C.2982852	0.0431881	-0.0062150	0.0081947
10	C.2499346	0.0376942	0.0159496	0.0020122
	C.2447612	0.0516450	0.0565263	-0.0305583
	C.2050046	0.C638199	0.0555087	-0.0697720
	C.1010417	0.0574376	0.0325901	-0.0531427
	0.0211686	0.0516889	0.0186088	-0.0145796
	0.0436169	0.0340282	0.0221411	-0.0122384
	C.C640945	0.0198620	0.0213370	-0.0173156
	C.0441581	0.0129448	0.0070885	-0.0061684
	0.0436985	0.0207582	0.0019025	0.0208735
	C.0666264	0.0370398	0.0078448	C.0268542
20	C.1229862	0.0347669	0.0331493	0.0178022
	C.1647573	0.0328743	0.0581214	0.0295819
	C.1026506	0.0373116	0.0489312	0.0269189
	C.C396913	0.0365711	0.0334101	0.0060398
	0.0311366	0.0250992	0.0251270	-0.0037312
	C.0264131	0.0179706	0.0163295	0.0016949
	C.0243113	0.0186164	0.0103082	0.0105062
	C.0197454	0.0099578	0.0030695	0.0021077
	C.0189284	0.0033767	-0.0007920	-0.0020957
	0.0224741	0.0046783	-0.0028097	0.0029712
30	C.0198431	0.0047526	-0.0045033	0.0014954
	C.0166920	0.0022479	-0.0018224	0.0010835
	C.0160C74	0.0014867	-0.0007726	-0.0000162
	C.0158241	0.0025406	-0.0003878	-0.0034613
	C.0161222	0.0032478	0.0043837	-0.0018311
	0.0165950	C.0050288	0.0083092	0.0012484
	C.0129701	0.0051804	0.0053669	0.0020165
	C.0128760	0.0023782	0.0013245	0.0018441
	C.0153729	0.0014390	0.0023334	0.0010064
	C.0183644	0.0032406	0.0063887	0.0007221
40	C.0230047	0.0048448	0.0093925	0.0029716
	C.0159719	0.0042358	0.0067734	0.0029668
	0.0130540	0.0026626	0.0040555	0.0010842
	C.0189874	0.0021083	0.0038831	0.0011460
	0.0143137	0.0025656	0.0006239	-0.0015329
	C.0107431	0.0040603	-0.0015958	-0.0061270

n = 9

τ	F_1	F_2	F_3	F_4
	0.2401385	0.0157454	0.0229736	0.0337343
	0.1214057	0.0172238	0.0141285	0.0117322
	0.3091171	0.0324817	0.0805578	0.0133671
	0.4472895	0.0537365	0.1310478	0.0334980
	0.3093244	0.0418949	0.0486420	0.0196557
-40	0.2452881	0.0178597	-0.0208220	0.0224930
	0.5575159	0.0690305	0.1428894	0.0691766
	0.8368248	0.1462203	0.3078181	0.1225551
	0.5348096	0.1039756	0.1763241	0.1000209
	0.2665747	0.0318683	0.0325463	0.0547944
	0.2523287	0.0238862	0.0105475	0.0352742
	0.2214793	0.0290418	0.0252598	0.0027142
	0.2060983	0.0377576	0.0638464	0.0022372
	0.2840666	0.0487943	0.0927468	0.0328402
	0.4317015	0.0538904	0.1019017	0.0231770
-30	0.3100602	0.0558462	0.0530197	-0.0083951
	0.2791994	0.0656393	0.0532749	0.0593872
	0.4698116	0.0599905	0.0936717	0.1161993
	0.4380972	0.0465916	0.0662906	0.0951037
	0.3851903	0.0561306	0.0645834	0.0985743
	0.4741773	0.0470168	0.1039429	0.0721330
	0.7161013	0.0372220	0.1570062	0.0180885
	0.8136485	0.0482941	0.1688581	0.0094701
	0.4172840	0.0489727	0.0637930	0.0402111
	0.3235554	0.0641325	0.0699449	0.0297768
-20	0.5871953	0.0855743	0.1929331	-0.0095855
	0.3951472	0.0655314	0.1523275	-0.0165083
	0.1535417	0.0255434	0.0378546	-0.0060074
	0.3660422	0.0229774	0.0501156	0.0446094
	0.5668160	0.0446152	0.1135624	0.0970998
	0.4254557	0.0360822	0.0696787	0.0672239
	0.2905034	0.0157832	0.0099403	0.0145910
	0.3428837	0.0198536	0.0558723	-0.0047961
	0.4530777	0.0340804	0.0783539	0.0178417
	0.4682348	0.0326936	0.0092546	0.0566486
-10	0.5625125	0.0326410	0.0310500	0.0028252
	0.7876555	0.0447829	0.1214767	-0.0335471
	0.6749450	0.0371222	0.0909013	0.0144521

(continued for n = 9)

σ	F_1	F_2	F_3	F_4
	C.37C92CC	0.0321831	0.0386221	0.0352300
	C.3492698	C.0544750	0.0653732	0.0232881
	0.4358923	0.0656762	0.0894805	-0.0142094
	0.4336890	0.0599073	0.0867104	0.0069938
	0.5112256	0.0734397	0.1346561	0.0497239
	0.7542901	0.0958252	0.2127053	-0.0298316
-1	C.0343217	0.0019237	0.0045046	-0.0059206
+1	C.0178023	0.0059511	0.0100704	C.0002979
	C.4726045	0.1108814	0.2166371	-0.0358720
	0.4224957	0.1077707	0.1225556	0.0588228
	C.3897453	0.1035894	0.0900321	0.0945293
	C.2882227	0.0683662	0.0891792	0.0401474
	C.1302797	0.0467427	0.0572133	0.0178539
	C.0301452	0.0479808	0.0197778	0.0123211
	0.0205536	0.0360613	0.0044804	-0.0021128
	0.0500999	C.0169907	0.0077250	0.0082997
10	C.0855232	0.0124189	0.0251676	0.0148177
	C.2000463	C.0102362	0.0324163	0.0089962
	C.2765217	0.0059307	0.0204257	0.0102608
	0.1418648	0.0060729	0.0029826	0.0135863
	0.0695533	0.0066876	0.0064210	0.0034815
	C.1245568	C.0059762	0.0185989	-0.0104154
	C.1053652	0.0036352	0.0135325	-0.0094404
	C.0695493	0.0067492	0.0144903	0.0032820
	C.0498498	0.0113270	0.0188772	0.0100922
	0.0595678	0.0087438	0.0175473	0.0000356
20	0.0964004	0.0090766	0.0242998	-0.0126249
	C.0661739	0.0208745	0.0242668	-0.0080222
	C.0357356	0.0292509	0.0213111	0.0021555
	C.0964645	0.0189646	0.0227819	0.0121556
	0.1293027	0.0138396	0.0183553	0.0224845
	0.0627332	0.0186830	0.0104725	0.0116501
	C.0118489	C.0122604	0.0031514	-0.0045541
	C.0064402	0.0028885	0.0001684	-0.0033303
	C.0109263	0.0015558	0.0022604	-0.0020794
	C.0322579	0.0044747	0.0090013	-0.0057137
30	C.0487902	0.0091281	0.0136790	-0.0106523
	C.0370512	C.0112045	0.0084508	-0.0126573
	C.0151624	0.0063997	0.0012795	-0.0038983
	C.0167728	0.0031917	-0.0000725	-0.0019279
	C.0246165	0.0037424	0.0011672	-0.0076396
	0.0139400	0.0026345	0.0001712	-0.0051444
	0.0047805	0.0025457	-0.0018137	-0.0008398
	0.0093920	C.0028907	-0.0032180	0.0013866
	C.0120692	0.0022225	-0.0029324	0.0015698
	C.0108854	0.0018120	-0.0010465	0.0003122
40	C.0144979	0.0014778	-0.0006147	-0.0012748
	0.0125779	0.0031885	-0.0002532	-0.0035923
	0.0086609	0.0046965	0.0020196	-0.0033470
	C.0105250	C.0026251	0.0031665	-0.0014573
	C.0159381	0.0014885	-0.0003635	-0.0030139
	C.0199821	0.0022120	-0.0035996	-0.0047302

n = 10

σ	F_1	F_2	F_3	F_4
	0.1807411	0.0116559	0.0079748	0.0240698
	0.2028278	0.0171553	0.0056461	0.0555967
	0.1421653	0.0144627	0.0070352	0.0289202
	0.0838589	0.0139142	0.0028301	-0.0145151
	0.1238375	0.0144565	-0.0048414	-0.0287928
-40	0.2499074	0.0207505	0.0395309	-0.0073787
	0.3323663	0.0488564	0.1016956	0.0021231
	0.4133238	0.0627370	0.1217178	-0.0192215
	0.5393858	0.0519287	0.1327986	0.0047209
	0.3752879	0.0500427	0.1100437	0.0367893
	0.0992950	0.0506030	0.0406429	0.0340881
	0.1410803	0.0436533	0.0244499	0.0262229
	0.2635351	0.0254023	0.0438311	0.0133109
	0.1790011	0.0112184	0.0300607	0.0038374
	0.0915968	0.0164507	0.0076662	-0.0030644
-30	0.1637092	0.0278315	-0.0018693	-0.0329767
	0.2348413	0.0471657	0.0127881	-0.0471043
	0.1262856	0.0669708	0.0094807	-0.0013657
	0.1551877	0.0551025	-0.0332930	0.0303102
	0.3111638	0.0481394	-0.0208712	0.0205714
	0.2512224	0.0565856	0.0315416	0.0105132
	0.1468128	0.0336959	0.0178849	0.0010537
	0.2852846	0.0140672	-0.0258013	-0.0199479
	0.4516960	0.0187696	-0.0264139	-0.0215088
	0.2737315	0.0306933	0.0018777	-0.0125145
-20	0.0769765	0.0306497	-0.0008013	-0.0223687
	0.0565012	0.0265959	-0.0057654	-0.0082884
	0.1059288	0.0343160	0.0253988	0.0082763
	0.2982119	0.0444031	0.0764226	0.0368644
	0.5647612	0.0620354	0.1468999	0.0724670
	0.8130199	0.0527048	0.1652405	0.0388028
	0.7278085	0.0315335	0.0729388	0.0040763
	0.3091198	0.0354363	-0.0021544	0.0091196
	0.1549651	0.0296026	0.0253299	0.0184055
	0.2375481	0.0156058	0.0378718	0.0187603
-10	0.1851310	0.0236480	0.0058859	0.0184785
	0.0826490	0.0363384	-0.0011998	0.0299125
	0.0523999	0.0260324	-0.0103131	0.0185794

(continued for n = 10)

σ	F_1	F_2	F_3	F_4
	0.0499968	0.0157121	-0.0243043	-0.0020548
	0.0290754	0.0259487	-0.0088525	0.0049591
	0.0713387	0.0398595	-0.0004665	0.0328724
	0.1959201	0.0373494	-0.0058856	0.0354830
	0.3073926	0.0297607	0.0262139	-0.0181461
	0.4776659	0.0393129	0.1012583	-0.0841248
-1	0.0287547	0.0017054	0.0059420	-0.0033185
+1	0.0087912	0.0017791	0.0011709	-0.0037375
	0.1442390	0.0641965	0.0348362	-0.0821310
	0.1882973	0.0461305	0.0287942	-0.0139526
	0.1951636	0.0304983	0.0185127	0.0114822
	0.1115043	0.0318112	-0.0032961	-0.0182634
	0.0493498	0.0466686	-0.0192125	-0.0331189
	0.0665032	0.0451463	-0.0092462	-0.0215521
	0.1034629	0.0408907	0.0211031	-0.0173840
	0.0746770	0.0519137	0.0314918	-0.0187664
10	0.0423003	0.0432819	0.0124302	-0.0036130
	0.0445169	0.0222053	0.0048395	0.0155265
	0.0375049	0.0145609	0.0029946	0.0180754
	0.0341000	0.0154690	0.0005254	0.0177174
	0.0502928	0.0121353	0.0007912	0.0152839
	0.0639293	0.0087163	-0.0060444	0.0085529
	0.0430824	0.0087748	-0.0054627	-0.0024023
	0.0307847	0.0071161	0.0040667	-0.0023285
	0.0340056	0.0067634	0.0080049	0.0055349
	0.0219702	0.0096636	0.0068494	-0.0001302
20	0.0135140	0.0154395	0.0095246	-0.0071685
	0.0203593	0.0137308	0.0122294	-0.0048435
	0.0418986	0.0102323	0.0064552	0.0093883
	0.0599624	0.0100030	-0.0032992	0.0181388
	0.0674021	0.0066338	-0.0074699	0.0139886
	0.0718039	0.0045210	-0.0073735	0.0129376
	0.0533578	0.0056192	-0.0077301	0.0066420
	0.0234577	0.0119998	-0.0038832	-0.0035374
	0.0129775	0.0169130	0.0065782	-0.0066040
	0.0130383	0.0124795	0.0108375	-0.0032104
30	0.0161955	0.0055544	0.0051801	0.0013006
	0.0178987	0.0029646	0.0009435	0.0019008
	0.0164418	0.0038607	0.0032388	0.0025305
	0.0156671	0.0060558	0.0047217	0.0028804
	0.0093867	0.0069971	0.0017185	0.0014318
	0.0089870	0.0045038	0.0016655	0.0024011
	0.0190877	0.0030368	0.0035707	0.0059903
	0.0235514	0.0050505	-0.0008469	0.0055062
	0.0222565	0.0065383	-0.0047036	0.0009683
	0.0200744	0.0042478	0.0001178	-0.0000140
40	0.0118918	0.0019230	0.0023367	0.0018337
	0.0090008	0.0022533	0.0023303	0.0035141
	0.0148764	0.0043422	0.0047205	0.0056918
	0.0131200	0.0057980	0.0058005	0.0056549
	0.0078349	0.0047581	0.0033683	0.0045428
	0.0119282	0.0029001	0.0004429	0.0035588

n = 11

σ	F_1	F_2	F_3	F_4
	0.2111773	0.0121694	0.0360269	-0.0182
	0.1522515	0.0126362	0.0260576	0.0035
	0.1571558	0.0173102	0.0211426	0.0234
	0.1575745	0.0228234	0.0401666	0.0055
	0.1592640	0.0175424	0.0391698	-0.0237
-40	0.1070916	0.0152234	0.0186043	-0.0275
	0.0664490	0.0191536	0.0140283	-0.0197
	0.0749436	0.0168347	0.0076076	0.0090
	0.0853812	0.0149981	-0.0059274	0.0294
	0.0747417	0.0133310	-0.0038453	0.0192
	0.1007007	0.0174260	0.0264565	0.0016
	0.2776822	0.0266260	0.0516001	0.0198
	0.3927533	0.0265219	0.0389740	0.0672
	0.3023162	0.0191876	0.0094407	0.0702
	0.2140320	0.0136015	-0.0039351	0.0399
-30	0.1906673	0.0096107	0.0072057	0.0086
	0.2171876	0.0176725	0.0350320	-0.0032
	0.1570165	0.0284007	0.0469111	0.0047
	0.0380426	0.0178340	0.0179241	0.0020
	0.0201752	0.0108777	-0.0111220	-0.0065
	0.0380551	0.0154936	-0.0139788	-0.0047
	0.0423533	0.0145360	-0.0094964	0.0031
	0.0538575	0.0100338	-0.0061250	0.0053
	0.1594267	0.0252237	0.0227426	0.0484
	0.2519758	0.0418235	0.0453604	0.0834
-20	0.1732064	0.0228082	0.0111825	0.0366
	0.1298555	0.0059975	-0.0127221	-0.0085
	0.1664470	0.0106345	-0.0082288	-0.0055
	0.1600014	0.0164701	-0.0049256	0.0220
	0.2625281	0.0143012	-0.0032165	0.0217
	0.3502020	0.0095935	-0.0126760	0.0067
	0.2117265	0.0149822	-0.0173232	-0.0232
	0.1669662	0.0208313	-0.0002976	-0.0293
	0.2424905	0.0273979	0.0475945	-0.0062
	0.1684822	0.0491075	0.0705065	0.0121
-10	0.2171105	0.0531462	0.0267916	0.0237
	0.3711274	0.0250151	-0.0112811	0.0340
	0.3574656	0.0149959	0.0284974	0.0142

(continued for n = 11)

σ	F_1	F_2	F_3	F_4
	0.3465255	0.0268983	0.0831336	-0.0257
	0.2365956	0.0266099	0.0554880	-0.0366
	0.0537741	0.0446637	-0.0041185	-0.0171
	0.0329458	0.0832070	-0.0460476	-0.0009
	0.0502719	0.0675820	-0.0457912	0.0071
	0.0545269	0.0126007	-0.0205031	0.0137
-1	0.0019670	0.0004506	-0.0006697	0.0003
+1	0.0031778	0.0025387	0.0015783	-0.0022
	0.0301430	0.0347032	0.0183671	-0.0248
	0.0088951	0.0234189	0.0021456	-0.0024
	0.0107380	0.0262334	-0.0099336	0.0035
	0.0473083	0.0223434	-0.0071254	0.0063
	0.0713724	0.0183203	-0.0008361	0.0088
	0.0499275	0.0259816	-0.0060620	-0.0064
	0.0407998	0.0317199	0.0055578	-0.0234
	0.0715984	0.0260566	0.0292385	-0.0125
10	0.0825651	0.0216656	0.0272441	0.0001
	0.0941920	0.0262803	0.0240269	-0.0150
	0.1184400	0.0240280	0.0348081	-0.0242
	0.0880872	0.0128843	0.0246234	-0.0145
	0.0651266	0.0067274	0.0109771	-0.0128
	0.0706210	0.0044634	0.0116954	-0.0117
	0.0575793	0.0050099	0.0126503	-0.0053
	0.0288468	0.0149052	0.0084653	0.0033
	0.0103339	0.0297675	0.0068703	0.0112
	0.0164767	0.0296954	0.0135747	0.0122
20	0.0396814	0.0149392	0.0094335	0.0104
	0.0642644	0.0057548	-0.0069036	0.0058
	0.0607901	0.0051223	-0.0101249	0.0026
	0.0800756	0.0052023	0.0054123	0.0002
	0.1062957	0.0048541	0.0122023	-0.0031
	0.0759183	0.0044840	0.0061220	0.0018
	0.0806051	0.0030962	0.0045530	0.0013
	0.0997709	0.0026900	0.0003949	-0.0033
	0.0567503	0.0044589	-0.0004632	-0.0000
	0.0208484	0.0081782	0.0056563	0.0000
30	0.0118486	0.0115456	0.0030900	0.0018
	0.0088293	0.0092766	-0.0022402	0.0064
	0.0078682	0.0049744	-0.0018693	0.0028
	0.0090377	0.0032357	-0.0000048	-0.0024
	0.0152188	0.0017497	0.0015468	-0.0010
	0.0144813	0.0010760	0.0016326	0.0015
	0.0102628	0.0016316	0.0014426	-0.0008
	0.0103961	0.0018736	0.0017127	-0.0033
	0.0083539	0.0020903	-0.0007629	-0.0027
	0.0062310	0.0022970	-0.0022886	-0.0013
40	0.0051164	0.0017446	-0.0003225	0.0004
	0.0077505	0.0011013	0.0009540	0.0012
	0.0115538	0.0012441	0.0010910	0.0008
	0.0064590	0.0016031	0.0009379	0.0004
	0.0016525	0.0013994	0.0005854	0.0001
	0.0043514	0.0015476	0.0002879	-0.0011

n = 12

σ	F_1	F_2	F_3	F_4
	0.1355859	0.0071449	0.0227428	0.01788
	0.1296110	0.0168273	0.0254009	0.03186
	0.0853376	0.0215616	0.0215138	0.02932
	0.0399049	0.0096179	0.0070381	0.01169
	0.0562011	0.0013997	0.0010202	0.00083
-40	0.0674475	0.0095832	0.0143833	-0.00848
	0.0677409	0.0203963	0.0204970	-0.00776
	0.0486473	0.0239095	0.0072344	0.00206
	0.0401544	0.0237769	0.0101679	0.00917
	0.0662765	0.0150193	0.0130177	0.01527
	0.0778868	0.0101646	0.0122538	0.00805
	0.0629289	0.0204311	0.0247638	0.00376
	0.0474385	0.0278876	0.0246734	0.01864
	0.0744723	0.0218815	0.0116133	0.01633
	0.1025717	0.0085635	0.0022965	-0.00189
-30	0.1224282	0.0099632	0.0159900	0.01482
	0.1596366	0.0181457	0.0356650	0.03709
	0.1145563	0.0204448	0.0335599	0.02001
	0.0616404	0.0352247	0.0383094	0.01417
	0.0539930	0.0420605	0.0356236	0.02002
	0.0772123	0.0239918	0.0158244	0.00588
	0.1507077	0.0080727	0.0042712	-0.00841
	0.1773140	0.0054143	0.0027082	-0.01249
	0.1296142	0.0098425	0.0065473	-0.00651
	0.0878899	0.0137743	0.0005211	0.00469
-20	0.1182492	0.0224030	0.0148267	-0.00077
	0.1441334	0.0329808	0.0310254	-0.02888
	0.1091341	0.0397271	0.0212990	-0.03811
	0.0574299	0.0406913	0.0228013	-0.02199
	0.0267809	0.0222037	0.0182751	-0.00178
	0.0334677	0.0072352	0.0079568	0.00788
	0.0813023	0.0057407	0.0038753	-0.00765
	0.1380388	0.0050600	-0.0033696	-0.01622
	0.1118540	0.0128629	-0.0050411	0.00227
	0.0448822	0.0266518	-0.0042355	0.01900
-10	0.0292189	0.0341072	0.0012643	0.02077
	0.0537697	0.0307376	0.0204289	0.01588
	0.0902749	0.0223448	0.0367350	0.01057

Bibliography

Bendat, J.S. and A.G. Piersol, 1966: Measurement and analysis of random data. John Wiley & Sons Inc., Chapter 7.

Blackman, R.B. and J.W. Tukey, 1958: The measurement of power spectra. Dover, pp. 189.

Charney, J., 1959: On the general circulation of the atmosphere. Rossby Memorial Vol., Rockefeller Inst. Press, New York, 178-193.

_____, 1963: A note on large scale motions in the tropics. J. Atmos. Sci., 20, 607-609.

Eliassen, A. and E. Palm, 1961: On the transfer of energy in stationary mountain waves. Geof. Publ., 22, 1-23.

Gates, W.L., 1961: Statistic stability measures in the atmosphere. AFCRL-TN-60-817, Scientific Report No. 3.

Harvard University, 1952: The Annals of the Computation Laboratory, Vol. 23; Tables of the error function and of its first twenty derivatives.

Manabe, S. and J. Smagorinsky, 1967: Simulated climatology of a general circulation model with a hydrologic cycle II. Monthly Weather Review, 151-169.

Maruyama, T., 1967: Large scale disturbances in the equatorial lower stratosphere. J. Meteor. Soc., Japan, 45, 391-407.

Morse P. and H. Feshbach, 1953: Methods of theoretical physics. McGraw-Hill Inc., pp. 1088-1094.

Obasi, G.O.P., 1965: On the maintenance of the kinetic energy of mean zonal flow in the southern hemisphere. Tellus, 17, 95-105.

Peixoto, J., 1960: Hemispheric temperature conditions during the year 1950. Planetary Circulations Project, M.I.T., Scientific Report No. 4.

Riehl, H., 1954: Tropical meteorology. McGraw-Hill Book Co. Inc., pp. 392.

Riehl, H., 1963: Stationary aspects of the tropical general circulation. Geof. Internacional, 53-68.

Shanks, J.L., 1967: Recursion filters for digital processing. Geophysics, Vol. XXXII, 33-51.

Shuman, F., 1957: Numerical methods in weather prediction, I. The balance equations. Monthly Weather Review, 85, 329-332.

Slater, L.J., 1960: Confluent hypergeometric function. Cambridge U. Press.

Smagorinsky, J., S. Manabe and J.H. Holloway, 1965: Numerical results from a nine-level general circulation model of the atmosphere. Mon. Wea. Review, 93, 727-760.

Starr, V.P. and R.M. White, 1952: Two years of momentum flux data for 31°N, Tellus, 4, 332-333.

Starr, V.P. and R.M. White, 1954: Two years of momentum flux data for 13°N, Tellus, 6, 180-181.

Treitel S. and E.A. Robinson, 1964: The stability of digital filters. Trans. Geoscience Electronics, V. 2.

Yaglom, A.M., 1962: Introduction to stationary random functions. Prentice Hall, Inc., pp. 235.

Yanai, M. and Maruyama T., 1966: Stratospheric wave disturbances propagating over the equatorial Pacific. J. Meteor. Soc., Japan, 44, 291-294.

Palmen, E., 1963: General circulation of the tropics. Symposium on tropical meteorology, World Meteorological Organization. TWS/Doc. 6.